

TECHNISCHE UNIVERSITÄT MÜNCHEN

Lehrstuhl für Bodenkunde

Degradation, chemical alteration and stabilisation
of pyrogenic plant residues in soil

André Hilscher

Vollständiger Abdruck der von der Fakultät Wissenschaftszentrum Weihenstephan für Ernährung,
Landnutzung und Umwelt der Technischen Universität München zur Erlangung des akademischen
Grades eines

Doktors der Naturwissenschaften

genehmigten Dissertation.

Vorsitzende: Univ.-Prof. Dr. I. Kögel-Knabner

Prüfer der Dissertation: 1. apl. Prof. Dr. H. E. Knicker
2. Univ.-Prof. Dr. J. Völkel
3. Priv.-Doz. Dr. Chr. Siewert

Die Dissertation wurde am 28.02.2011 bei der Technischen Universität München eingereicht und
durch die Fakultät Wissenschaftszentrum Weihenstephan für Ernährung, Landwirtschaft und Umwelt
am 15.06.2011 angenommen.

JORGE CHAM © 2009



WWW.PHDCOMICS.COM

THE ORIGIN OF THE THESES

Summary

Incomplete combustion of vegetation results in pyrogenic organic material (PyOM) which occurs ubiquitously in soils and sediments. Because of the potential refractory nature of such thermally altered products, they are expected to represent an important carbon (C) sink. However the recalcitrance of this material in soils is still heavily debated most probably due to the fact that up to now, no commonly accepted method is available for its identification and quantification and the processes involved in their degradation and humification are still not very well understood.

In order to fill this gap, the main objective of the present research was to study the alteration and stability of PyOM of varying charring degree during their humification in soil. The goal was to elucidate their impact on the quality and quantity of soil organic matter and its function as carbon and nitrogen sink. In order to meet these objectives, four studies were conducted at different scales. A first idea about the recalcitrance of PyOM was obtained in short-term high-resolution respiration experiments using PyOM of different charring degree, typical for fire-prone landscapes such as grassland (*Lolium perenne*) and pine forests (*Pinus sylverstris*). The effect of charring on the biomarker and lipid composition of different plant materials was studied to identify potential maker for PyOM in soil. Subsequently, the stability of those biomarkers against biotic degradation was tested in order to elucidate their applicability in *in situ* studies. Microcosm incubation experiments using ^{13}C - and ^{15}N -enriched PyOM were conducted for up to 28 months to study chemical alterations during their degradation by means of isotopic label recovery and solid-state NMR spectroscopy. Together with the isotopic enrichment, the setup of the experiment allowed the examination of the translocation potential within the soil column. Additionally, the effect of a co-substrate on PyOM mineralisation and aging was investigated. The used PyOM for all experiments was produced by charring plant materials for one min (1M) or four min (4M) at 350°C under oxic conditions. The applied charring conditions result in chars that are comparable to those remaining after natural wildfires.

The respiration experiments indicated that grass-derived PyOM showed the highest C mineralisation. During 7 weeks of aerobic incubation at 30°C in soil, up to 3.2% of the added PyOM-C was converted to CO_2 . More severe thermal alteration resulted in a decrease in the total C mineralisation to 2.5% of OC. In the pine-derived PyOM, only 0.7 (1M) and 0.5% (4M) of the initial C were mineralised. Co-substrate additions did not

enhance PyOM mineralisation during initial degradation. ^{13}C NMR spectroscopic analysis indicated structural changes during microbial degradation of PyOM. Concomitant with a decrease in O-alkyl/alkyl-C, carboxyl/carbonyl-C content increased, pointing to oxidation. Only the strongly thermally-altered pine PyOM showed a reduction in aromaticity. The small C losses during the experiment indicated conversion of aryl C into other C groups. As revealed by the increase in carboxyl/carbonyl C, this conversion must include the opening and partial oxidation of aromatic ring structures. Relatively short mean residence times of 14 (1M) and 19 years (4M) were obtained for the charred rye grass residues and up to 56 years for the pine wood char, which are in the range of unburned soil organic matter.

The second study focused on heat-induced alteration of n-alkanes, n-fatty acids (FA) composition as well as the content of the molecular marker levoglucosan (LG) in different plant materials. The results confirmed that charring of plant residues leads to typical thermal breakdown processes of n-alkanes and FA. In particular, the average chain length of n-alkanes is reduced by up to 4 carbons and the characteristic odd/even predominance of the fresh plant materials shifted to a balanced odd/even distribution with prolonging charring time. The unsaturated FA fraction was more depleted in relation to the saturated counterparts after the charring. Especially, linoleic acid ($\text{C}_{18:2}$) and α -linolenic acid ($\text{C}_{18:3}$) are depleted in the more charred grass, whereas oleic acid ($\text{C}_{18:1}$) is still present. Levoglucosan is detectable for all PyOM, whereas the pine residue charred for 1M contained the largest LG amount. A more progressive heating resulted a strong depletion of LG for both plant materials. The pine char showed a relative accumulation of vanillin, supporting that some lignin-type structures survived the 1M charring process.

The incubated pine chars were enriched in the n-alkane octadecane (C_{18}) and the mid-chain homologues in the range C_{22} to C_{26} . In contrast, the n-alkanes and FA fraction of the grass chars was more efficiently degraded with a loss of up to 39% of the initial amount. The study demonstrates that already during the initial phase of biodegradation of PyOM, n-alkanes and the FA fraction can be rapidly modified either by decomposition but also by biosynthesis most tentatively by fungi. Levoglucosan was efficiently decomposed. This indicates that care has to be taken, if this compound is used as a tracer in soils containing aged char because its instability against biodegradation may lead to an underestimation of the charcoal content. Another critical point is the thermal decomposition of the LG, which may lead to misinterpretation of the PyOM portion.

The third study extracted important aspects concerning the degradation of grass-derived PyOM, the transport of the residues within a soil column and distribution in soil organic matter fractions during a 28-month microcosm experiment. Therefore, the microbial recalcitrance of char and the transport within a soil column was studied, using ^{13}C - and ^{15}N -enriched PyOM. After 28 months, the ^{13}C PyOM recovery decreased to values between 62 and 65%. The respective ^{15}N PyOM recovery followed the same trend but tended to be higher. Most of the added PyOM isotopic label was recovered in the particulate organic matter (POM) fraction, being reduced by half at the end of the experiment. Already after one month, PyOM was detected in the POM-free mineral fractions. This fast association of PyOM with the mineral phase indicates that physical soil properties have to be considered for the elucidation of PyOM stability. Addition of fresh unlabelled grass material as co-substrate resulted in comparable trends as for the pure PyOM but the total recovery of the isotopic labels clearly increased with respect to the amount of mineral-associated PyOM. Most of the mineral-associated PyOM occurred in the clay separates ($< 2 \mu\text{m}$) for which the largest values were obtained for the experiment with the more intensively charred PyOM and co-substrate addition. The PyOM label was found in the collected leachate, indicating that PyOM was vertically transported and even left the soil column.

This study demonstrates the degradability of grass-derived PyOM. The addition of fresh plant material as an easily degradable co-substrate promoted the formation of partially decomposed PyOM and subsequently its association with the mineral phase, but did not increase the respective mineralisation rates. Detection of ^{13}C and ^{15}N content at different depths of the microcosm column demonstrated an additional loss of PyOM from top soil by way of mobilisation and transport to deeper horizons. Overall, all these processes have to be taken into account in order to obtain a more realistic view about the behaviour of PyOM in environmental systems and for estimation of the C and N sequestration potential.

The last study focused on structural modification of PyOM on a molecular scale. Solid-state ^{13}C and ^{15}N NMR studies were conducted to elucidate the humification processes at different stages of PyOM degradation. The chemical structure of the remaining PyOM after incubation was clearly different from the initial pyrogenic material. The proportion of O-containing functional groups was increased whereas that of aryl C and of N-containing heterocyclic structures was decreased, probably due to mineralisation and

conversion to other C and N groups. The observed degradation of aromatic C may include two simultaneous processes: (i) complete mineralisation to CO₂ and (ii) conversion to other C groups by partial oxidation. The relevance of the latter process is supported by the fact that oxygen-substituted aryl structures (O-aryl C) showed little if any decrease in spite of the considerable aryl C and total C losses. These reactions alter the chemical and physical properties of the char residue and make it more available for further microbial attack and for adsorption processes. The study presents direct evidence for the degradation of N-heterocyclic domains in charred plant remains adding new aspects to the understanding of the N cycling in fire-affected ecosystems.

In summary, the present research works underline that the observed degradation, stabilisation and translocation processes in soils should be considered as a whole, if a realistic assessment of the C and N sequestration potential of charred plant remains is desired. The different studies showed that PyOM is involved in the C and N turnover fluxes like other SOM. The view that PyOM preservation is dominated by its chemical recalcitrance should no longer be accepted. With regard to the climate change, PyOM cannot be generally counted as a potential carbon sink for long-term reduction of CO₂ in the atmosphere.

Zusammenfassung

Infolge unvollständiger Verbrennung der Vegetation wird pyrogenes organisches Material (PyOM) erzeugt, welches ubiquitär in Böden und Sedimenten anzutreffen ist. Aufgrund der potentiell refraktären Natur solch thermisch veränderter Verbindungen werden diese als wichtige Kohlenstoffsенke betrachtet. Aktuell wird vermehrt über die Rolle des PyOM als rekalcitranter Bestandteil der organischen Bodensubstanz diskutiert. Problematisch ist dabei, dass bis heute kein allgemein akzeptiertes Verfahren für die Identifikation und Quantifizierung von PyOM existiert und die Abbau- und Humifizierungsprozesse nicht ausreichend verstanden sind. Zur Klärung dieser Wissenslücken wird in der vorliegenden Arbeit auf die Veränderung und Stabilität von PyOM mit variierendem Verbrennungsgrad während seiner Humifizierung im Boden eingegangen. Schwerpunkt der Arbeit ist dabei der Einfluss des PyOM auf die Zusammensetzung und Quantität der organischen Bodensubstanz und seiner Funktion als Senke für Kohlenstoff (C) und Stickstoff (N). Um diese Ziele zu erreichen, wurden vier Studien auf verschiedenen zeitlichen und molekularen Ebenen durchgeführt.

Ein Einblick in den Abbau von PyOM wurde in hochauflösenden Respirationsexperimenten mit PyOM unterschiedlichen Verbrennungsgrades erhalten, welches typisch für brandgefährdete Gebiete wie Steppen (*Lolium perenne*) und Kieferwälder (*Pinus sylvestris*) ist. Der Einfluss der Verkohlungsstufe auf die Biomarker- und Lipid-Zusammensetzung verschiedener Pflanzenmaterialien wurde betrachtet, um potentielle chemische Marker für PyOM im Boden zu identifizieren. Zusätzlich wurde die biochemische Persistenz der Biomarker getestet, welche für ihre Anwendung in *In-situ*-Studien relevant ist. Mikrokosmos-Inkubationsansätze wurden unter Verwendung von ^{13}C - und ^{15}N -angereichertem PyOM über einen Zeitraum von 28 Monaten durchgeführt. Damit wurden chemische Veränderungen während des PyOM-Abbaus mittels isotopischer Bilanzierung und Festkörper- ^{13}C und ^{15}N -CPMAS-NMR-Studien (kernmagnetische Resonanzspektroskopie) festgestellt. Der Versuchsaufbau erlaubte weiterhin die vertikalen Verlagerungseigenschaften im Boden zu untersuchen. Zusätzlich wurde der Einfluss eines Co-Substrates auf Mineralisation und Humifizierung des PyOM betrachtet.

Das verwendete PyOM wurde für alle Studien durch die Verkohlungsstufe der Pflanzenmaterialien für den Zeitraum von einer (1M) oder vier Minuten (4M) bei einer Verbrennungstemperatur von 350°C unter oxidischen Bedingungen hergestellt. Diese

Rahmenbedingungen stellen die Vergleichbarkeit des erhaltenen PyOM mit den aus Vegetationsbränden resultierenden Rückständen sicher.

Das Gras-PyOM zeigte die höchste Kohlenstoffmineralisation während der aeroben Respirationsversuche bei einer Inkubationstemperatur von 30°C. Es wurde innerhalb von sieben Wochen insgesamt bis zu 3,2% (1M) des PyOM-Kohlenstoffs zu CO₂ umgesetzt. Eine Steigerung des Verkohlungsgrades bewirkte eine Abnahme der kumulativen Kohlenstoffmineralisation auf 2,5% (4M) des organischen Gesamtkohlenstoffgehaltes. Im Kiefer-PyOM wurden nur 0,7% (1M) bzw. 0,5% (4M) des Kohlenstoffvorrates mineralisiert. Die Bereitstellung eines Co-Substrates führte zu keiner Zunahme der PyOM-Mineralisation. Die Reduzierung der O-Alkyl/Alkyl-Kohlenstoffanteile wurde parallel von ansteigenden Carboxyl/Carbonyl-Kohlenstoffanteilen begleitet. Diese Beobachtung weist auf einen einsetzenden Oxidationsprozess des PyOM hin. Einzig für das intensiver verkohlte Kiefer-PyOM konnte eine Reduktion der Aromatizität festgestellt werden. Die geringen Kohlenstoffverluste während des Experiments stützen die Annahme, dass Aryl-Kohlenstoff in andere Kohlenstoffgruppen umgewandelt wurde. Im Hinblick auf die Zunahme des Carboxyl/Carbonyl-Kohlenstoffanteils könnte dieser Umbau mit einer Spaltung und partiellen Oxidation der aromatischen Ringstrukturen verbunden sein. Die abgeleiteten Verweilzeiten waren mit 14 (1M) bzw. 19 Jahren (4M) für das Gras-PyOM und von bis zu 56 Jahren für das verkohlte Kiefermaterial vergleichbar mit der von ungebranntem organischem Bodenmaterial.

Die zweite Studie fokussierte auf die thermisch induzierten Veränderungen der n-Alkane, n-Fettsäuren (FA), dem Pyrolyseindikator Levoglucosan (LG) sowie Lignin-Derivaten in verschiedenen Pflanzenmaterialien. Die erhaltenen Ergebnisse bestätigen, dass die Verkohlung von Pflanzenmaterial einen Zerlegungsprozess der n-Alkane und FA hervorruft. Die mittlere Kohlenstoffkettenlänge der n-Alkane wurde um bis zu vier Kohlenstoffatome verkürzt. Die charakteristische Dominanz der ungeraden n-Alkan-Kohlenstoffkettenzahl des frischen Pflanzenmaterials verschob sich mit zunehmendem Verkohlungsgrad zu einem ausgeglichenen Verhältnis. Infolge des Verkohlungsprozesses wurde die ungesättigte FA-Fraktion in Relation zu den gesättigten Homologen stärker dezimiert. Insbesondere Linolsäure (C_{18:2}) und α -Linolensäure (C_{18:3}) waren in dem stärker verkohlten Gras-PyOM nicht nachweisbar, wogegen Ölsäure (C_{18:1}) noch enthalten war. Levoglucosan war in allen PyOM feststellbar, wobei das Kiefer-PyOM (1M) den höchsten LG-Gehalt aufwies. Ein zunehmendes Fortschreiten des Verkohlungsprozesses bedingte

eine ausgeprägte Abnahme des LG-Gehaltes. Für das Kiefer-PyOM (1M) zeigte sich weiterhin eine relative Akkumulation des Vanillins, welches ein Indikator für das Vorhandensein von Lignin ist. Lignin-Strukturen können somit einen Bestandteil in verkohlten Pflanzenresten darstellen.

Das inkubierte Kiefer-PyOM war angereichert mit dem n-Alkan Octadekan (C_{18}) und den mittelkettigen Homologen in dem Bereich von C_{22} bis C_{26} . Im Gegensatz dazu wurde die n-Alkan- und FA-Fraktion des Gras-PyOM mit einem Verlust von 39% des Ausgangsgehaltes effizienter abgebaut. Diese Studie demonstriert, dass bereits während des beginnenden biotischen Abbaus von PyOM das n-Alkan- und FA-Verteilungsmuster durch Zerlegungsprozesse, aber auch durch Biosynthese - vorzugsweise durch Pilze - modifiziert werden kann. Levoglucosan wurde während der Inkubationsphase ebenfalls effizient abgebaut. Dieser Aspekt ist zu beachten, wenn diese Substanz als Indikator für PyOM im Boden herangezogen werden soll: Ihre Verwendung kann zu einer Unterschätzung des PyOM-Gehaltes führen, da gealtertes PyOM aufgrund seiner geringen biotischen Persistenz an LG verarmt sein kann. Ein weiterer kritischer Punkt ist die thermische Zersetzung des LG, welche ebenfalls zu einer Fehlinterpretation des PyOM-Anteiles führen dürfte.

Die dritte Studie behandelte den Abbau, die Verlagerung und die Inkorporation des PyOM in verschiedene organische Bodensubstanzfraktionen während eines Mikrokosmos-Experimentes über einen Zeitraum von 28 Monaten. Zu diesem Zweck wurde ^{13}C - und ^{15}N -angereichertes PyOM in Bodensäulen inkubiert. Am Ende des Versuches war die ^{13}C -PyOM-Wiederfindung auf Werte zwischen 62% und 65% gesunken. Die zugehörige ^{15}N -Wiederfindung folgte demselben Trend, tendierte aber zu höheren Werten. Nach einer Inkubationszeit von zwei Monaten wurde der Hauptanteil des PyOM in der partikulären organischen Substanz (POM) gefunden. Nach Abschluss des Versuches waren die betreffenden Wiederfindungen in der POM-Fraktion halbiert. Bereits nach einem Monat konnte PyOM in der POM-freien organo-mineralischen Fraktion nachgewiesen werden. Diese rasche Assoziation des PyOM mit der mineralischen Phase zeigt auf, dass auch physikalische Bodeneigenschaften (z.B. Textur) für die Abschätzung der PyOM-Stabilität im Boden zu beachten sind. Eine Zugabe von „frischem“, nicht isotopisch markiertem Gras als Co-Substrat resultierte in vergleichbaren Trends wie für das alleinig inkubierte PyOM. Jedoch konnte eine deutliche Steigerung des PyOM-Eintrages in die mineralische Phase ermittelt werden. Der Hauptanteil des mineralisch assoziierten PyOM war der Tonfraktion

zuzuordnen. Das PyOM mit dem höheren Verkohlungsgrad (4M) erzielte unter Co-Substratzugabe den höchsten Assoziationsgrad von PyOM mit der mineralischen Substanz. Es konnte ebenfalls gezeigt werden, dass PyOM in die unteren Bodenschichten der Bodensäulen verlagert wurde.

Zusammenfassend konnte mit diesem Experiment auch über einen längeren Zeitraum der kontinuierliche Abbau des PyOM bestätigt werden. Die Bereitstellung eines leicht zugänglichen Co-Substrates förderte die partielle Oxidation des PyOM und folglich seine Bindungsfähigkeit an mineralische Oberflächen. Die Mineralisationsraten wurden jedoch nicht gesteigert. Der Nachweis der ^{13}C - und ^{15}N -PyOM-Markierung in verschiedenen Tiefen der Bodensäulen weist auf eine potentielle Verlagerung des PyOM von der Bodenoberfläche durch Mobilisation und Verlagerung in untere Bodenhorizonte hin.

Eine andere Studie befasste sich mit den strukturellen molekularen Modifikationen während des PyOM-Abbaus im Boden. Zu diesem Zweck wurden Festkörper- ^{13}C und ^{15}N -CPMAS-NMR-Studien durchgeführt mit dem Ziel, Humifizierungsprozesse des PyOM zu quantifizieren. Die chemische Zusammensetzung des verbleibenden inkubierten PyOM unterschied sich deutlich von der des Ausgangsmaterials. Der Anteil an O-enthaltenden funktionalen Gruppen nahm zu, wogegen Aromaten bzw. N-heterozyklische Strukturen eine quantitative Abreicherung, bedingt durch Mineralisation und Umwandlung in andere C- und N-Gruppen, aufwiesen. Der beobachtete Abbau von aromatischen Verbindungen könnte in zwei simultan ablaufende Prozesse unterteilt werden: (1) der kompletten Mineralisation zu CO_2 und (2) der Umwandlung in andere Kohlenstoffgruppen. Die Relevanz des letzten Punktes ist durch die Tatsache gestützt, dass der Anteil von O-substituierten aromatischen Strukturen nicht oder nur wenig abnimmt - im Gegensatz zu dem beträchtlichen Verlust an Gesamtkohlenstoff sowie an aromatischen Verbindungen. Der festgestellte Alterungsprozess des PyOM bildet die Grundlage für einen fortschreitenden biotischen Abbau, aber auch für Adsorptionsprozesse an mineralische Oberflächen. Die Studie präsentiert direkte Hinweise für einen Abbau N-heterozyklischer Verbindungen in verkohltem Pflanzenmaterial, welche neue Aspekte im Hinblick auf den N-Kreislauf in feuerbeeinflussten Ökosystemen bieten.

Die durchgeführten Arbeiten zeigen, dass sich die untersuchten Abbau-, Stabilisierungs- und Verlagerungsmechanismen gegenseitig beeinflussen. Erst wenn diese Prozesse als Gesamtheit betrachtet werden, ist eine realistische Bewertung des Sequestrierungspotentials von verkohlten Pflanzenresten in Böden möglich. Es wurde

gezeigt, dass PyOM in gleicher Weise wie andere Fraktionen der organischen Bodensubstanz in den C- und N-Kreislauf eingebunden ist. Die Ansicht, dass die Präservierung von PyOM im Boden durch eine chemische Rekalzitranz begründet ist, sollte nicht länger akzeptiert werden. Im Hinblick auf den Klimawandel kann PyOM nicht als potentielle Kohlenstoffsенke zur langfristigen Reduzierung des CO₂-Anteiles in der Atmosphäre angesehen werden.

TABLE OF CONTENTS

SUMMARY	III
ZUSAMMENFASSUNG	VII
TABLE OF CONTENTS	XII
LIST OF FIGURES	XV
LIST OF TABLES	XVII
GLOSSARY	XIX

1. INTRODUCTION, OBJECTIVES AND STATE OF THE ART

1.1 General introduction	1
1.2 Objectives and state of the art.....	3
1.3 Techniques for PyOM quantification in soils and sediments	8
1.4 Solid-state ¹³ C and ¹⁵ N CPMAS NMR spectroscopy - a powerful tool for characterisation and quantification of PyOM	12
1.4.1 Basic NMR theory.....	12
1.4.2 Reliability and application of solid-state ¹³ C and ¹⁵ N CPMAS NMR spectroscopy in PyOM research.....	15

2. MATERIALS AND METHODS

2.1 Production of PyOM.....	21
2.2 Characterisation of PyOM and soil material.....	22
2.2.1 C / N content and ¹³ C / ¹⁵ N isotopic signature	22
2.2.2 Basic soil parameters.....	23
2.2.3 Specific surface area of PyOM.....	23
2.3 Setup of PyOM respiration experiment	23
2.4 Setup of ¹³ C and ¹⁵ N labelled PyOM incubation	25
2.5 Lipid analyses	27
2.6 Fractionation	27
2.6.1 DOM extraction.....	28
2.6.2 Density fractionation	28

2.6.3 Particle size fractionation	28
2.7 Solid-state ^{13}C and ^{15}N CPMAS NMR spectroscopy	29
2.7.1 HF pre-treatment	29
2.7.2 Solid-state ^{13}C CPMAS NMR spectroscopy	30
2.7.3 Solid-state ^{15}N CPMAS NMR spectroscopy	31
2.8 Quantification of C and N groups of incubated PyOM	31
2.9 Statistical analysis and data fitting	32
3. MINERALISATION AND STRUCTURAL CHANGES DURING THE INITIAL PHASE OF MICROBIAL DEGRADATION OF PYROGENIC PLANT RESIDUES IN SOIL	
3.1 Chemical changes in the plant materials during the thermal treatment	33
3.2 PyOM mineralisation during incubation	38
3.3 Impact of co-substrate addition on char mineralisation	40
3.4 Changes of the chemical quality of PyOM during incubation	41
3.5 Influence of co-substrate addition on degradation level	45
3.6 Implication of structural properties on the degradation of PyOM in soil	47
3.7 Role of the priming effect for char degradation	48
3.8 Elucidation of residence times	49
4. MODIFICATION OF PLANT BIOMARKERS BY CHARRING AND DURING THE INITIAL PHASE OF BIODEGRADATION OF PYROGENIC ORGANIC MATTER IN SOIL	
4.1 Influence of charring on lipid content	51
4.2 n-Alkanes pattern of the fresh and incubated PyOM	51
4.3 Free fatty acid pattern of the fresh and incubated PyOM	57
4.4 Degradation of biomarkers for plant source material and biomass burning	59
5. DEGRADATION OF ^{13}C AND ^{15}N LABELLED GRASS-DERIVED PYOM, TRANSPORT OF THE RESIDUES WITHIN A SOIL COLUMN AND DISTRIBUTION IN SOIL ORGANIC MATTER FRACTIONS DURING A MICROCOSM EXPERIMENT	
5.1 Characterisation of isotopically labelled grass material during thermal treatment	62
5.2 Reproducibility of PyOM recovery	67
5.3 Recovery of ^{13}C and ^{15}N labelled PyOM in soil column	70
5.4 Relocation of PyOM in soil column	71

5.5 ^{13}C and ^{15}N PyOM partitioning in soil fractions of the A layer	73
5.5.1 DOM fraction	73
3.5.2 POM fraction.....	76
5.5.3 PyOM interactions with mineral surfaces	77
5.5.4 Particle size fractions	79
5.6 Elucidation of residence time	82
6. CARBON AND NITROGEN DEGRADATION ON MOLECULAR SCALE OF GRASS- DERIVED PYROGENIC ORGANIC MATERIAL DURING INCUBATION IN SOIL	
6.1 Efficiency of HF treatment of PyOM-enriched mineral fractions on NMR sensitivity	85
6.2 Reproducibility of C group recovery	87
6.3 C-group distribution of incubated PyOM	88
6.4 Degradation of PyOM-derived C.....	90
6.5 Chemical structure of leached PyOM.....	95
6.6 Turnover of pyrogenic N	96
6.7 Is black nitrogen a recalcitrant N pool?	98
6.8 Structural alteration of PyOM by degradation.....	99
6.9 Stability of PyOM and environmental implications	99
7. CONCLUSIONS AND OUTLOOK.....	101
8. REFERENCES	104
9. DANKSAGUNG	126
<i>CURRICULUM VITAE</i>	129
PUBLICATIONS	132

LIST OF FIGURES

Figure 1: Combustion continuum for PyOM	1
Figure 2: Pools and fluxes of PyOM.....	2
Figure 3: Overview about uncertainty of biogeochemical PyOM fates in soil	3
Figure 4: Overview of quantification methods within the PyOM continuum.....	9
Figure 5: Selected examples for chemical shift assignment in solid-state ^{13}C CP MAS NMR	14
Figure 6: Selected examples for chemical shift assignment in solid-state ^{15}N CP MAS NMR	15
Figure 7: Cultivation of isotopically enriched rye grass	22
Figure 8: Setup of PyOM respiration experiment	25
Figure 9: Setup of ^{13}C and ^{15}N PyOM incubation experiment	26
Figure 10: Schematic of conducted fractionation.....	29
Figure 11: Solid-state ^{13}C and ^{15}N NMR spectra of rye grass and ^{13}C NMR spectra of pine wood as a function of oxidation time at 350°C	35
Figure 12: Cumulative $\text{CO}_2\text{-C}$ release of PyOM produced from rye grass and pine wood without and with co-substrate addition.....	39
Figure 13: Changes in respiration rates of grass-derived PyOM during the very early phase of incubation.....	40
Figure 14: Solid-state ^{13}C NMR spectra of incubated PyOM without and with co-substrate addition in comparison to fresh PyOM	43
Figure 15: Abundances of n-alkanes from rye grass and pine wood and the respective fresh and incubated PyOM.....	55
Figure 16: Abundances of fatty acids from rye grass and pine wood and the respective fresh and incubated PyOM.....	59
Figure 17: Solid-state ^{13}C and ^{15}N NMR spectra of isotopically enriched fresh rye grass and charred residues produced under oxic conditions for 1 and 4 min at 350°C	65
Figure 18: Recovery of ^{13}C and ^{15}N labelled PyOM in the soil layers as a function of incubation time.....	72
Figure 19: Temporal development of recovery of ^{13}C and ^{15}N labelled PyOM in different SOM fractions of the A layer vs. incubation time	75

Figure 20: C/N and $^{13}\text{C}/^{15}\text{N}$ ratios of DOM fraction of the A layer	76
Figure 21: Influence of charring degree on association of ^{13}C and ^{15}N enriched PyOM with the mineral phase.	78
Figure 22: Influence of co-substrate addition on association of ^{13}C and ^{15}N enriched PyOM with the mineral phase	79
Figure 23: Solid-state ^{13}C NMR spectra of HF-treated and untreated mineral-associated PyOM... ..	87
Figure 24: Time course of the relative distribution and total recovery of the different PyOM C groups during the 28 months of incubation.....	89
Figure 25: Solid-state ^{13}C NMR spectra of the vertical down moved PyOM fraction for the last 8 months of incubation.....	96
Figure 26: Time course of the relative distribution and total recovery of the different PyOM N groups for the A layer during the 28 months of incubation	97
Figure 27: Solid-state ^{15}N NMR spectra of the vertical relocated PyOM leachate fraction after 28 months of incubation.....	98

LIST OF TABLES

Table 1: Gravimetric elemental concentration, specific surface area, micropore surface area and volume associated with heating of rye grass and pine wood at 350°C under oxic conditions.....	34
Table 2: Relative intensity distribution in solid-state ¹³ C NMR associated with heating of rye grass and pine wood at 350°C under oxic conditions.	36
Table 3: Relative intensity distribution in solid-state ¹⁵ N NMR associated with heating of rye grass at 350°C under oxic conditions.....	37
Table 4: Relative intensity distribution in solid-state ¹³ C NMR for PyOM produced from rye grass and pine wood after 7 weeks of incubation.	44
Table 5: Changes in abundances of the different types of C for PyOM produced from rye grass and pine wood after 7 weeks of incubation.	44
Table 6: Degradation of co-substrate during incubation.	46
Table 7: Relative intensity distribution in the solid-state ¹³ C NMR and the total contribution of PyOM water extracts	46
Table 8: Abundance and molecular ratios for n-alkanes and fatty acids of the fresh and charred plant materials.....	54
Table 9: Abundance and molecular ratios for n-alkanes and fatty acids of the incubated PyOM ...	56
Table 10: Specific biomarker abundances of fresh and charred plant materials and respective recovery from the incubated PyOM.....	60
Table 11: Elemental and isotopic composition of fresh and burnt rye grass and isotopic losses during charring at 350°C under oxic conditions.....	64
Table 12: Intensity distribution of solid-state ¹³ C and ¹⁵ N NMR spectra of fresh rye grass and its residue (PyOM) charred at 350°C under oxic conditions.	66
Table 13: Reproducibility of recovery of ¹³ C and ¹⁵ N from isotopically enriched PyOM from 2 month incubated samples.....	69
Table 14: Recovery of ¹³ C and ¹⁵ N from isotopically enriched PyOM in size fractions of A layers of the soil microcosms after 28 months incubation.....	81
Table 15: Estimation of decomposition kinetics of PyOM fitted to a two-component decay model	83

Table 16: Elemental composition and isotopic ^{13}C and ^{15}N contents before and after HF treatment of the mineral fraction with C and N-enrichment factors E_{C} and E_{N}	86
Table 17: Reproducibility of the intensity distribution and the total recovery for PyOM C groups after 2 months of incubation	88
Table 18: Decomposition kinetics for the different C groups of fresh rye grass and PyOM revealed by fitting with a first order decay model.....	92
Table 19: Correlation coefficients between total recoveries of PyOM C groups during 28 months of incubation	93

GLOSSARY

1M	Charring time of 1 min
4M	Charring time of 4 min
ACL	Average chain length
B ₀	Magnetisation vector
BC	Black carbon
BD	Bloch decay
BN	Black nitrogen
BV	Blank value
C	Carbon
C _{tot}	Total carbon
CPI	Carbon preference index
CP	Cross polarisation
CS	Co-substrate addition
DB	Distribution
DD	Dipolar dephasing
DOC	Dissolved organic carbon
DOM	Dissolved organic matter
DP	Direct polarisation
E _C	Enrichment factor of carbon
E _N	Enrichment factor of nitrogen
EM	Electromagnetic radio frequency pulse
EOP	Even to odd predominance
FA	Fatty acid
FAME	Fatty acid methyl ester
GC-MS	Gas chromatography mass spectroscopy
Gr0M	Rye grass (<i>Lolium perenne</i>)
Gr1M	Rye grass charred for 1 min
Gr4M	Rye grass charred for 4 min
H	Proton
HF	Hydrofluoric acid
LG	Levoglucosan
MAS	Magic angle spinning

m/z	Mass to charge ratio
N	Nitrogen
NIST	National Institute of Standards and Technology
NMR	Nuclear magnetic resonance spectroscopy
O	Oxygen
OC	Organic carbon
OEP	Odd to even predominance
OM	Organic matter
p	Error probability
POM	Pine wood (<i>Pinus sylvestris</i>)
P1M	Pine wood charred for 1 min
P4M	Pine wood charred for 4 min
POM	Particulate organic matter
PyOM	Pyrogenic organic material
Q	Relative recovery
R ²	Coefficient of determination
RC	Recovery
R _{s/l}	Ratio of short and long carbon chains
SD	Standard deviation
SIM	Single ion monitoring
SOC	Soil organic carbon
SOM	Soil organic matter
SSB	Spinning side band
t _{1/2}	Half-time period
T _{1C}	Spin-lattice relaxation time of ¹³ C
T _{1H}	Spin-lattice relaxation time of ¹ H
t _c	Contact time
T _{CH}	Polarisation transfer time
TIC	Total ion currency
WHC	Water holding capacity
WRB	World Reference Base for soil resources

1. Introduction, objectives and state of the art

1.1 General introduction

Vegetation fires do not only convert large amounts of biomass to CO₂, they produce also pyrogenic organic material (PyOM), which occurs ubiquitously in soils and sediments. The annual natural production of this material, also known as black carbon (BC), was calculated to range between 4×10^{13} g and 24×10^{13} g (Kuhlbusch and Crutzen, 1995). Its formation depends on several factors, such as type of fuel, temperature and duration of charring, so its chemical composition and morphology are expected to vary considerably (Fig. 1). It was suggested that PyOM represents a continuum of combustion products ranging from slightly charred biomass, which may be still accessible for microbial degradation, to highly condensed refractory soot (Masiello, 2004).

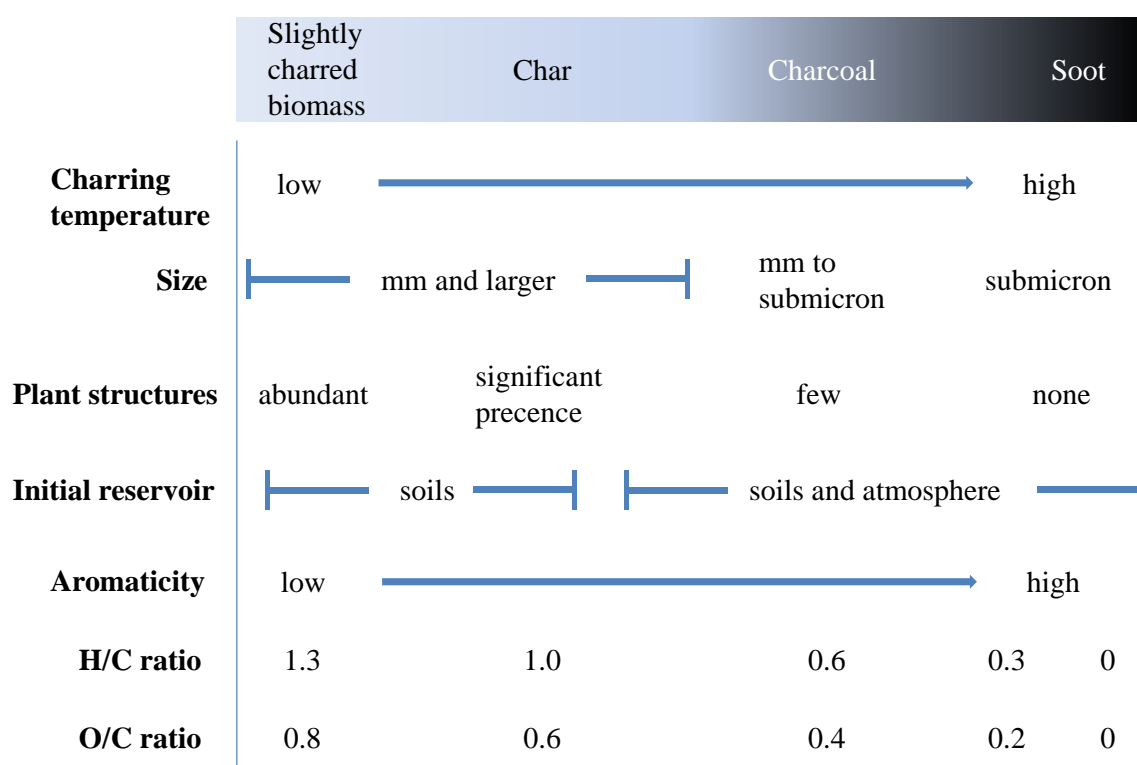


Figure 1: Combustion continuum for PyOM [adapted from Masiello (2004) and Hammes et al. (2007)].

Common char models assume that all PyOM is characterised by fused aromatic rings with varying cluster size (Schmidt and Noack, 2000; Preston and Schmidt, 2006). Due to the refractory nature of such thermally condensed products, they are expected to play an important carbon (C) and nitrogen (N) sink in the global cycle (Fig. 2). Residence times of

thousands of years were calculated based on radiocarbon (^{14}C) dated char in soils (Saldarriaga and West, 1986; Glaser et al., 2001). Its recalcitrance is also supported by its occurrence in deep marine sediments (Middelburg et al., 1999). However, according to Masiello (2004), PyOM and its transformation products should contribute up to 125% of soil organic carbon (SOC), if one assumes that biomass burning since the last glacial maximum occurred at the same rate as now. This strongly indicates that the recalcitrance of PyOM may have been overestimated. The same conclusion was postulated by Kim et al. (2004), who estimated that it would only require $< 80,000$ yrs. to convert the entire pool of actively cycling C to BC, assuming that no degradation occurred.

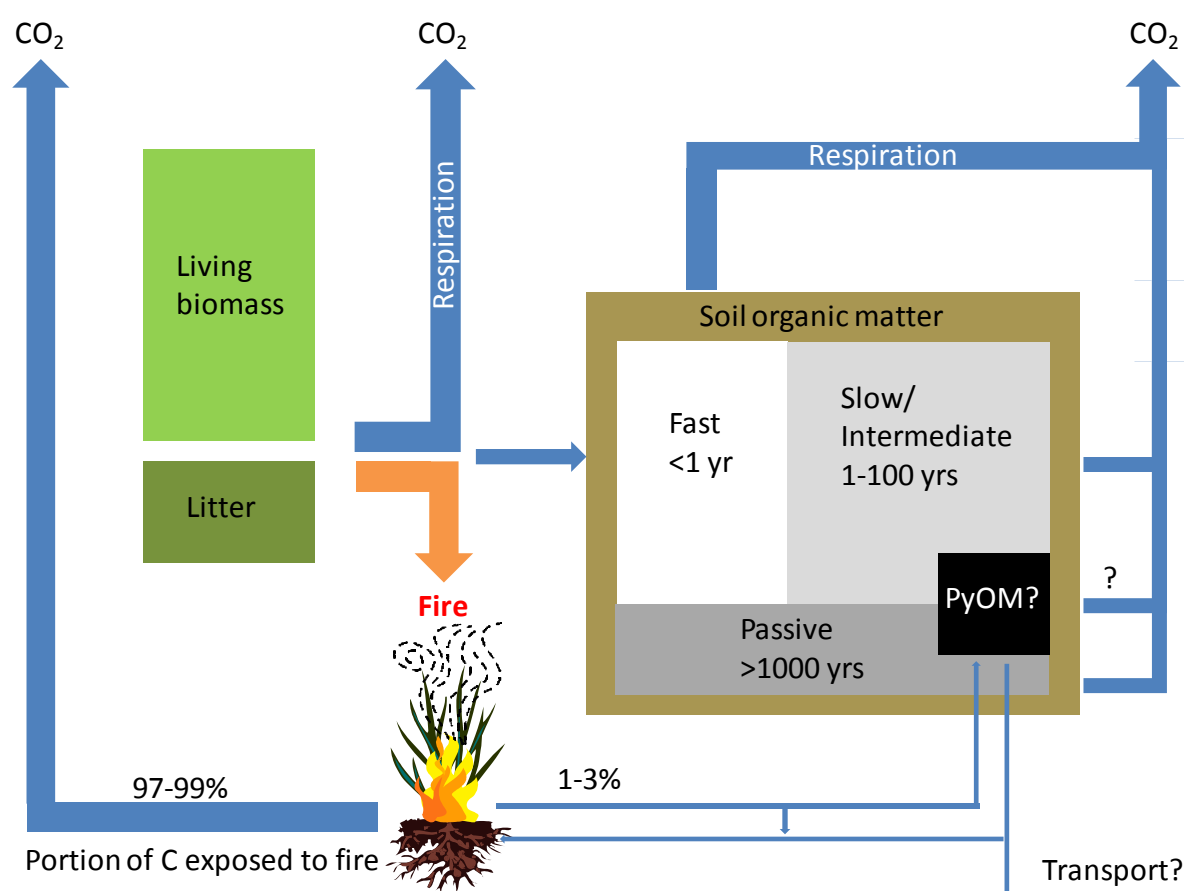


Figure 2: Pools and fluxes of PyOM [adapted from Preston and Schmidt (2006)].

The observation that PyOM may be degraded faster than commonly assumed is underlined by recent field studies of Amazonian dark earth (Solomon et al., 2007), sandy savannah soil at a fire trial site (Bird et al., 1999) and in fire-affected Siberian Scots pine forest soil (Czimczik et al., 2003). One reason may be that a description of PyOM formed by vegetation fires as a polycondensed aromatic network may be oversimplified, as recently demonstrated by the analysis of the chemical structure of model chars derived

from biopolymers and plant residues (Knicker et al., 2008). The latter rather supports an alternative concept which assumes PyOM to be a heterogeneous mixture of thermally altered biopolymers with aromatic domains of relatively small cluster size, but considerable substitution with N, O and S functional groups (Knicker, 2007). Such a structure would allow fast oxidation, facilitating further microbial attack and dissolution in the soil solution.

1.2 Objectives and state of the art

The present work focuses on the biochemical degradation potential and humification of PyOM in soil. The main investigation intentions are illustrated in Figure 3.

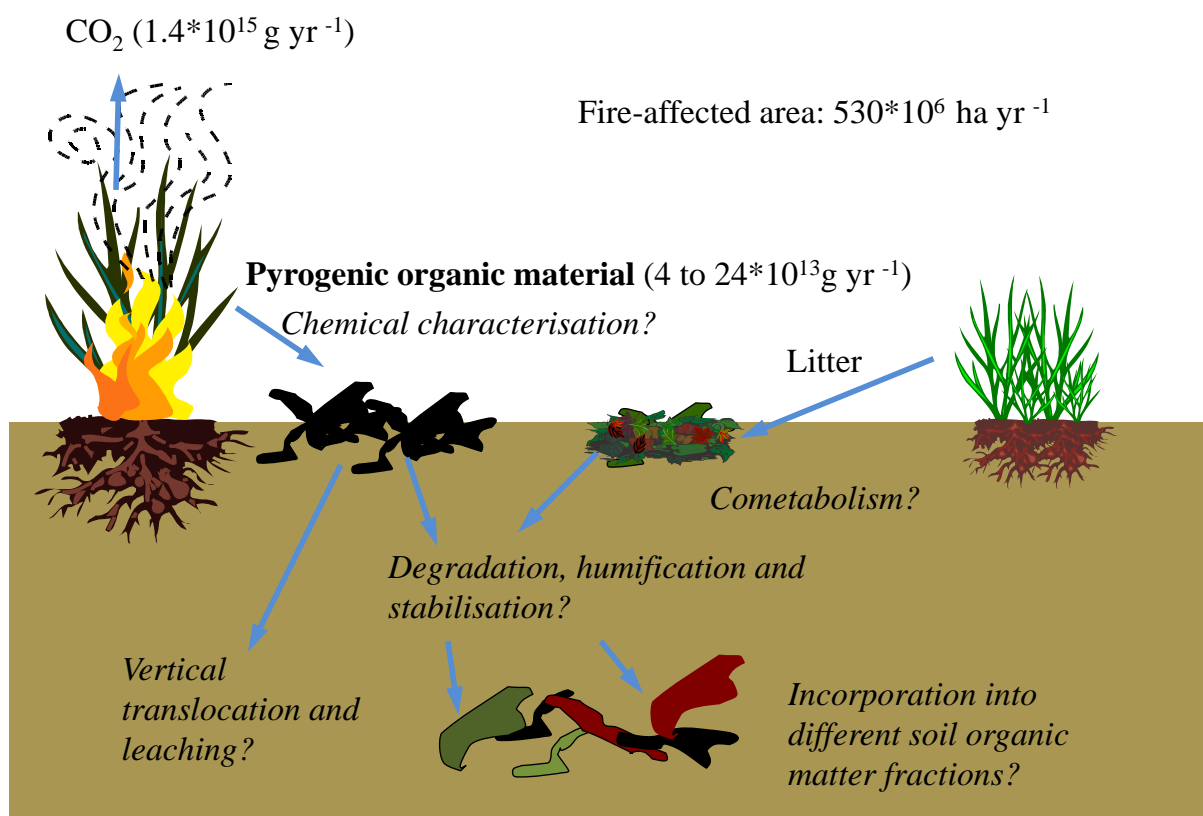


Figure 3: Overview about uncertainty of biogeochemical PyOM fates in soil [adapted from Knicker (2007)]. Numbers derive from Kuhlbusch and Crutzen (1995).

Research topic I: Study of the impact of plant source material and charring intensity on the initial PyOM degradation (Chapter 3).

For elucidation of the recalcitrance of PyOM in soil, not only knowledge of its chemical structure is required but also understanding of its degradation and humification mechanism. One of the first pioneers was Potter (1908), who showed that wood charcoal was partly mineralised after 20 days incubation at temperatures between 20°C and 40°C. In addition, Shneour (1966) demonstrated the degradability of BC by reporting that, after 96 days of incubation, 2% of graphitic C were mineralised. Cheng et al. (2006) postulated that abiotic chemisorption of oxygen were more important for oxidation of BC than biotic processes during a 30-day incubation experiment at 30°C and 70°C. However, Hamer et al. (2004) found a close correlation between glucose addition and additional BC mineralisation during biotic incubation for model chars, which could suggest a co-metabolic degradation pattern. One must bear in mind that in natural environments possible co-substrates are fire-unaffected litter from dying trees or regrowing vegetation, which have a more complex matrix than pure glucose. Therefore, the mechanisms of the priming effect may be more complex than commonly considered (Fontaine et al., 2003). For that reason, the present study quantifies the PyOM mineralisation with and without co-substrate availability to reveal aspects concerning the biochemical PyOM stability in the initial post fire phase.

Research topic II: Modification of plant biomarkers by charring and its biodegradability during the initial PyOM degradation (Chapter 4).

Wildfires convert not only large amounts of biomass to CO₂, but they also thermally alter the C pools of soils. According to a recently suggested concept, this pool consists of the combustion residues of different biomacromolecules whose chemical structure depends upon the charring conditions (Knicker et al., 2008a). Beside of charred carbohydrates, peptides and lignin residues, thermally-altered lipids can represent an important fraction of this pyrogenic organic matter (González-Vila et al., 2001).

Compared to other plant components such as cellulose or lignins, lipids are less abundant. Lipids enter the soil with the litter where they are altered or re-synthesised by microbes. In certain environment, they are more resistant against degradation than other biomolecules. Within the lipid fraction, n-alkanes and aromatic hydrocarbons are less efficiently biodegraded than medium chain fatty acids and alcohols (Tu et al., 2001; Wiesenberg et al., 2004).

Wiesenberg et al. (2009) demonstrated for charred grass materials that biomass burning causes changes of lipid pattern. The authors reported that charring at 500°C resulted in a pronounced n-alkane chain length shift to short chain homologues, maximising at C₁₈, dominated by even numbered homologues. In this context, Almendros et al. (1988) and Tinoco et al. (2006) suggests that such thermally altered lipids can be incorporated as constituents of the soil lipid fraction of fire-affected Mediterranean soils under pine. Until now, however, knowledge is missing how decomposition of PyOM affects the nature of thermally altered lipid fractions in soil.

Wiesenberg et al. (2009) pointed out that the composition of aliphatic and aromatic hydrocarbons of fire-affected recent and fossil soils offers specific fingerprint indicators for diagnosis of vegetation burning and burning conditions. Eckmeier and Wiesenberg (2009) analysed lipids from buried ancient topsoils that contained charred organic matter. The authors associated the found particular pattern of short-chain and even carbon numbered n-alkanes with a maximum at C₁₆ or C₁₈ to the occurrence of charred biomass. However, studies are lacking about the fate of such PyOM-derived lipids during humification. The latter, however, is needed, if one intends to apply the findings from laboratory heating experiments to natural soils and sediments.

Lignin is the most abundant polymeric aromatic organic substance in the plants. For example, the content of lignin ranges from 20-40% in wood. Sharma et al. (2004) and Knicker et al. (2008a) demonstrated that the lignin backbone is a major constituent of plant chars. Therefore, it is of interest if biomarkers for lignin detection (e.g. vanillin) will be affected by the charring process and the incubation in soil.

Levoglucosan (1,6-Anhydro-β-1D-glucopyranose; LG), the major tracer from the thermal decomposition of cellulose (Lakshman and Hoelsche, 1970), is a further significant indicator for biomass burning. Levoglucosan is frequently used as atmospheric tracer for detection of forest fires (Simoneit et al., 1999). Recently LG served as tracer for

contributions from vegetation combustion to soils (Otto et al., 2006; Kuo et al., 2008) and sediments (Elias et al., 2001). Elias et al. (2001) reported a correlation between LG and the counted charcoal particles for a sediment core from a lake in Carajas (Southeastern Amazonia). In this context Kuo et al. (2008) examined systematically the LG levels of charcoal produced from tree plant materials under controlled combustion conditions (150-1050°C, 0.5-5 h). The authors reported large differences of LG yield in the char across the plant species and the charring temperature. They concluded that it is difficult to use LG as a quantitative biomarker for char characterisation in environmental media. Studies are needed dealing with environmental stability of LG to clarify the application of LG as an indicator for contribution of charred biomass in soils.

In general, the identification and application of specific biomarkers for detection of char in soils and sediments is mostly based on studies using freshly produced charred plant materials (e.g. (Wiesenberg et al., 2009)). However, the assumption that char is slowly degraded and the biomarkers could be preserved for a long-term period may be oversimplified. Studies dealing with a systematic investigation of possible modification and degradation of PyOM-derived biomarkers are lacking.

Research topic III: Quantification of PyOM incorporation into different SOM fractions and vertical PyOM translocation through a soil column (Chapter 5).

Little is known about incorporation mechanisms and quantity of PyOM incorporated into soil fractions. Many questions arose with respect to the processes that caused transformation and mobilisation of PyOM in soils. One is related to the organic N incorporated into the PyOM structure. During fire events, the organic N pool is converted into more recalcitrant N forms (Sanchez and Lazzari, 1999; Knicker et al., 2005b). Since the labile N reserves are the major N source for biomass production by soil microorganisms and plants, the fire does not only affect the C cycle but also the N cycle (Gärdenäs et al., 2011). However, studies dealing with “black nitrogen” decomposition and contribution dynamics are lacking, although this knowledge is required for estimates of long-term impact of fires on ecosystems.

A further question that needs to be approached concerns the turnover of PyOM and how it is affected by interaction with the mineral phase. According to Skjemstad et al. (1996) and Kuzyakov et al. (2009), charred residues are found primarily in the <math><53\ \mu\text{m}</math> soil fractions, within other authors have reported an accumulation of aromatic structures (Baldock et al., 1992; Rodionov et al., 2006). The results confirm that the analysis of the fine size fraction in particular is required for understanding the role of the mineral phase in PyOM preservation. For example, how the PyOM distribution among size fractions is influenced by the charring degree is unknown.

A further fraction of interest with respect to PyOM stability is the water-soluble extract. According to Hockaday et al. (2007), it is composed mainly of condensed aromatic ring structures that are also present in soil pore, river and ground water samples. The dissolution and export of this water-soluble PyOM fraction is still an unmeasured C and N flux.

Research topic IV: Biochemical alteration of PyOM in soil on a medium-term scale (Chapter 6).

We still lack knowledge about the degradation and humification processes and the stability of different PyOM structures, which is required for understanding the C sequestration potential. In particular, knowledge concerning the chemical structure of PyOM is also important for the establishment of more accurate PyOM quantification methods because common degradative techniques based on the chemical recalcitrance of polycondensed aryl structures (Hammes et al., 2007; Knicker et al., 2008a) are characterised by low specificity. Chemical modification of these aryl domains during the degradation process may decrease their chemical recalcitrance and thus may be responsible for an underestimation of the PyOM content assessed by traditional methods.

Recent studies (Covington and Sackett, 1992; Prieto-Fernandez et al., 2004) reported an increase of inorganic N immediately after fire. During the post-fire phase, this inorganic N can be rapidly lost by erosion due to the missing of a plant cover and/or leakage with seepage water. A considerable part of the remaining fire-affected organic N was shown to occur in heterocyclic N structures derived from heat-transformed proteins (Knicker et al.,

1996b; Almendros et al., 2003; Knicker et al., 2008a). On the other hand, this “black nitrogen” (Knicker, 2007) is probably characterised by an increased resistance to biological degradation, leading to a preferential accumulation of heterocyclic N compounds in fire-affected soils. A recent study indicated a low chemical stability of the N fraction in char against acid digestion with potassium dichromate (Knicker, 2010). To which extent this may also be true for biochemical stability is still not known. At the moment are no studies available in which degradation and humification processes of black N have been addressed. The biochemical degradation of PyOM-derived N compounds was investigated in the present part of the work.

A further aspect, which presently receives much attention, is the amendment of so-called biochar to incorporate additional photosynthetically fixed carbon into the soil. The presence of such char in soil could contribute to a long-term C storage and thus to the mitigation of increasing atmospheric CO₂ concentrations (Lehmann, 2007). The extent of a C sequestration effect on a long-term scale as well as the influence of biochar addition on the quality of soil organic matter (SOM) is still not clear.

1.3 Techniques for PyOM quantification in soils and sediments

A number of techniques have been developed to determine PyOM in soils and sediments (Schmidt et al., 2001; Nguyen et al., 2004; Hammes et al., 2007; Bird and Ascough, 2010). In general, the PyOM identification can be divided into spectroscopic (Rositani et al., 1987; Kim et al., 2004; Knicker et al., 2005a; Lehmann et al., 2005), visual/microscopic (Kruge et al., 1994; Brodowski et al., 2005a), thermal (Gustafsson et al., 1997; Dell'Abate et al., 2000; Dell'Abate et al., 2003), chemical (Wolbach and Anders, 1989; Song et al., 2002; Simpson and Hatcher, 2004; Knicker et al., 2008b) and UV photo-oxidizing (Skjemstad et al., 1996; Skjemstad et al., 1999) methods. Different molecular markers were also applied for the identification of PyOM (Glaser et al., 1998; Brodowski et al., 2005b; Otto et al., 2006; Wiesenberg et al., 2009). All methods basically have to differentiate between three forms of carbon, inorganic carbonates, thermally unaltered organic carbon, such as humic substances or plant material, and PyOM. It is important to note that most of the techniques can only be applied to a part of the PyOM continuum (Fig. 4). This fact makes it difficult to compare results obtained with different quantification techniques (Masiello, 2004).

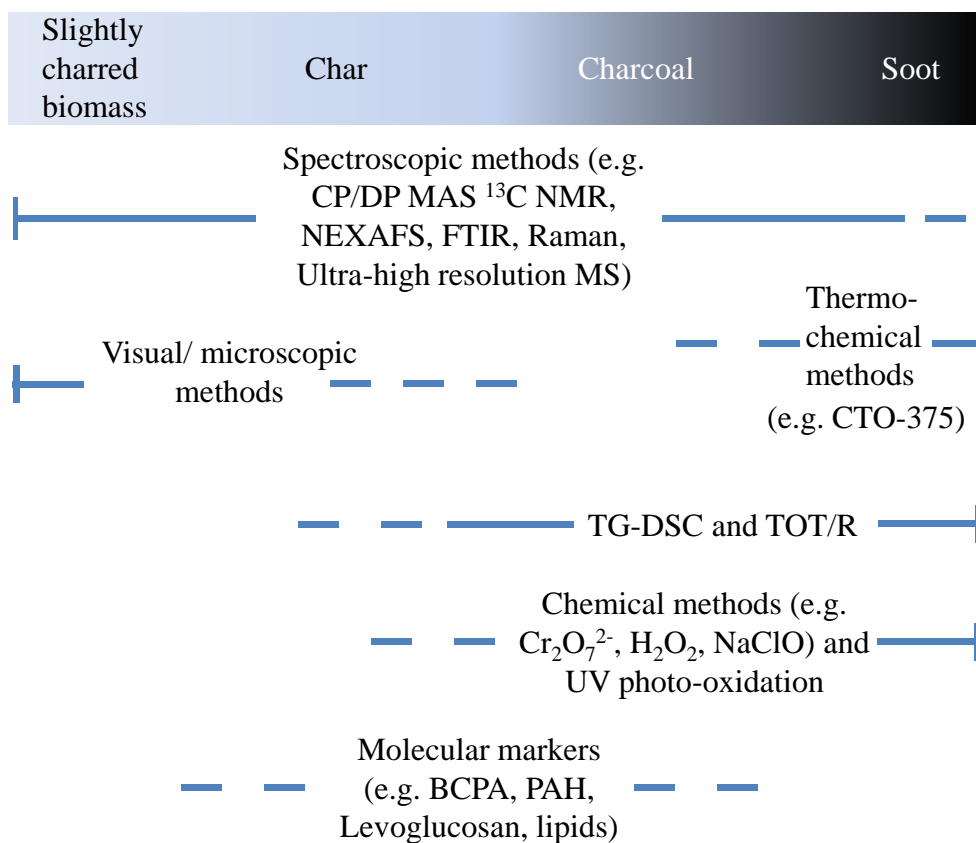


Figure 4: Overview of quantification methods within the PyOM continuum [summarised from Hedges et al. (2000); Schmidt and Noack (2000); Masiello (2004); Lehmann et al. (2005); Hammes et al. (2007); Plante et al. (2009); Bird and Ascough (2010)] CP/DP MAS ^{13}C NMR Solid-state cross polarisation/ direct polarisation magic angle spinning ^{13}C nuclear magnetic resonance spectroscopy; NEXAFS Near edge X-ray absorption fine structure spectroscopy; FTIR Fourier transformation infrared spectroscopy; MS Mass spectroscopy; CTO-375 Chemo-thermal oxidation at 375°C ; TG-DSC Thermogravimetry and differential scanning calorimetry analysis; TOT/R Thermal/optical transmittance and reflectance; $\text{Cr}_2\text{O}_7^{2-}$ Acid dichromate oxidation; H_2O_2 Peroxide Oxidation; NaClO Sodium hypochlorite oxidation; BCPA Benzene polycarboxylic acids; PAH Polycyclic aromatic hydrocarbons.

Visual methods quantify the number of char pieces visible under an optical microscope. However, this procedure detects only relative large PyOM particles and cannot capture soot or PyOM degradation products. Further, the presence of pyrite and other dark-colour debris makes it difficult to quantify PyOM (Schmidt and Noack, 2000). Optical methods provide morphological description of PyOM particles, which can give information on sources and transport distances. Scanning electron microscopy coupled with energy-dispersive X-ray spectroscopy (SEM/EDX) provides additional information

about the elemental composition of the scanned particles (Brodowski et al., 2005a). However, the resolution is too fine for practical use in quantification (Nguyen et al., 2004).

Thermo-chemical methods oxidise or volatilise labile carbon and leave a resistant residue for quantification as PyOM (Gustafsson et al., 2001). Such methods were developed for atmospheric PyOM particles such as soot and are not directly applicable to soils and sediments. Soils can contain closely associated organic matter that is not easy to thermally degrade and the formation of artefacts by charring of non-PyOM is also possible (Schmidt and Noack, 2000). Thermogravimetry and differential scanning calorimetry analysis (TG-DSC) determine carbon species by recording the mass loss during the thermal oxidation of the sample. The initial weight loss based upon the exothermic oxidation of labile carbon such as carbohydrates (300°C to 350°C). The exothermic loss at higher temperatures (above 450°C) is attributed to more refractory SOM and PyOM-derived carbon species (De la Rosa et al., 2008; Plante et al., 2009). The position of the DSC peaks reflect the chemical composition of the sample. The disadvantages of this method are mineral impurities such as clays which will contribute to measured weight loss as they lose water on heating. The occurrence of non-PyOM with high C content like coal may overestimate PyOM contribution (Hammes et al., 2007).

Chemical oxidation techniques (e.g. acid oxidation with dichromate) separate labile organic matter from condensed PyOM assuming that the oxidation process follows a first-order kinetic (Wolbach and Anders, 1989). These techniques often involve removal of carbonates and silicates as a pre-treatment step. The studies of Knicker et al. (2007) and Knicker et al. (2008b) indicate that aromatic PyOM structures can also be attacked and paraffinic compounds can survive the procedure because of their hydrophobic character which obscures quantification. Therefore, such chemical methods should be combined with analytical techniques for characterising the chemical composition of the oxidation residue. The chemical oxidation efficiency varies due to the chemical heterogeneity of PyOM. Therefore it is necessary to determine a correction factor for the respective char material to ensure realistic quantification (Knicker et al., 2008b).

UV photo-oxidation (Skjemstad et al., 1993) relies on the relative stability of PyOM to high-energy UV radiation compared to other SOM fractions. This method seems to be more gently in comparison with chemical oxidation approaches (Hammes et al., 2007) resulting in higher PyOM values for soot and chars. Another critical point is that UV radiation affects only the surface of soil aggregates. Skjemstad et al. (1993) demonstrated

that a considerable proportion of SOM of clay and silt fractions of Australian soils was not affected by this method. Some SOM was protected in the interior of microaggregates. This fact may result in overestimation of PyOM content if no further techniques are used, which allow a more detailed characterisation of the residue.

The benzene polycarboxylic acids (BPCA) method converts aromatic structures via oxidation with HNO_3 into BPCAs (Glaser et al., 1998). The PyOM quantity is calculated as the sum of the threefold to sixfold carboxylated benzoic acids. However, this technique does not quantitatively detect very large and highly condensed PyOM components. Therefore, the results are multiplied by a correction factor of 2.27 to estimate the PyOM content. The BPCA method provides only a minimum estimation for other types of PyOM (Hammes et al., 2007) because this factor was obtained from commercial charcoal and may not be applicable to all kinds of PyOM. Further, the method has a risk of overestimation by detection of non-BC-derived compounds (Glaser and Knorr, 2008). For example, aspergillin, the black pigment of the fungi *Aspergillus niger* (Lund et al., 1953), was reported to contain aromatic compounds which are detected as BPCA.

There are intentions to use levoglucosan (Elias et al., 2001; Otto et al., 2006), polycyclic aromatic hydrocarbons (PAH) (Kim et al., 2003) or n-alkane distribution pattern (Eckmeier and Wiesenberg, 2009) for determination of PyOM in soils and sediments. Levoglucosan is produced by thermal degradation of cellulose and may indicate the presence of charred plant residues. Charring of plant materials result in domination of even numbered C chains and shortening of the chain length of the alkane fraction (Wiesenberg et al., 2009). Therefore, the alkane distribution pattern may provide information of charring conditions and the presence of PyOM. However, knowledge is missing about stability of such markers against biotic degradation and modification, which may have implications for the accuracy.

Spectroscopic techniques, such as Fourier transformation infrared spectroscopy (FTIR), solid-state cross-polarisation magic angle spinning ^{13}C nuclear magnetic resonance spectroscopy (^{13}C CPMAS NMR) and near edge X-ray absorption fine structure spectroscopy (NEXAFS), provide information on molecular scale, allowing detection of aromatic domains. However, there are not only PyOM-derived aromatic sources. The presence of lignin-derived aromatics (De la Rosa et al., 2009) may result in overestimation of PyOM. Therefore, spectroscopic techniques are often combined with chemical or UV

photo-oxidation pre-treatments, removing non fire-affected labile C compounds. However, ^{13}C NMR and NEXAFS are costly and laboratory capacity is limited.

The present work applies solid-state ^{13}C and ^{15}N CPMAS NMR spectroscopy for the investigation of the degradation and humification of PyOM in soil. Former studies demonstrated that NMR technique provides useful information concerning chemical alteration of plant residues by charring and the chemical structure of PyOM (Knicker et al., 1996a; Freitas et al., 1999; Baldock and Smernik, 2002; Almendros et al., 2003; Knicker et al., 2005a; Knicker et al., 2008a). The studies showed that carbohydrate fraction was converted into dehydrated compounds which produced intense signals in the aromatic region of the ^{13}C CPMAS NMR spectra. The respective ^{15}N CPMAS NMR spectra revealed that amide N was converted to heterocyclic structures such as pyrroles, imidazoles and indoles (Knicker et al., 1996a).

The following chapter provides information about the basic NMR theory and some aspects concerning quantifiability of CPMAS ^{13}C and ^{15}N NMR spectra.

1.4 Solid-state ^{13}C and ^{15}N CPMAS NMR spectroscopy - a powerful tool for characterisation and quantification of PyOM

1.4.1 Basic NMR theory

An advantage of NMR spectroscopy is that it can be used as a non-invasive technique for analysing environmental heterogeneous solid materials (Grassi and Gatti, 1995; Bortiatynski et al., 1996; Preston, 1996; Kögel-Knabner, 1997). In contrast to the described thermo and chemical methods, application of NMR technique avoids possible chemical alteration, such as cracking, rearrangement, dehydrogenation or polymerisation. The NMR spectroscopy allows analysing and quantifying of a sample as a whole without previous extraction, derivatisation or oxidation step. It provides chemical information on atomic and molecular scale and allows examination of physicochemical properties of certain molecular domains (Veeman, 1997). However, there are a few important points to account concerning acquisition parameters and spin interactions for obtaining a representative PyOM characterisation (Knicker et al., 2005a). For better understanding the basics of theory and important NMR techniques will be explained in the following.

NMR bases on the concept that many atomic nuclei behave as magnetic dipoles. The magnitude of the magnetic dipole is proportional to a fundamental property of the atomic

nucleus, the spin angular momentum (Rabi et al., 1938). The spin aligns itself parallel (low energy state) or antiparallel (high energy state) to an external magnet field (B_0). An applied electromagnetic radio frequency pulse (RF) causes the nuclei to absorb energy from the RF pulse if the resonance condition is fulfilled (Bloch et al., 1946). The frequency of RF pulse (ω_1), which is perpendicular orientated to B_0 , has to correspond to the resonance frequency. The resonance condition is described by $\omega_1 = \omega_L = -\gamma \times B_0$ with the Larmor frequency (ω_L) and the gyromagnetic ratio (γ). The magnetic moment (μ) of the nucleus precesses with the Larmor frequency (ω_L) around the z-axis of B_0 in a Cartesian coordinate system. The gyromagnetic ratio is a nuclear constant of each elemental nucleus and represents the ratio of its magnetic dipole moment to its angular momentum. The highlight of the resonance condition is that the adsorbed energy amount equals a multiple of the energy difference (ΔE) between the spin levels. The adsorbed ΔE forces the net magnetisation (M) of the spin system along the z-axis to flip in direction of the y-axis. The magnitude of its y-component (M_y) will periodically alter because the transversal magnetisation is still precessing with ω_L around the z-axis.

The magnetic field of the electron cloud around the nucleus shields the nucleus of interest. Consequently the effective magnetic field (B_{eff}) is reduced, resulting in a shift of the specific resonance frequency (ω_1). A short intense RF pulse is applied for detection of all individual nuclei with different resonance conditions at the same time. Such a short pulse generates a symmetric frequency band around ω_1 . The pulse technique is based on the Heisenberg uncertainty principle $\Delta E \times \Delta t \geq h (2\pi)^{-1}$ where h denotes the Planck's constant.

After termination of the pulse, the spin system returns to its thermal equilibrium by radiating energy at a specific resonance frequency, which depends on the strength of the magnetic field. The relaxation is described by two time constants T_1 and T_2 . The longitudinal (or spin-lattice) relaxation time T_1 is the decay constant for the recovery of the z component of the nuclear spin magnetisation (M_z) towards its thermal equilibrium value. The transverse (or spin-spin) relaxation time T_2 is the decay constant for the component of M which is perpendicular to B_0 (M_{xy}). T_2 is the time frame that is needed for the redistribution of the energy among the spins. A detector in y-direction records the alteration of the magnetisation M_y as a voltage signal. The detected relaxation decay pattern has an oscillating amplitude and is called free induction decay (FID). The

overlapping FIDs of the individual nuclei are converted from the time into frequency domain by the mathematical Fourier transformation (FT).

The location of detected resonance frequency lines is depending from the applied strength of B_0 . Therefore, the resonance frequencies of nuclei are given as chemical shift (δ) with respect to a reference (ω_{Ref}). The chemical shift is defined with δ (ppm) = $(\omega_1 - \omega_{\text{Ref}}) / \omega_{\text{Ref}} \times 10^6$. Commonly tetramethylsilane (TMS; 0 ppm) is used as reference for ^{13}C NMR spectroscopy. For ^{15}N NMR spectroscopy no common reference exists. In the present work nitromethane (0 ppm) is used as reference. The comparison of spectra using different references is only possible by using conversion factors. Figure 5 and 6 show some important chemical shift assignments in solid-state ^{13}C and ^{15}N NMR spectroscopy, respectively.

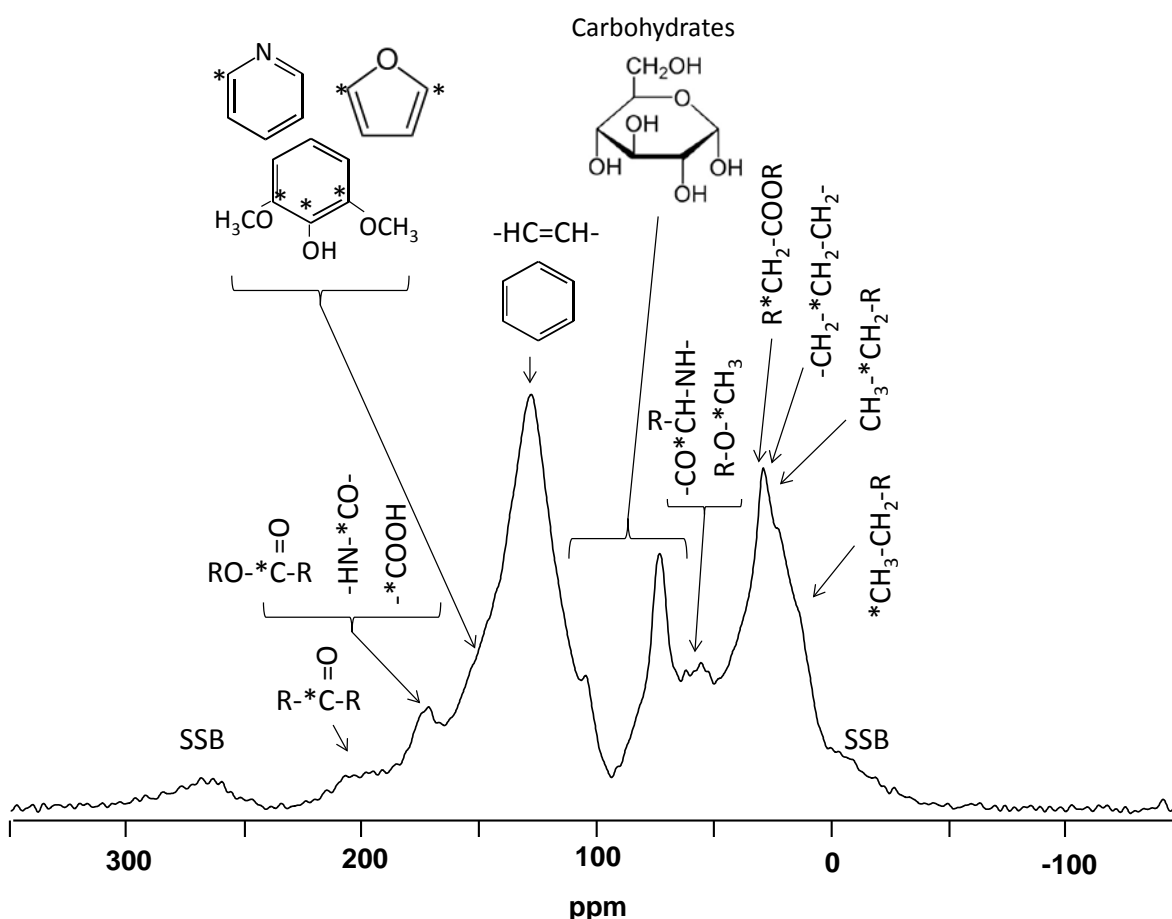


Figure 5: Selected examples for chemical shift assignment in solid-state ^{13}C CP MAS NMR (meant C is marked with asterisk, SSB Spinning side band).

When NMR spectroscopy is applied to solid samples, such as SOM or PyOM, the anisotropic chemical shift is one reason why NMR spectra display broad spectral lines. The

reason is that the electron shielding effect is depending on the orientation of the molecule with respect to the external field B_0 . Orientation dependent interactions are proportional to the term $3\cos^2\theta-1$. If θ equals the magic angle (θ_m) of $54^\circ44'$, the term vanishes. Therefore, solid samples are spun at several kilohertz around an axis that makes θ_m (magic angle spinning, MAS) (Schaefer and Stejskal, 1976). However, spinning side bands (SSB) occur in case of insufficient spinning rate. The SSBs appear at a frequency distance equal to the spinning frequency on each side of the parent signal (Fig. 5). Such SSBs can overlap with other main signals. In the case of occurring SSB, their signal areas can be added to the respective parent signal and subtracted in case of signal overlapping for allowing correct quantification of the NMR spectra.

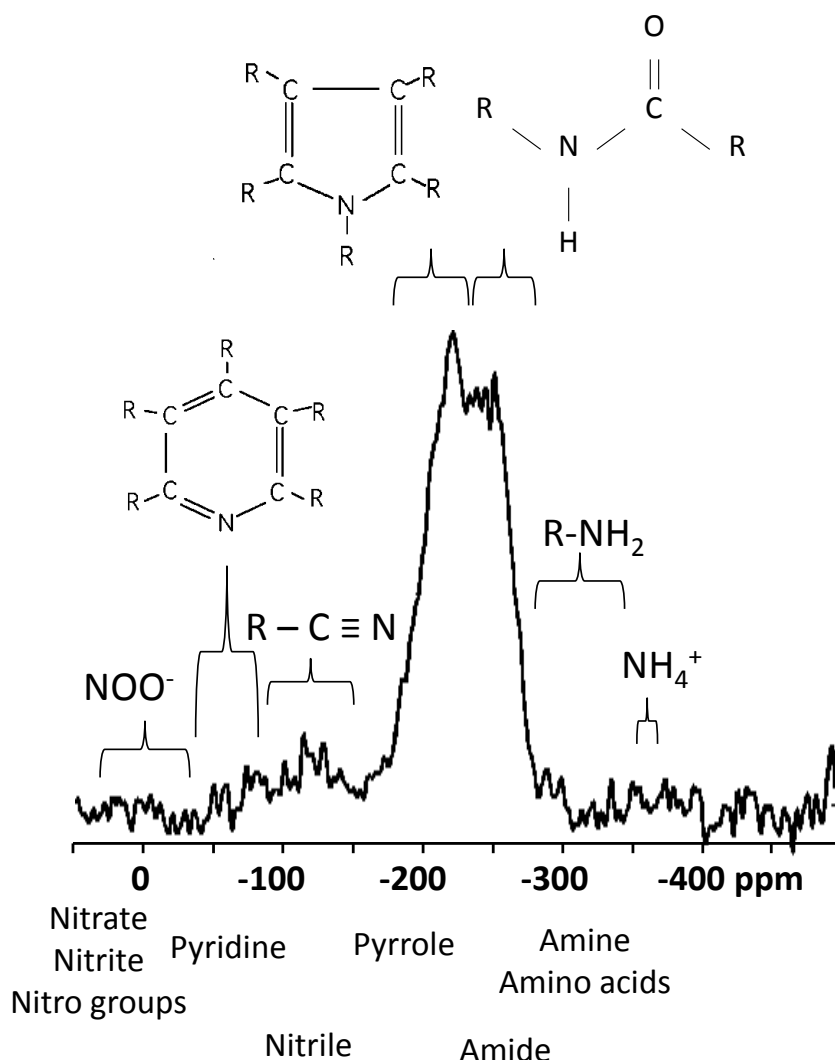


Figure 6: Selected examples for chemical shift assignment in solid-state ^{15}N CP MAS NMR.

The cross polarisation (CP) technique is applied in order to enhance the sensitivity of ^{13}C or ^{15}N NMR measurement. Therefore, ^1H nuclei with a high relative abundance of 99.9

atom% and short spin-lattice relaxation time (T_{1H}) are magnetised by a RF pulse (B_{1H}) and the magnetisation is subsequently transferred to ^{13}C or ^{15}N nuclei with a low natural abundance of 1.1 atom% and 0.4 atom% and relatively long T_1 . A polarisation transfer between two spin systems can only occur if the Hartmann-Hahn condition $-\gamma_H \times B_{1H} = -\gamma_X \times B_{1X}$ with $X = ^{13}\text{C}$ or ^{15}N is fulfilled. This means that a magnetisation transfer is only possible if the energy amount (ΔE_H) between the energy levels of the ^1H spin system has the same magnitude than ΔE_X of the X spin system. The Hartmann-Hahn condition can be achieved by a simultaneous irradiation of the ^1H and X spin systems with the RF fields B_{1H} and B_{1X} during a contact time (t_c). The RF fields B_{1H} and B_{1X} have to be adjusted that ΔE_H and ΔE_X of the two spin system is equal (spin lock).

The ^{13}C or ^{15}N -intensity signal is only observable if the condition between the cross-polarisation transfer time (T_{XH}) and the ^1H spin-lattice relaxation time in the rotating frame ($T_{1\rho H}$) is satisfied with $T_{XH} \ll t_c \ll T_{1\rho H}$. The cross-polarisation transfer time T_{XH} describes the time frame that is necessary for the transfer of the magnetisation from ^1H to the ^{13}C or ^{15}N spin system. In general, T_{XH} increases with the distance of the X nucleus from the protons and the molecular motion. The $T_{1\rho H}$ represents the relaxation of the protons in the presence of the field B_0 together with the time-dependent magnetic field B_1 . The field B_1 rotates in the plane perpendicular to B_0 at the Larmor frequency of the nuclei in the B_0 . In case $T_{XH} > T_{1\rho H}$, the relaxation of the protons becomes already affective before the cross polarisation is completed and the signal is completely suppressed.

The spin system has to be completely returned to the thermal equilibrium before a new rf pulse can be applied. The pulse delay should be $5 \times T_{1H}$ for avoiding saturation effects of the spin system. The relaxation time of the X spin system has not to be considered since the polarisation is induced by the ^1H spin system.

1.4.2 Reliability and application of solid-state ^{13}C and ^{15}N CPMAS NMR spectroscopy in PyOM research

The presence of paramagnetic and ferromagnetic species, such as Fe, Cu or Mn, affects NMR spectroscopy via loss of B_0 field homogeneity and shortening of $T_{1\rho H}$ (Smernik and Oades, 2000a). This can lead to considerable shortening of $T_{1\rho H}$ to an extent that the condition T_{CH} or $T_{NH} \ll T_{1\rho H}$ is not fulfilled, resulting in ineffective CP and line broadening. In this context Schöning et al. (2005) reported a selective O/N-alkyl C suppression due to presence of Fe. Such a selective effect on the O/N-alkyl C fraction of

^{13}C CP MAS NMR spectra was also shown for a Terric Humisol, containing a high concentration of paramagnetic Cu (Preston et al., 1984). For avoiding interactions with paramagnetic compounds, NMR samples can be pre-treated with dilute hydrofluoric acid (HF), as described by Goncalves et al. (2003). The advantage of HF treatment is (i) the removal of most of the mineral phase concentrating the C in the residue and (ii) removal of interfering paramagnetic minerals for improving NMR observability.

There are many NMR studies confirming that HF treatment does not alter chemical composition of OM (Skjemstad et al., 1994; Schmidt et al., 1997; Knicker et al., 2000; Gelinas et al., 2001; Goncalves et al., 2003). The latter is supported by identical NMR spectra of mineral-free organic litter layers obtained before and after the HF procedure (Dai and Johnson, 1999; Eusterhues et al., 2003). In this line, the C/N ratio does often not change by the HF procedure (Schmidt et al., 1997; Goncalves et al., 2003). However, Dai and Johnson (1999) and Schöning et al. (2005) reported lower recoveries and enrichment ratios of N compared to the corresponding OC values. The higher N loss during HF treatment may be explained by a preferred loss of easily soluble amino acids and amino sugars (Mathers et al., 2002) and inorganic N that were protected through sorption before HF treatment.

Dai and Johnson (1999) showed ^{13}C NMR spectra for soil HF-extracts of Spodosols (Podsol) that indicated a preferential removing of O-alkyl C and carboxyl C during the extraction. The observation may be attributed to the release of carbohydrates and OM which were associated with iron oxides (Oades et al., 1987). Especially HF treatment of subsoil horizons of acid forest soils can result in a preferential loss of mineral-associated OM (Eusterhues et al., 2003). In spite of this observation, the respective NMR spectra from HF-treated and untreated soils were almost identical. It can be summarised that HF treatment only dissolves soil minerals and mineral-associated OM whereas the remaining OM is nearly unaffected (Eusterhues et al., 2003).

A preferential loss of N containing compounds or O-alkyl C is not expected for PyOM because it does not contain free amino acids or carbohydrates like sugars (Knicker et al., 1996a). Therefore, HF pre-treatment can be considered as a useful tool to ensure quantitative NMR spectroscopy of PyOM samples.

For charred residues produced at high heating intensity under oxygen exclusion the formation of aromatic clusters with proportion of core C with a distance to the next ^1H

exceeding three bonds is expected (Schmidt and Noack, 2000). This distance is too high for efficient cross polarisation and thus such core C cannot be quantitatively detected by CPMAS ^{13}C NMR (Smernik et al., 2002). However, in contrast to soot, such graphitic polyaromatic domains play a minor role in chars produced under wildfire condition (Knicker et al., 2008a). Since temperatures above 700°C are required for the formation of graphitic structures (Freitas et al., 1999). At such high temperatures, most unprotected organic matter is expected to be volatilised under oxidic conditions.

Knicker et al. (2005a) showed that the condensation degree of plant residues charred by vegetation fires is low. The atomic H/C ratio between 0.6 and 0.4 of the aromatic moiety of charred peat and barbeque charcoal revealed that on average every second to third C is connected to a proton (Knicker et al., 2005a). The observed protonation degree of aromatic domains allows efficient cross polarisation that is required for a correct quantification of the NMR spectra.

Dipolar dephasing (DD) NMR experiments allow to discriminate between weak and strong proton dipolar coupling of ^{13}C nuclei (Alemany et al., 1983). The DD procedure includes an interruption of high power proton-decoupling for a certain time delay t_{dd} directly after t_c but before the ^{13}C acquisition. This allows the ^1H spin system to interact with ^{13}C nuclei, resulting in dephasing of ^{13}C signals (signal broadening). In general, ^{13}C nuclei without direct attached H and high molecular motion have weak ^1H dipolar coupling and will be visible in a spectrum obtained with $t_{\text{dd}} > 40 \mu\text{s}$. The DD NMR experiments with charcoal and charred peat support that almost every second aryl C is directly connected to neighbouring H (Knicker et al., 2005a). In this line, variable contact time (VCT) measurements of different PyOM revealed that the condition $T_{\text{CH}} < T_{1\rho\text{H}}$ was fulfilled for aryl C which is necessary for efficient cross polarisation. The CP time T_{CH} did not tend to increase with prolonging charring degree of the PyOM (Knicker et al., 2005a). This indicates that graphite-like structures were not formed because that would cause in decreasing protonation degree of aryl structures, resulting in increasing ^1H - ^{13}C distance and larger T_{CH} values.

Bloch decay (BD) or direct polarisation (DP) NMR spectroscopy represents another opportunity to determine directly C species. However, $T_{1\text{C}}$ is an order of magnitude or more slower than $T_{1\text{H}}$ (Smernik and Oades, 2000a). Commonly, recycling delays of 60-90 s are applied for BD MAS NMR determination of natural OM samples (Smernik and Oades, 2000a). Comparing CP and BD MAS NMR spectra of PyOM an underestimation of

aryl domains is often reported (Skjemstad et al., 1999; Mao et al., 2000; Smernik and Oades, 2000b; Keeler and Maciel, 2003; Fang et al., 2010). Knicker et al. (2005a) explained this observation by an expense of O/N alkyl and alkyl C in BD NMR due to saturation because of application of relaxation delays that were too short. The assumption is supported by NMR studies of Teeaar and Lippmaa (1984), determining a very long T_{1C} of 266 s for crystalline cellulose. This requires a recycle delay of 22 min ($5 \times T_{1C}$) to avoid ^{13}C -spin saturation. In spite of the fact that fresh peat does not contain considerable amounts of char, the respective BD NMR measurements showed also differing results from CP NMR spectra (Knicker et al., 2005a). The latter is best explained by saturation effects in the O-alkyl C and alkyl-C fraction and may explain the observed higher aryl C contribution in BD NMR. In this line, the studies of Simpson and Hatcher (2004) and Hammes et al. (2006) supported a comparable ^{13}C BD MAS NMR efficiency in comparison with the corresponding CP MAS NMR spectra for charred wood and grass, containing little or no O-alkyl C.

The application of CP technique minimises possible spin-saturation effects of O-alkyl C because of much shorter recycle delay of the ^1H spin system. The reliability of the CP NMR was also supported by experiments with standards containing PyOM and untreated peat mixed in defined ratios (Knicker et al., 2005a). The authors demonstrated that almost all aryl C was efficiently cross polarised. Thus, the CP technique does not underestimate aryl C in PyOM if the contribution of soot-like or graphitic material can be excluded.

Another useful tool in PyOM characterisation is solid-state ^{15}N NMR spectroscopy. Unfortunately this technique is hampered by two factors. The most abundant isotope of N is ^{14}N with 99.6 atom%. However, it is impossible to perform ^{14}N high resolution NMR because of the large quadrupole moment. The dipolar ^{15}N isotope has a low natural abundance and a low negative gyromagnetic ratio. These factors cause a 50 times lower sensitivity for ^{15}N NMR compared to ^{13}C NMR. Therefore, ^{15}N -enriched sample material is often used for ^{15}N NMR studies e.g. Ripmeester et al. (1986); Cheshire et al. (1990); Knicker and Lüdemann (1995). The CP technique can also be applied for improvement of the sensitivity of ^{15}N NMR spectroscopy in SOM with natural ^{15}N abundance (Knicker, 1993). Knicker et al. (1999) confirmed that CP technique applied to humic fractions spiked with ^{15}N -enriched trinitrotoluene did not reveal a major intensity loss compared to the respective ^{15}N direct polarisation NMR spectrum. The authors could not find additional

peaks in the ^{15}N BD NMR spectrum, indicating that ^{15}N CP NMR detected all organic N groups. The ^{15}N NMR studies of Knicker et al. (1996a) and Knicker et al. (1996b) applied successfully solid-state ^{15}N NMR to coal and charred plant residues. The authors extracted acquisition parameters allowing quantitative characterisation of heterocyclic bound N compounds by application of solid-state ^{15}N CP MAS NMR spectroscopy. However, inorganic N species were not quantitatively determined via CP technique with a contact time of 0.7 to 1 ms because of their high mobility (NH_4^+) or weak interaction with the ^1H spin system (NO_3^-) (Knicker and Lüdemann, 1995).

It can be summarised, that the application of ^{13}C and ^{15}N CP MAS NMR technique is quantitative for SOM and wildfire-derived PyOM.

2. Materials and Methods

2.1 Production of PyOM

For the production of the ^{13}C and ^{15}N labelled PyOM, rye grass (*Lolium perenne* L.; Gr) was used, which represents a typical plant fuel consumed by grassland fires. Seeds of rye grass were cultured on quartz sand in a closed plexiglass chamber, located in a phytotron (Lehrstuhl für Zierpflanzenbau, TUM) that allowed the automatic control of climatic and light conditions (Fig. 7). The grass was grown with ^{13}C -enriched CO_2 gas (^{13}C : 99atom%) and ^{15}N -labelled potassium nitrate nutrient solution (^{15}N : 98atom%; Knicker (2002)). After two weeks the grass shoot stems were harvested. The pots with the cut plants were reintroduced into the chamber for further growth. After yielding sufficient shoot material, the pots were removed from the chamber and the roots were manually separated from quartz sand.

In comparison with the natural abundance of 1.1 atom% for ^{13}C and 0.4 atom% for ^{15}N it was possible to produce plant material which was highly isotopically enriched (^{13}C : 23.5atom%; ^{15}N : 62.8atom%). The combined aboveground and belowground biomass was dried to constant weight at 40°C and cut into small pieces (5 to 10 mm).

In contrast to other studies (Smernik et al., 2000; Baldock and Smernik, 2002; Hamer et al., 2004; Trompowsky et al., 2005; Hammes et al., 2006), oxic conditions were used for the charring process, since pyrolysis conditions are unlikely to occur during natural aboveground fires. Approximately 5 g of the plant material was put in a 1-mm layer on a ceramic tray preheated at 350°C . The tray was introduced into a preheated muffle oven to allow charring at 350°C under oxic conditions to ensure that plant material was immediately exposed to the target charring temperature. This temperature was reported to result in char that is comparable to that remaining after natural wildfires (Almendros et al., 1990). Two combustion times of one (1M) and four minutes (4M) were applied to obtain material with different charring degree (Hilscher et al. 2009). These relatively short charring times were applied to account for the high speed with which natural fires commonly move.

For the respiration incubation study, unlabelled rye grass (*Lolium perenne*; Gr) and pine wood (*Pinus sylvestris*; P) was used to produce the PyOM. The rye grass was cut into small pieces (5 to 10 mm) and the pine wood was ground to a particle size of 1 mm. The charring conditions were similar as for the labelled grass material.

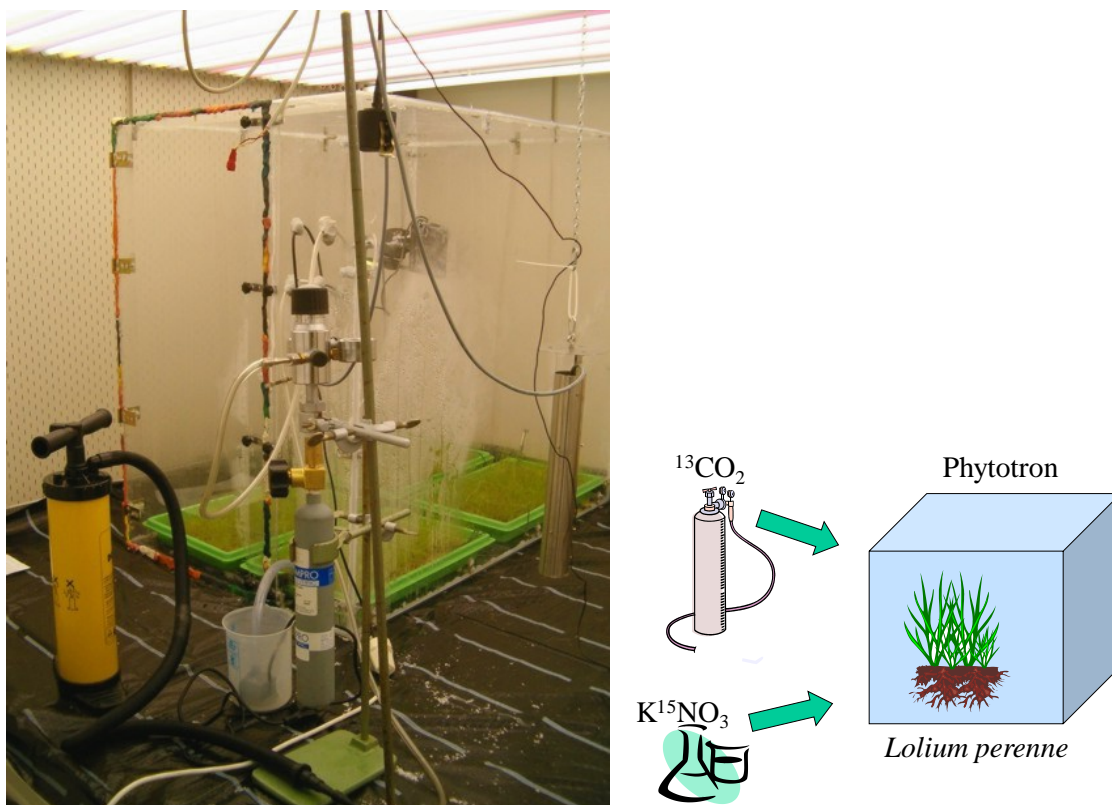


Figure 7: Cultivation of isotopically enriched rye grass.

2.2 Characterisation of PyOM and soil material

2.2.1 C / N content and ^{13}C / ^{15}N isotopic signature

Total C and total N contents of the PyOM and soil mixtures were measured in duplicates using dry combustion (975°C) with an Elementar Vario EL microanalyser detecting N as N_2 and C as CO_2 . Detection limits for C and N were $0.4\ \mu\text{g}$ and $1\ \mu\text{g}$, respectively. The ^{13}C and ^{15}N contents of the samples were measured with a quadrupole mass spectrometer (InProcess Instruments GAM 200) connected to the microanalyser. Because of low ^{13}C and ^{15}N enrichments of the B and C sub layers of the soil incubates, these samples were determined using an elemental analyser (CHN NA1500, Carlo Erba) coupled to an isotope ratio mass spectrometer (Isochrom III Micromass-GVI Optima; CNRS Laboratoire de Biogéochimie et Ecologie des Milieux Continentaux) with an analytical precision for isotope measurements of 0.3‰.

The contribution of $\text{NH}_4^+\text{-N}$ to the PyOM was detected in a $1\ \text{mol l}^{-1}$ KCl extract using indophenol blue colorimetric method on a spectrophotometer (Milton Roy, Spectronic 601) at 655 nm.

2.2.2 Basic soil parameters

The soil substrate for the incubation experiment was obtained from a fire-unaffected Bw horizon of a Cambisol (IUSS Working Group WRB, 2006) under Norway spruce near Leuk, Canton Valais, Switzerland, (GPS 46.33678° N, 7.64394° E). After air-drying the soil was passed through a 5 mm sieve. The low organic C (OC) concentration of the soil (3.4 g kg⁻¹) allowed an efficient ¹³C and ¹⁵N tracing of compounds derived from the isotopically enriched PyOM. No inorganic C was recovered after heating the soil at 550°C for 5 h. A soil pH value of 6.8 was measured with a glass electrode in the supernatant of a suspension obtained by mixing soil with 0.01 M CaCl₂ solution in a mass to volume ratio of 1:2.5.

The soil texture was determined after oxidising the OC with 30% (w/w) H₂O₂ solution and removing Fe oxides with a dithionite-citrate-bicarbonate solution at room temperature. The texture was obtained by combination of wet sieving (2000 - 63µm) and the use of a Micrometrics Sedigraph 5100 (Buchan et al., 1993) to differentiate silt (63 - 2µm) and clay (< 2µm). The soil contained 34% sand, 42% silt and 23% clay, which classifies it as a loamy soil (IUSS Working Group WRB, 2006).

2.2.3 Specific surface area of PyOM

The specific surface area was determined using N₂ adsorption at -195.8°C with an Autosorb 1 (Quantachrome Corp., Syosset, NY). The calculations were performed according to the BET equation (Brunnauer et al., 1938). Micropore surface area and volume were calculated according to de Boer et al. (1966). Prior to analysis, the samples were degassed under vacuum at 40°C overnight in order to remove adsorbed volatile compounds from the surfaces. In addition, micropore area and volume were obtained from CO₂ adsorption at 0°C. Calculations were conducted according to the method of Dubinin and Radushkevich (1947). Sample pre-treatment was the same as for the N₂-adsorption measurements.

2.3 Setup of PyOM respiration experiment

Each of the char samples obtained from the grass and wood after 1 or 4 min of charring was mixed with the soil in a ratio of 1/10 (w/w). Of each sample 30 g were placed in a 250 ml incubation vessel. For the degradation study, 10 and 4 replicates were prepared of the rye grass char and for the pine wood char, respectively. In addition, 10 replicates of

pure soil material were used to determine the background respiration (blank value, BV) of the native soil organic matter. All samples were inoculated with 1 ml of a microbial suspension. Therefore, a soil mixture of A horizons of 6 Cambisol, 3 Luvisol and one Fluvisol was rewetted to 60% of its maximal water hold capacity and pre-incubated at 20°C (2 days). Then, the inoculum was extracted with deionised water and the supernatant was filtered (5 µm pore size). With the use of the soil mixture, it was intended to assure a microbial population which is representative for soils. To simulate the input of fresh unburnt litter entering the soil system after the death of fire-affected vegetation, 150 mg of unburnt and finely ground rye grass was added as a co-substrate (CS) to one of the two replicates of each series after 1 and 3 weeks of incubation.

The water content of the sample mixtures was adjusted to approximately 60% of the maximum water holding capacity and the samples were incubated for 48 days at 30°C under aerobic conditions in a Respicond apparatus (Nordgren Innovations, Sweden) located at the Institut für Landschaftsarchitektur, Forschungsanstalt für Gartenbau Weißenstephan (Fig. 8). This system measures the respiration every 15 min by determining changes in the electrical conductivity induced by absorption of CO₂ in 10 ml of a 0.6 M KOH solution placed inside the incubation vessel (Nordgren, 1988). The amount of the absorbed CO₂ (c_t) is calculated as $c_t = \alpha (1 - R_0 \times R_t^{-1})$ with α equals the proportionality constant relating the decrease in conductivity to the absorbed CO₂ amount. The electrical resistance of the KOH solution at time t is R_t , and at $t = 0$ it is R_0 .



Figure 8: Setup of PyOM respiration experiment

2.4 Setup of ^{13}C and ^{15}N labelled PyOM incubation

Soil columns (16 for each PyOM treatment) with three layers were prepared. The uppermost layer comprised 120 g soil mixed with 400 mg PyOM obtained from the grass after 1 min or 4 min charring (A layer). This corresponds to an addition of 41 mg ^{13}C and 8 mg ^{15}N for the PyOM 1M incubates and 38 mg ^{13}C and 9 mg ^{15}N for PyOM 4M, respectively, equivalent to a total C input of 0.49 and 0.45 t ha⁻¹. To determine potential PyOM vertical movement, two sub-layers, B and C, composed of 200 g soil each, were enclosed in a nylon net. The net allowed it to separate the different layers at the end of the experiment. The C and B soil layers kept in the net (3 cm high each) were put into a polyethylene beaker, overlaid with the A layer (2 cm high; Fig. 9). The whole column was covered with a perforated Al foil to avoid drying out. The bottom of the polyethylene beaker was perforated to allow release of water and soil material. The leachate was weekly collected in underlying glass dishes and freeze-dried. During the whole incubation period between 0.6 g and 1.3 g of leachate was collected.

In addition, 9 columns of soil without added PyOM were incubated and used to determine the natural SOM content and its possible alteration at different stages of the degradation experiment (BV). All samples were inoculated with 1 ml of a microbial suspension to ensure that an active microbial population was present. This inoculum was obtained from a forest litter layer that was shaken with deionised water (1:5). Subsequently, the supernatant was filtered (5 μm pore size) to avoid input of particulate organic material from the forest litter (Knicker, 2003).

The water content of the soil samples was adjusted to ca. 60% of the WHC and the samples were incubated for one to 20 months at 30°C in the dark under aerobic conditions. The water content was checked weekly and adjusted by weighing the soil column and adding the mass difference as water. On average, 10 ± 7 ml of water were added weekly to each beaker and could disperse within the soil column.

To simulate the input of fresh unburned litter derived from dying vegetation affected by fire, 400 mg of unburned, finely ground unlabelled rye grass were added as co-substrate (CS) to one of the two replicates of each series after 4, 10 and 16 months incubation. The soil columns with CS were incubated for a period of up to 28 months. With this design it was also intended to identify a possible co-metabolic priming effect (Fontaine et al., 2003) during PyOM decomposition. For the 2 month incubation experiment, duplicates were prepared to provide material for controlling the reproducibility.

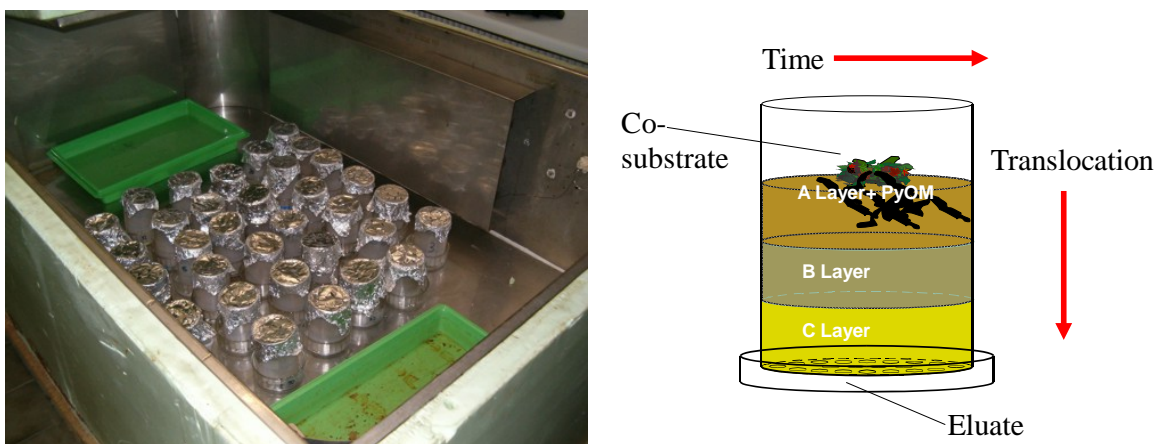


Figure 9: Setup of ^{13}C and ^{15}N PyOM incubation experiment.

After the incubation, the A layer was first collected. Then, the B and C layers were taken and the nylon net was removed to collect the incubated soil. The nylon net was cleaned with water and the obtained soil residues were added to the respective layer. Thereafter the soil was air-dried.

2.5 Lipid analyses

Aliquots of the incubated labelled PyOM samples (10 g; respiration experiment) and fresh and charred plant material (1 g) were Soxhlet-extracted with a dichloromethane-methanol (3:1 v:v) mixture for 8 h (González-Vila et al., 2003). Prior to extractions, the cellulose extraction thimbles were Soxhlet-extracted with same dichloromethane-methanol mixture, to remove any contaminant lipid. In order to remove elemental sulphur, activated (2M HCl) copper curls were added to each extraction. The total lipid extract was filtrated and subsequently the filtrate was dried up with sodium sulphate. The lipid amount was determined by gravimetry and related to the respective sample weight before analysis by gas chromatography (GC; Hewlett-Packard 5730A) and gas chromatography–mass spectrometry (GC–MS; Hewlett-Packard GCD). The total lipid extract was derivatised by adding 2M trimethylsilyldiazomethane for the methylation of polar compounds. In addition silylation of the samples was accomplished by using *N,O*-bis(trimethylsilyl)-trifluoroacetamide. Thus, the acids from the polar fraction were identified as their methyl or silyl esters.

Separation of the total lipid extract was achieved using a SE-52 fused silica capillary column (30 m × 0.32 mm i.d., film thickness 0.25 µm). The column temperature was programmed to increase from 40 to 100 °C at 30 °C min⁻¹ and then to 300 °C at 6 °C min⁻¹. Helium was used as carrier gas at a flow rate of 1.5 ml min⁻¹. Mass spectra were measured at 70 eV ionising energy. Individual compounds were identified by low resolution mass spectrometry and by comparison with mass spectra libraries (NIST and Wiley). Traces corresponding to selected homologous series of biomarkers families were obtained by single ion monitoring (SIM), such as ion at *m/z* 85 for *n*-alkanes and ion at *m/z* 74 for FAMES (fatty acid methyl esters). Relative compound abundances were calculated by using the software of the Data Review Chemstation, assuming that a constant relationship exists between the percentage of the total chromatogram area and the amount of the corresponding lipid extract.

2.6 Fractionation

The A layer of the ¹³C and ¹⁵N labelled PyOM incubates was separated into different soil organic matter fractions to obtain a more detailed view about the char degradation and stabilisation process (Fig. 10).

2.6.1 DOM extraction

The dissolved organic matter (DOM) was extracted after shaking an aliquot of 80 g of the incubated soil sample with 300 ml deionised water for 15 h. After centrifugation for 30 min at 3500 rpm, the supernatant was decanted, pressure filtered using a 0.45 μm polypropylene membrane and freeze-dried (Rennert et al., 2007).

2.6.2 Density fractionation

An aliquot of the DOM-extraction residue (60 g) was subjected to density fractionation with a Na-polytungstate solution (300 ml, density 1.8 g cm^{-3} ; Kölbl and Kögel-Knabner, (2004)). The particulate organic matter (POM) was recovered as material floating on the Na polytungstate solution after centrifugation for 10 min at 3000 rpm. The obtained POM fraction was separated by using a 20 μm sieve. The extraction was repeated (3 x) and both the light fractions and the mineral residue (sediment) were washed with deionised water to remove remaining Na polytungstate. Salt removing was complete when the conductivity of the washing water was smaller than 50 $\mu\text{S cm}^{-1}$ for the sediment and 3 $\mu\text{S cm}^{-1}$ for the POM, respectively. The mineral residue and POM were freeze-dried. The two POM particle size fractions were combined to calculate the POM recovery.

2.6.3 Particle size fractionation

For particle size fractionation, the mineral residue of the density fractionation step (30 g) was re-suspended in deionised water (mixing ratio: 1:5) and subjected to ultrasonication with a Branson Sonifier 250 with an energy input of 250 J ml^{-1} to disintegrate the aggregates. The mineral residue was fractionated into gravel plus sand fraction (5 mm to 63 μm) and coarse silt fraction (63 to 20 μm) via wet sieving. The finer fractions were separated into medium silt (20 to 6 μm), fine silt (6 to 2 μm) and clay (< 2 μm) by sedimentation in deionised water using Atterberg cylinders and freeze-dried.

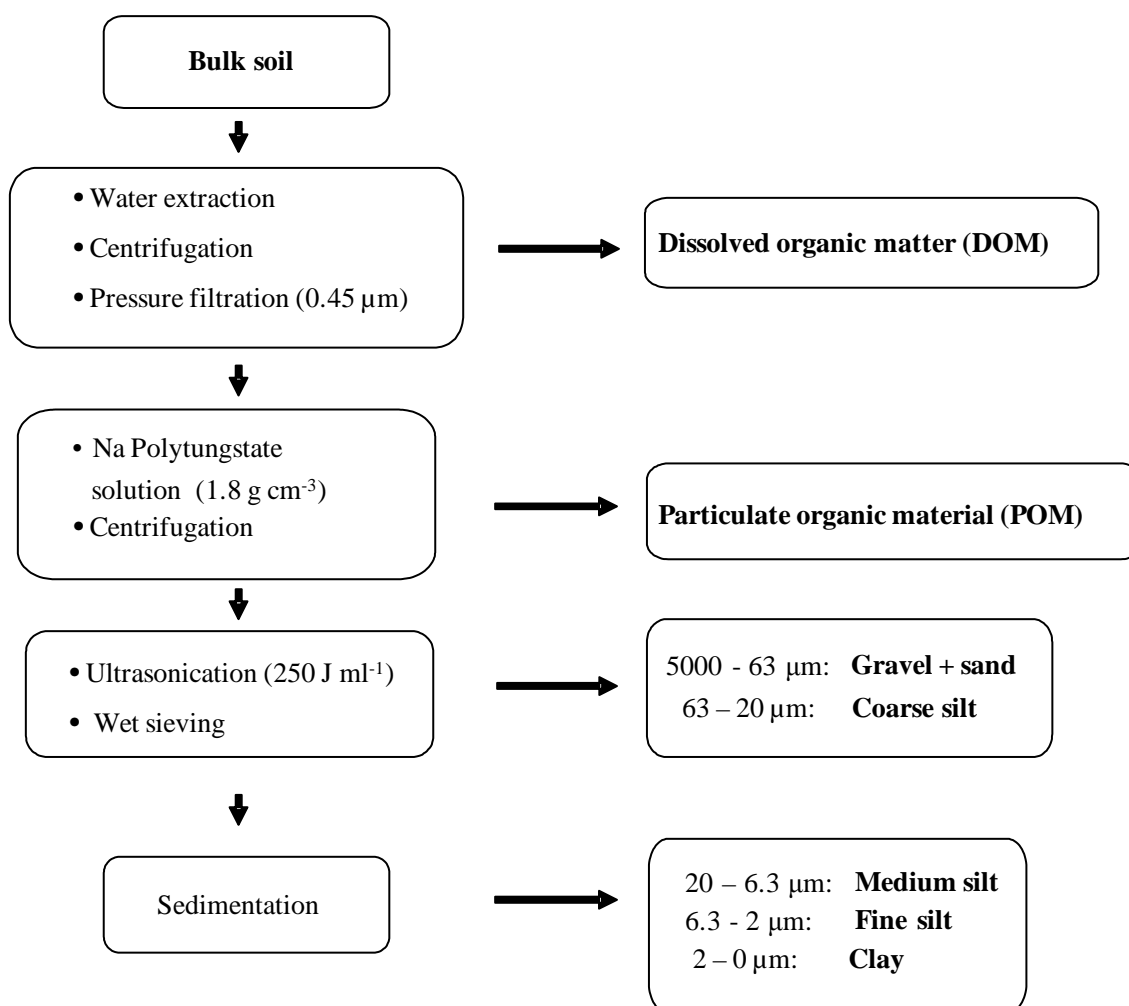


Figure 10: Schematic of conducted fractionation.

2.7 Solid-state ¹³C and ¹⁵N CPMAS NMR spectroscopy

2.7.1 HF pre-treatment

The soil incubates and particle size fractions were demineralised with HF according to Goncalves et al. (2003) to improve the sensitivity of the following solid-state ¹³C and ¹⁵N NMR spectroscopic analyses. Approximately 5 g sample material was shaken with 50 ml of 10% (w/w) HF for 3 h in a polyethylene bottle. After centrifugation, the supernatant was removed and discarded. The procedure was repeated five times at room temperature. The remaining sediment was washed five times with 50 ml deionised water and freeze dried.

2.7.2 Solid-state ^{13}C CPMAS NMR spectroscopy

All PyOM samples were analysed by using a Bruker DSX 200 spectrometer operating at a resonance frequency of 50.32 MHz. The cross polarisation magic-angle spinning (CPMAS) technique (Schaefer and Stejskal, 1976) was applied with a spinning speed of 6.8 kHz. A ramped ^1H pulse was disposed during the contact time of 1 ms in order to circumvent spin modulation during the Hartmann–Hahn contact (Peersen et al., 1993; Cook et al., 1996). A Pulse delay of 300 ms for PyOM samples was applied, following the recommendation of Knicker et al. (2005a). Knicker et al. (2005a) showed that the condensation degree of plant residues charred by vegetation fires is low enough to ensure efficient cross polarisation, which is required for correct quantification of the spectra. Depending on the ^{13}C content of the samples, between 2000 and 150000 scans were accumulated. Line broadenings between 10 and 100 Hz were applied. The ^{13}C chemical shifts were calibrated relative to tetramethylsilane (0 ppm) with glycine (COOH at 176.08 ppm). Using the instrument software (XWIN-NMR V2.6), the contribution of the different C groups to total C was determined by integration of their signal intensity in the respective chemical shift regions (Knicker et al., 2005a). The regions from 245 to 185 ppm and from 185 to 160 ppm are assigned to carbonyl and carboxyl/ amide C, respectively. Between 160 and 110 ppm, resonance lines of olefins and aryl C are detected. The chemical shift region between 140 and 160 ppm is assigned to substituted aryl C. Commonly, the region between 110 and 45 ppm is assigned to O/N-alkyl C. However, in samples with high aryl C content, the latter dominate the intensity between 110 and 90 ppm (Knicker et al., 2007). Accordingly, for the PyOM, this region was assigned to originate predominantly from aryl C signal. Resonances of alkyl C are expected between 45 and 0 ppm. Owing to insufficient averaging of the chemical shift anisotropy at a spinning speed of 6.8 kHz, spinning side bands (ssbs) of the aryl C signals occur at a frequency distance of the spinning speed at both sides of the central signal (300 to 245 ppm and 0 to -50 ppm). Their contributions were considered by adding their intensities to that of the parent signal as described by (Knicker et al. (2005a). The ssbs of the carboxyl-C signal contribute to the intensity in the chemical shift region between 325 to 300 ppm and between 45 ppm and 0 ppm. Because one ssb of the carboxyl C is superimposed by the alkyl-C signal (45 to 0 ppm), the integral of the second ssb in the region of 325 to 300 ppm was doubled and added to the carboxyl-C main signal. The same ssb integral was subtracted from the intensity of the alkyl C region.

2.7.3 Solid-state ^{15}N CPMAS NMR spectroscopy

The solid-state ^{15}N NMR spectra were obtained using a Bruker DMX 400 operating at 40.56 MHz. The contact time was 1 ms, and a 90° pulse width of 6.5 ms, a pulse delay of 300 ms and a line broadening between 50 and 200 Hz were applied. Between 50,000 and 1,000,000 scans were accumulated at a magic-angle spinning speed of 4.5 kHz. The chemical shift was standardised to the nitromethane scale (0 ppm) and adjusted with ^{15}N -labeled glycine (-347.6 ppm). The integrals were assigned to heterocyclic N compounds (-145 to -245 ppm) and to peptide-like structures (-245 to -285 ppm) according to Knicker (2000).

2.8 Quantification of C and N groups of incubated PyOM

The total ^{13}C and ^{15}N amount of the incubated PyOM was calculated by mass balance using the sample weights, their respective total C or N concentrations as well as their ^{13}C or ^{15}N abundance given in atom%. The results were corrected for the natural ^{13}C and ^{15}N background by subtraction. The latter was determined via control soil incubates with natural ^{13}C and ^{15}N abundance which had been prepared for each time series.

To calculate the amount for each C and N group of the PyOM incubate, the proportion of the integrated signal area of the respective chemical shift region of the ^{13}C or ^{15}N NMR spectra was multiplied by the total ^{13}C or ^{15}N amount of the incubate. The respective amount of each C group of the control soil (B_v) was subtracted from the respective C group of the PyOM incubate.

The recovery (RC) of the total ^{13}C and ^{15}N amounts from the incubated PyOM in the soil layers and SOM fractions was calculated by mass balances using the sample weight (w) and respective total C or N concentrations (c) as well as the ^{13}C or ^{15}N abundance (Y) in atom%.

$$RC = (w \times c \times Y)_{\text{after}} \times (w \times c \times Y)_{\text{before}}^{-1} \times 100[\%] \quad (1)$$

The relative recovery (Q) of ^{13}C and ^{15}N derived from isotopically enriched PyOM of the mineral fraction was calculated by setting the recovery of the 1M PyOM (RC_{1M}) treatments to 100% related to the respective 4M PyOM (RC_{4M}) values.

$$Q = RC_{4M} \times (RC_{1M})^{-1} \times 100[\%]. \quad (2)$$

2.9 Statistical analysis and data fitting

Mean values and standard deviations were calculated with Microsoft Excel (2007) and further statistical analysis was carried out with the software SigmaPlot 2000, version 11.0 (SPSS Inc.).

An one way repeated measures ANOVA was applied to identify significant treatment effects as a function of time. A Tukey's honest significant difference test was used to determine which PyOM fractions and treatments were significantly different from each other. Statistical significance was assigned at the $p \leq 0.05$ level (error probability).

Decomposition of labelled PyOM was described with a two-component model (Voroney et al., 1989)

$$y = a \times e^{(-k1 \times t1)} + b \times e^{(-k2 \times t2)} \quad (3)$$

and using the software SigmaPlot 2000, version 11.0 (SPSS Inc.). Terms a and b describe the fast and slowly decomposable OM pool, respectively, whereas k displays the turnover constant rate at the respective time t . This equation allows description of the kinetics of a two-phase decomposition process. Based on Eq. 3, half-life periods of the labelled substrates were calculated with

$$t_{1/2} = \ln 2 / k. \quad (4)$$

The decomposition dynamic of the C groups of the PyOM was described with a first order decay model

$$y = a \times e^{(-k1 \times t1)} \quad (5)$$

The data of Knicker and Lüdemann (1995) were used to compare the degradation dynamics of the PyOM with the respective dynamics of fresh unburned rye grass (*Lolium perenne* L.). They performed a long-time degradation experiment with comparable incubation conditions with regard to water content and temperature.

For testing potential correlations between C groups, a Pearson product moment correlation test was applied. Statistical significance was assigned at the $p \leq 0.05$ level.

3. Mineralisation and structural changes during the initial phase of microbial degradation of pyrogenic plant residues in soil

This chapter discusses the influence of charring intensity and plant source material on the chemical structure of PyOM. Model chars were biotic incubated in order to investigate the impact of charring degree on the mineralisation dynamic during the initial degradation stage in soil. A further interest was to test if the supply of a microbial available co-substrate promotes the PyOM mineralisation.

3.1 Chemical changes in the plant materials during the thermal treatment

After one minute of thermal treatment of the grass (Gr1M) and pine wood residues (P1M), an increase of the C content and a relative enrichment of N was observed (Table 1). The latter resulted in a clear decrease of the atomic C/N ratio of the wood char, although the values are still high. The low N content confirms the minor role of N compounds as structural constituents of wood chars. In contrast, the narrow atomic C/N ratios of the grass char underline that in this material such N compounds comprise an important fraction.

Figure 11 shows the solid-state ^{13}C NMR spectra of the fresh and charred plant residues. Most of the intensity in that of the fresh rye grass is observed in the region assigned to O-alkyl C between 110 and 45 ppm (Table 2). Here, the resonance lines at 64, 74 and 84 ppm are characteristic for cellulose (Maciel et al., 1982). The intensity of its di-O-alkyl C appears at 105 ppm. A further strong signal is observable in the alkyl-C region (45 to 0 ppm). According to previous studies, in the present sample this signal derives mainly from peptides and peptide-like constituents rather than from paraffinic units in plant waxes (Knicker et al., 1996b). This is supported by the expressed signal at 174 ppm, which can be assigned to carboxyl and amide C groups (Knicker et al., 1996b).

Table 1: Gravimetric elemental concentration, specific surface area, micropore surface area and volume associated with heating of rye grass (*Lolium perenne*) and pine wood (*Pinus sylvestris*) at 350°C under oxic conditions.

Sample	C		N	C/N atomic	C loss	N loss	Specific surface area (N ₂) m ² g ⁻¹	Micropore surface area (N ₂) m ² g ⁻¹	Micropore volume (N ₂) cm ³ g ⁻¹	Micropore surface area (CO ₂) m ² g ⁻¹	Micropore volume (CO ₂) cm ³ g ⁻¹
	mg g ⁻¹	%									
Rye grass	416	30	16								
Gr1M	505	42	14	44	35	6.5	0	0	0	68	0.03
Gr4M	468	43	13	53	39	5.3	0	0	0	84	0.04
Pine wood	492	1	523			6.8	0	0	0	57	0.03
P1M	621	2	326	16	-	6.6	0	0	0	187	0.08
P4M	657	4	218	51	-	244.1	142.4	0.08	0.08	690	0.30

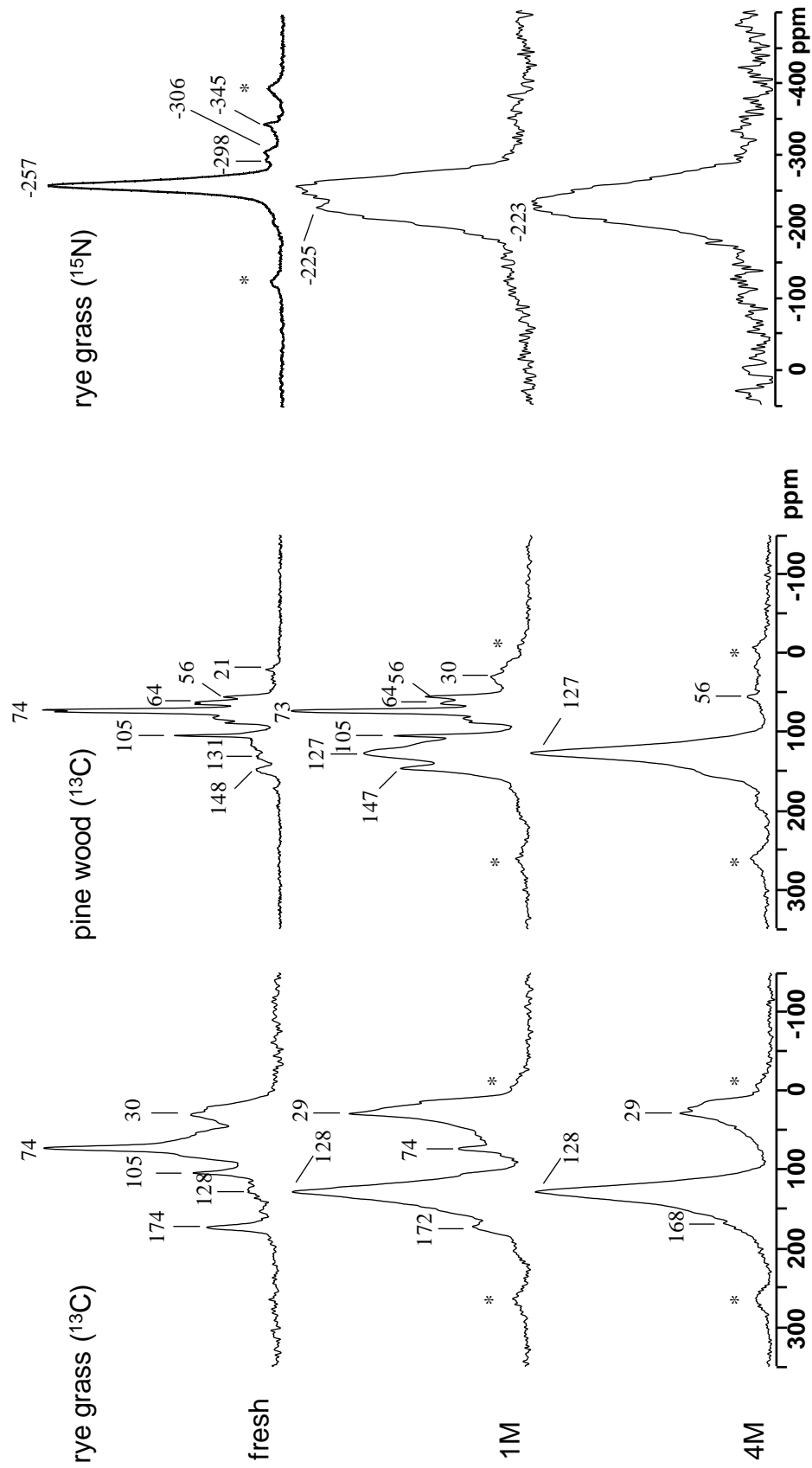


Figure 11: Solid-state ^{13}C NMR and ^{15}N NMR spectra of rye grass and pine wood as a function of oxidation time at 350°C . Spinning side bands are marked with asterisk.

Table 2: Relative intensity distribution in solid-state ^{13}C NMR (% of total intensity) associated with heating of rye grass (*Lolium perenne*) and pine wood (*Pinus sylvestris*) at 350°C under oxidic conditions.

Sample	Carbonyl/ Carboxyl C	O-Aryl C	Aryl C	O-Alkyl C	Alkyl C
	245-160 ppm	160-140 ppm	140-90 ppm	90-45 ppm	45-0 ppm
Rye grass	9	2	7	65	18
Gr1M	10	11	39	12	27
Gr4M	11	14	49	6	20
Pine wood	3	5	14	73	4
P1M	6	13	34	38	8
P4M	8	16	67	5	5

The ^{13}C NMR spectrum of the pine wood reveals a higher relative O-alkyl C content than the rye grass. The small peak at 21 ppm together with a weak signal in the region of carboxyl C is in line with the occurrence of acetate. The higher contents of lignin and tannins of the wood samples in relation to grass residues is supported by the resonance line in the aryl C region (Table 2). Typical signals for methoxyl C, aryl C and O-aryl C associated with lignin are commonly observed at 56 ppm, 131 ppm, and 148 ppm (Hatcher, 1987).

The spectra of both plant chars show an increase in aromaticity with charring time. Almost half of the total ^{13}C intensity derives from aromatic C structures. The remaining methoxyl C (64 ppm) and O-aryl C (147 ppm) signals in the ^{13}C NMR spectrum of P1M indicate that some lignin-type structures survived the charring process (Fig. 11), which is in accordance with the relatively high resistance of the lignin backbone towards thermal oxidation (Sharma et al., 2004). The higher lignin content of the pine wood vs. the grass material may also be responsible for the smaller C loss during charring (Table 1).

Increasing the charring time to 4 min increased the carbon loss for the pine wood and grass to 51% and 53%. Concomitantly, the atomic C/N value decreased, supporting preferential accumulation of N-containing compounds.

The solid-state ^{13}C NMR spectra of these more thermally treated chars showed no signals attributable to cellulose and the main signal at 128 ppm in the aromatic region confirms that they can be taken as representative of severely charred material. The aromatic C intensity in the spectrum of P4M is much higher than that in the spectrum of Gr4M (Table 2). The spectrum of Gr4M, on the other hand, reveals a substantial

contribution of heat-recalcitrant alkyl C (Fig. 11), which may be assignable to cyclic peptides as they were observed by Meetani et al. (2003) charring peptides at a temperature between 285°C and 285°C although using a N atmosphere.

Figure 11 includes the solid-state ^{15}N NMR spectra of the heat-treated grass materials. Because of the low N content of the pine-derived PyOM, it was not possible to obtain their ^{15}N NMR spectra (Table 3). The solid-state ^{15}N NMR spectrum of the unburnt grass is dominated by a signal at -257 ppm from amides (Fig. 11 and Table 3). The resonance lines at -298 ppm and -306 ppm can be assigned to NH groups. A pronounced signal at -345 ppm is in the chemical shift region of free aliphatic amino groups. With increasing burning time, the relative intensities of the amide signal and the resonance line at -345 ppm decrease. The latter completely disappears, indicating the degradation of proteins and free amino acids. This may be explained by thermolytic degradation of these compounds or their conversion to heterocyclic compounds (Sharma et al., 2003). The most important observation in the spectra is the strong increase in the relative signal intensity in the region of indoles, imidazoles and pyrroles (-145 to -240 ppm; Table 3). This might be caused by their selective preservation due to their resistance against thermal degradation or, as discussed above, by their neoformation through rearrangement of amide structures or peptides under the influence of heat (Knicker et al., 1996b).

Table 3: Relative intensity distribution in solid-state ^{15}N NMR (% of total intensity) associated with heating of rye grass at 350°C under oxic conditions.

Sample	Pyridine/ Imine-N -25 to -145 ppm	Pyrrole-N -145 to -240 ppm	Amide-N -240 to -285 ppm	Guanidine-N -285 to -325 ppm	Amino/ NH^{4+} -N -325 to -375 ppm
Rye grass	0	3	83	9	4
Gr1M	4	56	34	3	2
Gr4M	5	64	25	4	3

As determined from N_2 adsorption, the specific surface areas of all PyOM samples, except of P4M are low (around $6 \text{ m}^2 \text{ g}^{-1}$). The latter shows a significant larger surface area of $244 \text{ m}^2 \text{ g}^{-1}$ and considerable micropore surface and volume (Table 1). A comparable trend is observed for CO_2 adsorption, although here higher values were obtained. Low specific surface areas of naturally occurring charcoals have also been reported (Kwon and Pignatello, 2005). However, surface area and pore volume of charcoals depend upon both the nature of the source material and the respective method of its production and they increase with charring temperature and time (Pastor-Villegas et al., 2006; Jindarom et al.,

2007). The increasing pore volume is mainly due to partly devolatilisation of OM (Pastor-Villegas et al., 2007). This explains the considerably high values obtained for the severely charred P4M. Because CO₂ has a higher sorption affinity for coals, it is also frequently used for surface area measurements. Moreover, the higher temperature, at which the measurements are performed compared to N₂ adsorption give a higher kinetic energy to the gas molecules (de Jonge and Mittelmeijer-Hazeleger, 1996) facilitating CO₂ molecules to enter into micropores. Thus, significantly larger micropore areas and volumes are measured with this adsorption gas. On the other hand, micropores can be partly blocked by tarry matter or decomposition products formed during the charring (Pastor-Villegas et al., 2007).

For the PyOM in the present study, it was observed an increase in the micropore surface area and volume with the degree of burning, when using CO₂ (Table 1). The micropore surface of the pine chars is up to a factor of 8.3 greater than for the rye grass chars. A larger surface area of PyOM may promote the microbial accessibility and thus increase its degradability. In conclusion, the examples clearly demonstrated that the different source materials and charring conditions used in the present study resulted in chars with differences in chemical composition, as well as accessibility of surfaces, both of which are expected to affect microbial degradation.

3.2 PyOM mineralisation during incubation

The blank value (BV) CO₂ C-corrected curves determined for the cumulative OC mineralisation of the PyOM are given in Fig. 12. For the grass and pine chars, the BV contribution is less than 8% and 25%, respectively. Because of the different C contents of the PyOM (Table 1), it was necessary to normalise the CO₂-C using the corresponding PyOM-C input for a better comparison. The highest C mineralisation rates were observed for the grass-derived chars. After the first three days, more than 1% of the initial carbon of Gr1M was converted to CO₂. At the end of the incubation after 48 days, the value increased to 3.1% (Fig. 12). The incubated blank soil showed a SOC mineralisation of 2.9% at the end of the incubation, demonstrating that PyOM can be mineralised with rates comparable to that of SOM during this initial degradation phase.

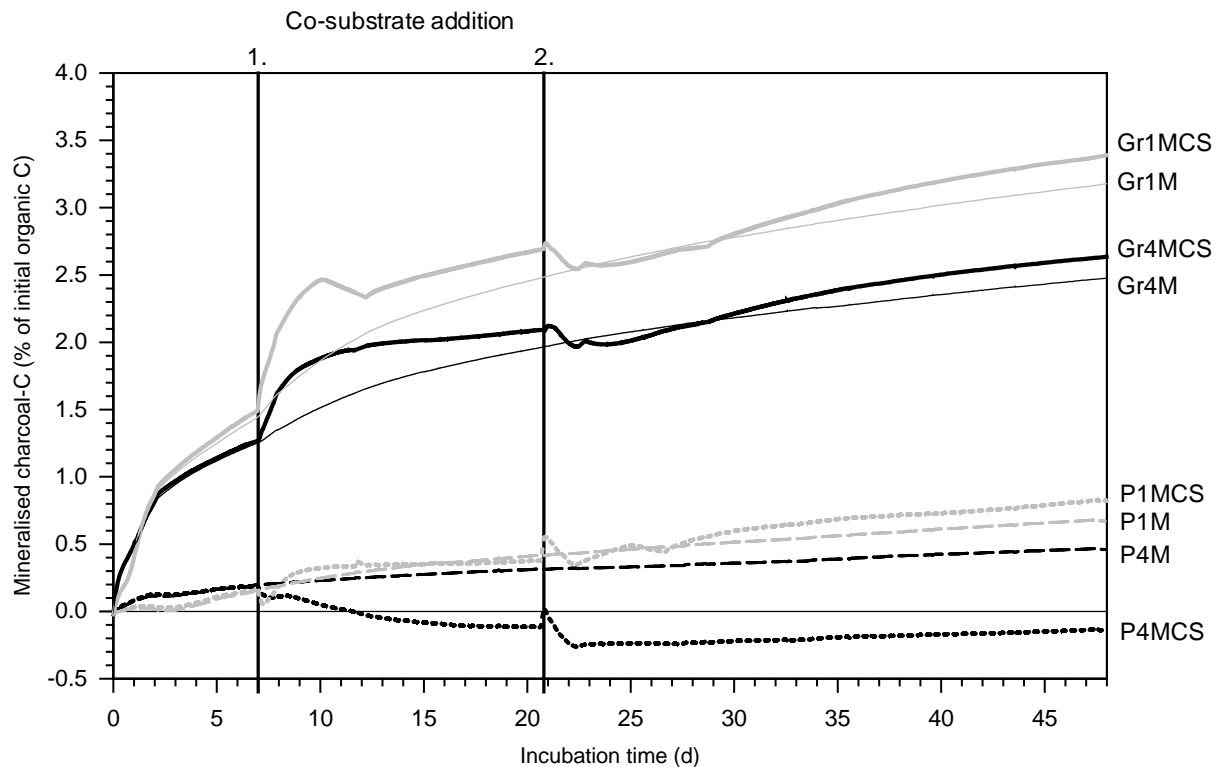


Figure 12: Cumulative CO₂-C release of PyOM produced from rye grass and pine wood at 350°C without and with co-substrate addition. Values are corrected by subtraction of CO₂-C emission of the blank values. The curves are fitted from the mean values of up to 5 replicates with a relative standard deviation < 5%.

The stronger thermal alteration of Gr4M resulted in a smaller total C turnover of 2.4%, which is 22% lower than for Gr1M. However, within the first 15 h of incubation, Gr4M was more efficiently mineralised than Gr1M (Fig. 13). During the first 2 h, Gr4M showed a maximum respiration rate of 0.6 CO₂-C mg (C g h)⁻¹ which is slightly higher than that of Gr1M [0.3 CO₂-C mg (C g h)⁻¹]. Therefore, in spite of the higher aromaticity of GR4M, this sample must contain a fraction which is microbially more available, at least at the beginning of the incubation. After this short initial response, a second maximum occurred during the second day, but at this time it was more expressed for Gr1M [0.27 CO₂-C mg (C g h)⁻¹]. Possibly this is related to alteration of the microorganism community, but may also be explained in terms of complete consumption of the more labile fraction, forcing the microorganism to rely on a more stable C source.

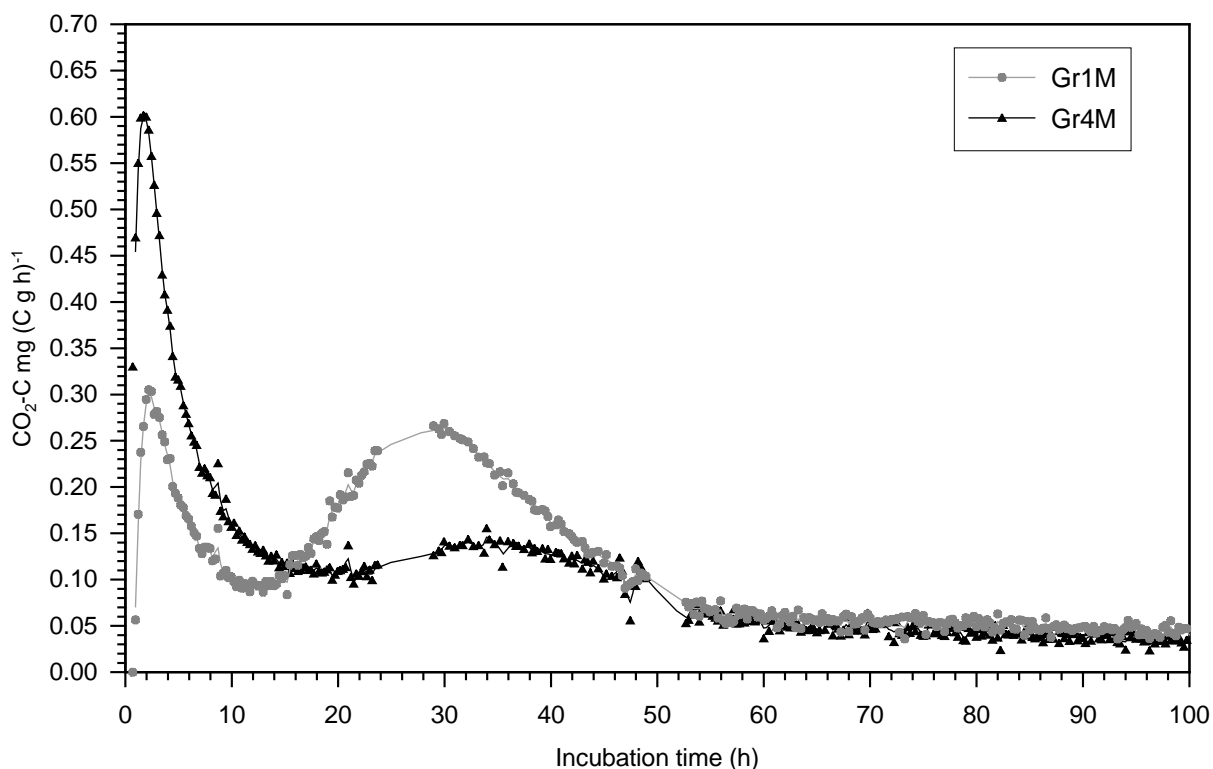


Figure 13: Changes in respiration rates of grass-derived PyOM during the very early phase of incubation. Values are corrected by subtraction of CO₂-C emission of the blank values.

Comparable to the grass chars, the pine chars show decreasing mineralisation with increasing burning degree (Fig. 12), but the effective CO₂ release is much lower. Only 0.66% and 0.46% of the initial charcoal C of P1M and P4M were mineralised. Likewise, a higher microbial activity at the beginning of the experiment for the char with the higher aromaticity is evidenced, confirming that increased charring can result in the production of a small fraction of relatively easily degradable C compounds. After 30 days, no further decline in the mineralisation rate was evidenced for all PyOM samples, indicating that this easily degradable fraction may have been completely consumed.

3.3 Impact of co-substrate addition on char mineralisation

Fig. 12 depicts the respiration curves for the different chars to which a second C source (fresh rye grass) was added as a co-substrate that was readily available to microorganisms. As shown for the incubates without co-substrate addition, the grass chars experienced more intense mineralisation (Fig. 12). Up to 3.4% of Gr1MCS was converted to CO₂ whereas only 0.8% of P1MCS was mineralised. It is noticeable that P4CS had a lower CO₂-C release than the blank (BVCS). The comparison of the BV-corrected mineralisation curves with that of the pure char incubations allows the quantification of a

potential priming effect. During the first three days after the first co-substrate addition, the char mineralisation enhanced by 31.9% for Gr1MCS and by 22.8% for Gr4MCS in relation to the incubation with solely char (Fig. 12). This indicates that a more efficient charring process is connected to a weaker positive priming effect. However, 14 days after the co-substrate addition, the amount of mineralised C already decreased to values that were only 9.2% and 7.5% higher than those for the respective samples without co-substrates. Thus, although addition of fresh grass led quickly to an acceleration of the degradation, its consumption readjusted the turnover rates to values already observed for the pure chars. A second co-substrate addition resulted in no statistical significant positive priming effect for the grass chars “incubates” at day 48.

P1MCS reflects a comparable degradation pattern as the grass chars after addition of the co-substrate (Fig. 12). On the other hand, relative to P4M, P4MCS shows a continuing decline in total CO₂ production when compared to BVCS after the first supply of fresh grass material. This effect may be explained by a char-induced inhibition of the degradation of the uncharred grass residues, possibly because soluble constituents of the grass residues diffuse into the char particles. After being adsorbed, they may turn into material that is physically protected against further mineralisation. Such stabilisation in the inner voids of char was recently evidenced with a range of organic pollutants (Cornelissen et al., 2005; Wu et al., 2007). Its occurrence in the present experiment is supported by the very high microporosity of P4M obtained from CO₂-adsorption, which is up to 8.3 and 3.7 times higher than that of Gr4M and P1M (Table 1), respectively, and the fact that no micropores were detected from N₂ adsorption with Gr1M, Gr4M and P1M. The latter strongly indicates that their micropores are too small or are blocked by organic decomposition products and therefore not accessible to N₂ molecules. After the second co-substrate addition we observe a continuous increase of the microbial activity for P4MCS (Fig. 12, day 21 to 48), possibly because of higher co-substrate availability after saturation of the char adsorption places.

3.4 Changes of the chemical quality of PyOM during incubation

Fig. 14 compares the solid-state ¹³C NMR spectra of the untreated and incubated chars and Table 4 lists the respective BV-corrected intensities for each chemical shift region. For the grass-derived char treatments, 7% of the total C and for the pine wood chars, only 5% are attributed to BV. Consequently, the natural organic matter of the soil

material contributes only slightly to the ^{13}C NMR signal of the PyOM. After incubation, it was found a decrease from 27% to 22% in the alkyl C region for Gr1M (Table 4). Furthermore, the shift of the signal at 29.2 ppm to 26.8 ppm (Fig. 14) indicates the formation of acetyl groups, possibly caused by degradation processes and accumulation of short aliphatic C chains by microbial modification. The observed alkyl C decrease corresponds to 56 mg g^{-1} of the bulk char C (Table 5). Comparably, Gr4M reveals a consumption of alkyl C from 20 to 16% and a pronounced shift of the alkyl C peak from 28.6 to 22.8 ppm (Fig. 14).

Note that, with the exception of P4M, the relative aryl C content of all samples shows no major alteration caused by the degradation, but an increasing content of carboxyl/carbonyl C is evidenced for Gr1M, Gr4M and P4M, supporting the idea that oxidation occurred (Fig. 14). Independent of the burning time of the grass chars this group increased to 25 mg g^{-1} and 32 mg g^{-1} of the bulk C for Gr1M and Gr4M at the end of the experiment.

In spite of the higher aromaticity of Gr4M vs. Gr1M, both samples show comparable carboxyl/carbonyl C contents (14%) after termination of the incubation. This can be explained by the formation of smaller C clusters by pyrolytic breakdown processes during the more intense thermal treatment of Gr4M. Such small PyOM clusters could be more available for microbiological attack, resulting in the observed similar carboxyl/carbonyl C content.

In contrast to the grass chars, the pine chars exhibit smaller total amounts of alkyl C that could serve as a potential C source for the microorganisms (Table 2). However, although P1M contains a high O-alkyl C contribution (38%), very tentatively derived from fire-unaffected carbohydrate moieties or anhydrosugars, this C source does not increase the degradation efficiency. For this sample, a loss of 30 mg g^{-1} of the bulk C was calculated, which is in the range observed for Gr1M with an O-alkyl C content of 12%. Possibly, in P1M O-alkyl C is not available for the microorganisms because of its physical protection within partly charred domains and/or of a low content of available N forms. Note that no mineral nutrient solution was added in order to simulate natural conditions.

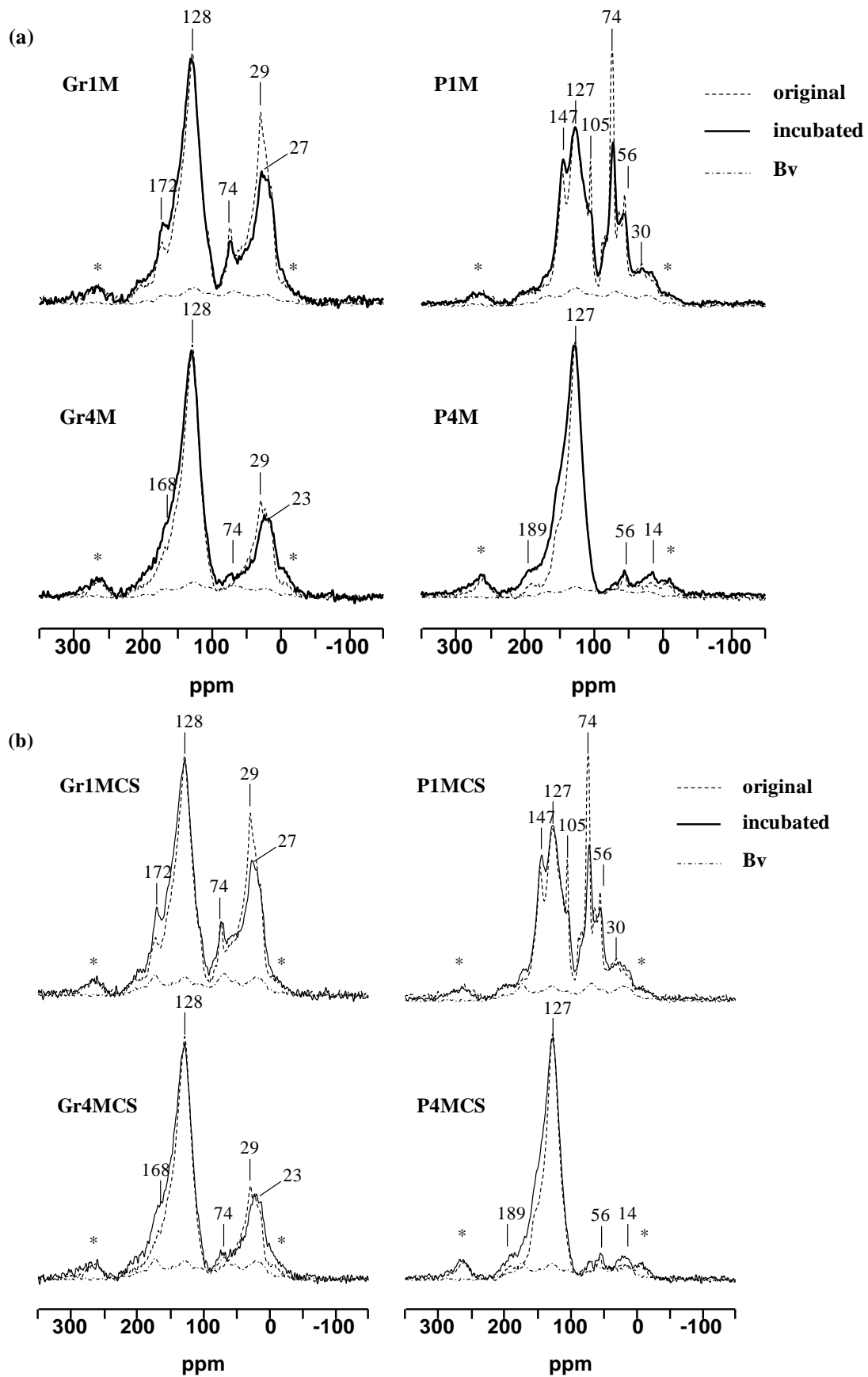


Figure 14: Solid-state ^{13}C -NMR spectra of incubated PyOM without (a) and with co-substrate addition (b) in comparison to fresh PyOM. Spinning side bands are marked with asterisk.

Table 4: Relative intensity distribution in solid-state ^{13}C NMR for PyOM produced from rye grass and pine wood after 7 weeks of incubation.

Sample	Carbonyl/ Carboxyl C	O-Aryl C	Aryl C	O-Alkyl C	Alkyl C
	relative distribution (% of total C intensity) ^a				
Gr1M	13	13	43	9	22
Gr1MCS	12	13	42	11	22
Gr4M	14	16	50	4	16
Gr4MCS	15	16	49	3	16
P1M	6	14	36	36	9
P1MCS	6	14	36	35	9
P4M	14	19	60	2	4
P4MCS	12	19	61	3	4

^a Values are corrected by subtraction of blank values calculated on a C balance for each chemical shift region.

Table 5: Changes in abundances of the different types of C for PyOM produced from rye grass and pine wood after 7 weeks of incubation.

Sample	Carbonyl/ Carboxyl C	O-Aryl C	Aryl C	O-Alkyl C	Alkyl C	Total loss ^b
	mg (g C bulk) ⁻¹ ^a					
Gr1M	25	15	18	-35	-56	-32 A
Gr1MCS	15	16	10	-15	-60	-34 A
Gr4M	32	9	1	-22	-45	-25 B
Gr4MCS	38	13	-10	-25	-42	-27 B
P1M	1	12	10	-30	1	-7
P1MCS	-3	15	19	-40	0	-9
P4M	57	36	-71	-22	-4	-4
P4MCS	44	33	-56	-14	-6	1

^a Values are standardised to C content of bulk sample; positive value indicates formation; total sum equals CO₂-C loss (mineralisation).

^b Values with different letters are significantly different at $\alpha = 0.05$ as determined by a Tukey's HSD post hoc analysis.

A decrease from 67 to 60% in intensity of the chemical shift region of H/C-aryl C (140 to 90 ppm) was found for P4M. However, the intensity in the O-aryl C (160 to 140 ppm) region increased concomitantly from 16 to 19%. An explanation for this behaviour may be a modification of the aryl rings by substitution of aromatic ring C with hydroxyl or carboxyl groups. Since the total C loss during the experiment was only 4 mg g⁻¹ (Table 5), this indicates that the aromatic ring structures must have been attacked and altered. This is supported by a total reduction of the aromatic C content of 35 mg g⁻¹. As revealed by the

increase in carboxyl/ carbonyl C contribution of 57 mg g^{-1} , this observation is best explained via opening and partial oxidation of aromatic ring structures (Hatakka, 1994; Hofrichter et al., 1997) and formation of carboxyl C.

According to the intensity distribution, a considerable fraction of the carboxyl C must be associated with aryl rings, since the contribution of the other substitutable C groups is with 6% (Table 4) too low to account for the total amount (14%) of this polar functional group. Knicker et al. (2005a) showed that the size of the polyaromatic rings in charcoal produced at 350°C is unlikely to exceed that of naphthalene-like structures with up to five substituents or clusters of maximal six condensed rings. Assuming a maximal cluster size of 6 aromatic rings connected by two bridging C (Knicker et al., 2005a), 45% of the aryl C in the chemical shift region between 90 and 140 ppm is protonated and can be regarded as substitutable aryl C. This corresponds to 27% of the total C of P4M. Knowing that 14% of the total C is assignable to carboxyl C, it can be calculated that almost every second substitutable aryl C of the cluster is connected to a carbonyl/carboxyl group. These high carbonyl C contents are in agreement with recent field and laboratory studies (Brodowski et al., 2005a; Lehmann et al., 2005; Cheng et al., 2006; Liang et al., 2006; Solomon et al., 2007). It is remarkable that, despite the relatively small mineralisation rates for the chars, especially for P4M, considerable alteration was observed with respect to the chemical composition (Table 4).

3.5 Influence of co-substrate addition on degradation level

At the end of the incubation, 50% of the fresh grass residues that were added as co-substrate were mineralised (Table 6). Consequently, relative to the non-treated samples, the addition of co-substrate increased the BV to 10% and 8% of the total C for the grass and pine char, respectively. The low O-alkyl C recovery of 18% at day 48 (Table 6) indicates that the easily degradable parts of fresh grass residues were preferentially consumed, leading to a relative enrichment in aryl C and alkyl C. The effective degradation stage of the CS is supported by a total recovery of carbonyl/ carboxyl C of 184%. In contrast, the total aryl C amount was not decreased.

Table 6: Degradation of co-substrate (CS) during incubation.

	Carbonyl/ Carboxyl C	Aryl C	O-Alkyl C	Alkyl C	Total
<i>Relative intensity contribution (%)</i>					
Fresh grass	9	8	65	18	100
Incubated grass	33	16	24	27	100
<i>Total contribution (mg)</i>					
Fresh grass	11	11	84	23	129
Incubated grass	21	10	15	17	64
Recovery (%)	184	98	18	76	50

Within the time frame of the incubation, the addition of the co-substrate resulted in no significant changes in the degradation pattern of the different PyOM samples (Table 4). It seems that co-substrate addition had no major effect on the char degradation process, because possible decomposable sources may already be available in the starting PyOM. This is supported by a preferred consumption of alkyl C with up to 60 mg g⁻¹ for the grass chars and up to 40 mg O/N-alkyl C g⁻¹ for the pine chars (Table 4). A comparable observation was reported by Cheng et al. (2006) using manure as co-substrate during 120 days of microbial char degradation. Aside from incompletely combusted sugar residues, a possible source of microbially usable compounds in the PyOM may be the “water-soluble” fractions, with its substantial contribution of 3.6% and 3.9% to the total C (C_{tot}) of Gr1M and Gr4M (Table 7). The signal at 162 ppm in their solid-state ¹³C NMR spectra is indicative of the presence of low molecular weight acids or carboxyl C directly bound to aromatic rings. As demonstrated in former studies considerable amount of microorganisms and fungi are able to survive on such structures as the only energy source (Woo and Park, 2004; Ben Said et al., 2008). The altered PyOM contains such substituted aryl compounds as shown in Table 4. These compounds could serve as a substrate for microorganisms and induce a further progressive degradation of the aged PyOM.

Table 7: Relative intensity distribution in the solid-state ¹³C NMR (% of total C) and the total contribution of PyOM water extracts.

	Carbonyl/ Carboxyl C	O-Aryl C	Aryl C	O-Alkyl C	Alkyl C	total
<i>Relative intensity contribution (%)</i>						
Gr1M	18	6	28	17	32	100
Gr4M	25	10	34	11	19	100
<i>Contribution to PyOM (%)</i>						
Gr1M	0.6	0.2	1	0.6	1.2	3.6
Gr4M	1	0.4	1.3	0.4	0.7	3.9

In contrast, the pine-derived chars delivered only small amounts of water-extractable organic matter, comprising 0.13% and 0.03% of the C_{tot} of P1M and P4M, respectively. Those yields were too low to allow the acquisition of usable solid-state ^{13}C NMR spectra. Assuming that this fraction is preferentially consumed by the microorganisms, these low yields are in line with the lower CO_2 release during incubation.

3.6 Implication of structural properties on the degradation of PyOM in soil

Subjecting different vegetation residues to increasing charring time showed that both time and source affect the chemical structure of the char products, confirming the high degree of heterogeneity for PyOM (Knicker, 2007). Comparable to the previous study (Baldock and Smernik, 2002), greater severity of the fire and limited oxygen supply go along with an increase in aromaticity. However, the presence of peptide-like structures in the source material is connected to the contribution of alkyl C in the respective charred material (Knicker et al., 2008a), as observed by comparing the pine and grass chars (Table 2). More severely charring of peptides results in formation of heterocyclic compounds (Knicker et al., 1996b) (Table 2). The solid-state NMR spectroscopic analyses clearly showed that these differences in the alkyl C and aryl C content affect the decomposability of the PyOM.

Baldock and Smernik (2002) analysed the degradability of chars produced from *Pinus resinosa* sapwood at increasing charring temperatures and confirmed that a higher aromaticity of char reduces the mineralisation rate. However, Gr1M and P1M were produced under the same charring conditions and have also comparable aryl C content (Fig. 11), but their effective char mineralisation reveals strong differences, indicating that aromaticity is not the only factor controlling the extent of CO_2 release. Although P1M contains more O-alkyl C than Gr1M, the first experienced slower mineralisation. Possibly, the O-alkyl C was protected from microbial attack by being within the partly charred lignin network (Knicker et al., 2008) or the condensation degree of the aromatic domains is higher. Alternatively, the lower N content of the pine char may limit the microbial activity. However, here one has to bear in mind that, as indicated in the solid-state ^{15}N NMR spectra, even for the grass char, the N is mostly immobilised in heterocyclic structures that are generally assumed to have low microbial accessibility.

The grass-derived PyOM samples were subjected to microbial attack of the heat resistant aliphatic C region. However, Cheng et al. (2006) observed disappearance of the

aliphatic C after incubation at 70°C, also under sterilised conditions, which was more pronounced than that at 30°C with microbial activity, demonstrating that oxidation may also occur under abiotic conditions. This implicates that the observed degradation of PyOM may be attributed to biotic and abiotic oxidation. The observed formation of carbonyl/carboxyl groups during the incubation of PyOM can increase the water solubility and thus leaching into deeper soil horizons and loss by way of transport from soils to aquatic systems. Further, the decreasing hydrophobicity by these polar groups makes the PyOM more available for further microbial attack, and also for adsorption to the mineral phase, and thus for stabilisation.

3.7 Role of the priming effect for char degradation

Hamer et al. (2004) reported relative priming effects of up to 100% even after 60 days by incubating chars at 20°C with supplements of glucose. The present study indicates also a cometabolic process occurring directly after the first addition of the co-substrate on the seventh day of incubation, but the second addition showed no clear effect and at the end of the experiment only a trend of higher metabolic activity caused by the co-substrate was visible. One explanation for this observation is the competition of microorganism groups with different surviving strategies (Fontaine et al., 2003). According to Fontaine et al. (2003), a potential priming effect results from the competition for energy and nutrient acquisition between microorganisms specialised in the decomposition of fresh organic matter (r-strategist) and those feeding on humified SOM (K-strategist). Within the short period of the experiments, only the r-strategists will develop quickly by decomposing the easily available co-substrate or uncharred plant remains and leaving partly degraded residues. Fontaine et al. (2003) claim further that these residues can be used by the K-strategists, giving them an advantage against the r-organisms when the easily available substrate is almost completely consumed. Assuming that the K-strategists are more efficient at degrading the polymeric structure of char, they will be the main agent responsible for char mineralisation at an advanced stage. However, in samples with co-substrate addition, they will have an additional source of substrate composed of partly degraded residues left by the r-strategists. This is in line with the observation that at the end of the incubation, the co-substrate was depleted in easily usable compounds. The better adaptation of the K-strategists to the remaining substrate can also explain the higher accumulated C mineralisation during the last two weeks of the incubation in the samples with co-substrate addition.

3.8 Elucidation of residence times

The mean mineralisation rate for the last 10 days was used for elucidation of possible a residence time for the PyOM without co-substrate addition. Therefore, the data were fitted with a two-component first-order decay model. During this part of the incubation, no further decline in respiration rate was observed. Relatively short mean residence times of 14 and 19 years were obtained for the charred rye grass residues Gr1M and Gr4M and up to 56 years for the pine wood chars. The findings are in agreement with those of Hamer et al. (2004), who determined residence times for charred straw residues and charred wood of 39 and 76 years, respectively. However, these are minimum turnover times because they are based on a 7 week incubation under controlled aerobic conditions. Such conditions will certainly not be available in natural environments. Cold and dry periods or anaerobic conditions in sediments can result in much slower degradation rates or even cause their preservation over a long term. Although not definitively known, it is likely that most microorganisms which oxidise the aromatic structure of char are lignin degraders, which need oxic conditions to activate their enzyme systems (Hatakka, 1994; Hofrichter et al., 1997). This could explain the high age of some PyOM findings in sediments and buried soil horizons with mostly anaerobic conditions (Schmid et al., 2001; Cao et al., 2006). However, preservation via oxygen deficiency is also a common feature of organic compounds other than char. Consequently, PyOM may not necessarily play such an important role as a long time C sink in the global C cycle in all environments. The relatively fast turnover times of plant chars estimated in the present and other studies (Hamer et al., 2004) could contribute to the unexpectedly low PyOM contribution in different field studies of fire affected sites. Dai et al. (2006), for example, described only minor effects on the size of the soil BC pool in a temperate mixed grass savannah, although the site was affected by 2 to 3 fires. Czimczik et al. (2003) noted that PyOM was not a major fraction of the soil OC pool in unburned or burned forest Siberian pine forest floors and attributed this either to rapid in situ degradation or possible relocation. The field work of Bird et al. (1999) supports the turnover times obtained for the incubations, indicating that they may be valid under natural environment conditions. They predict for well-aerated tropical soil environments that charcoal can be significantly degraded, even in a short time span.

Additionally, the mineralisation kinetic of the pure PyOM confirms that microbial degradation of severely fire-altered residues can occur already in the initial post-fire phase

even without supply of co-substrate. This further indicates that, even after intensive fires leaving almost no thermally unaltered plant residues, the newly developed microorganism communities need no additional nourishing substrate, at least at the very early post-fire phase.

4. Modification of plant biomarkers by charring and during the initial phase of biodegradation of pyrogenic organic matter in soil

The present chapter focuses on the effect of charring on the biomarker and lipid composition of different plant materials. Further, the stability of those biomarkers and lipids against biotic degradation during 7 weeks of incubation of the respective plant chars in soil was investigated. Until now, knowledge is missing how decomposition of PyOM affects the nature of thermally altered lipid fractions and if they can be used as an indicator for PyOM determination in soil.

4.1 Influence of charring on lipid content

The lipid contents of the fresh rye grass and the pine wood are comparable with 67 and 62 mg g⁻¹ and typical for these plant materials (Wiesenberg et al., 2009). The respective PyOM extracts indicate a consecutive decrease in total lipid yield with prolonged charring time (Table 8). The grass-derived PyOM contains up to 3.6 times more lipids than that of pines. The lowest lipid content was determined for the more charred pine (P4M) with only 3 mg g⁻¹. The lower amount of lipids detected for the PyOM compared to that of the fresh plant material is better explained by cracking and volatilisation losses during the charring process (Yokelson et al., 1997; Simoneit and Elias, 2001).

4.2 n-Alkanes pattern of the fresh and incubated PyOM

The total abundance of the n-alkanes is with 55 µg g⁻¹ in the same range as reported by Wiesenberg et al. (2009) for fresh rye grass. Untreated rye grass straw (Gr0M) is characterised by a predominance of long chain odd numbered n-alkanes in the range of C₂₅ to C₃₃ and C₂₉ as the dominant homologue within the aliphatic hydrocarbons (Fig 15). The observation is well established for higher plants and described in detail by Eglinton et al. (1962) and Eglinton and Hamilton (1967). The fresh pine wood (P0M) showed higher contributions of mid chain n-alkanes maximising at C₁₉ and smaller long chain n-alkanes contents (C₂₅ to C₃₃; Fig. 15). This points to a smaller contribution of epicuticular waxes in the pine wood. The grass-derived PyOM reveals an enrichment of the n-alkanes fraction with factor 3.6 (Gr1M) and 2.6 (Gr4M) relative to the fresh grass (Table 8). The higher

content of n-alkanes is attributed to a selective enrichment caused by higher thermal stability compared to other plant components and a possible synthesis by breakdown processes of other lipid fractions, e.g. the decarboxylation of fatty acids (FA). The molecular ratios of n-alkanes, in particular the average chain length (ACL) and the carbon preference index (CPI) decrease with prolonging charring time for the grass-derived PyOM (Table 8). This means that the relative predominance of long chain odd numbered n-alkanes declines for the respective PyOM and larger amounts of mid chain even numbered n-alkanes (C_{19} to C_{25}) are present. The latter is caused by thermally induced break down process of long chain odd numbered n-alkanes which was also observed by González-Pérez et al. (2008) in fire-affected soils from Andalusia (Southern Spain). The thermal degradation is confirmed by the decrease of CPI_{long} (C_{25} to C_{31}) from 8.2 to 1.2 and the shift in the short to long n-alkanes ratio $R_{s/l}$ from 0.5 to 4.1 (Table 8). The dominance of even homologues caused by thermal degradation is also reported by Wiesenberg et al. (2009) for grass and by Almendros et al. (1988), Tinoco et al. (2006) and Eckmeier and Wiesenberg (2009) for soils.

During the 7 weeks of aerobic incubation in soil, the cumulative content of n-alkanes of the grass-derived PyOM was reduced. The recovery is with 61% for the Gr1M incubate (Gr1M_{Ink}) lower than for Gr4M_{Ink} with 85% (Table 9). The higher recovery for Gr4M_{Ink} may be explained by physical entrapment. The ACL of Gr1M_{Ink} is two carbon homologues shorter than for the fresh grass PyOM, indicating degradation of long chain homologues ($> C_{26}$) and/or biosynthesis by microorganisms (Fig. 15). The observation is reflected by increasing $R_{s/l}$ ratio (Table 9). The CPI index for the incubated grass-derived PyOM is in the same range between 0.9 and 1.1 than for the fresh PyOM (Table 9).

Ambles et al. (1994) performed a biodegradation study of pure eicosane (C_{20}) added to a rendzina soil and reported a faster disappearing by 71% after one week and 89% after 8 weeks in contrast to the high C_{20} recovery in the present study (Fig. 15). The authors found out that the mineralisation of eicosane was a limiting process counting only 25% of the added C_{20} . The decrease was mainly due to biotransformation processes or transfer into other soil organic matter fractions. The observed decline of n-alkanes fraction of the PyOM incubates may be a combination of these processes.

The incubated pine chars showed in comparison with the grass chars a different modification of the n-alkanes. In general, the recovery is 2 to 3 times higher compared to the grass-derived PyOM (Table 9). However, the content of the total n-alkanes of the fresh

pine chars is up to 7 times lower than that of the grass-derived chars (Table 8). Especially octadecane (C_{18}) and the mid-chain homologues in the range C_{22} to C_{26} showed an increase (Fig. 15). The observed alteration is comparable for both pine chars, only the abundance of the n-alkanes is reduced by the factor 2.2 for P4M_{Ink}. The unexpected n-alkane formation may be explained by biosynthesis of mycelial hydrocarbons. A fungus-like exhalation of the char incubates supports the growth of mycelium. Generally, fungi biomass contains n-alkanes in the range from C_{15} to C_{36} with the predominance of long-chain C_{19-30} homologues (Merdinger and Devine, 1965; Merdinger et al., 1968; Jones, 1969) which is in agreement with the observed n-alkane formation. Marseille et al. (1999) interpreted also large concentrations of C_{25} and C_{27} n-alkanes of decomposed forest litter layers as the result of microbial production most probably by fungi.

The study reveals that the n-alkane amount of PyOM can be quickly reduced as shown for the grass chars. However, a modification and synthesis is also possible due to microbial activities during the degradation process. The plant source material and thus the chemical composition of the respective PyOM seems to have a strong influence on this process. Eckmeier and Wiesenberg (2009) propose the occurrence of short-chain n-alkanes (C_{16-20}) in ancient soils to use as molecular marker for prehistoric biomass burning. However, the present study indicates that this may only be valid if microbial activities can be excluded. Otherwise, thermally-altered and microbially-derived n-alkanes may be difficult to distinguish. In this context, the study of Kuhn et al. (2010) provides a further source of short chain n-alkanes with an even to odd predominance (EOP) in Australian woodland and grassland soils. They postulated that the origin could derive from vegetation, containing short chain n-alkanes (C_{14-20}) with pronounced EOP. Such short chain n-alkanes were not identified for the used plant species of this study.

Table 8: Abundance and molecular ratios for n-alkanes and fatty acids of the fresh and charred plant materials.

Sample	Total lipid					n-Alkanes					saturated FA					unsaturated FA	
	extract	Total ^a	ACL ^b	CPI ^c	CPI _{long} ^d	R _{s/i} ^e	Total ^a	ACL ^b	CPI ^f	R _{FA s/i} ^g	Total ^a	ACL ^b	CPI ^f	R _{FA s/i} ^g	Total ^a	Portion ^h	C _{18:1,3} /C _{18:0}
	mg g ⁻¹	μg g ⁻¹					μg g ⁻¹			μg g ⁻¹				μg g ⁻¹	%		
Gr0M	67	55	25.7	3.7	8.3	0.5	4307	16.7	24.5	10.7	5622	56.6	19.4				
Gr1M	41	199	22.2	1.2	1.4	2.7	3540	16.4	10.2	12.8	1525	30.1	5.5				
Gr4M	12	142	21.5	1.0	1.2	4.1	1127	16.4	8.6	14.3	98	8.0	0.6				
P0M	62	41	20.8	2.3	-	5.9	191	17.2	40.6	4.3	448	70.2	28.2				
P1M	18	39	21.6	1.1	1.2	6.5	119	15.9	6.9	8.5	62	34.4	7.1				
P4M	3	21	21.3	0.9	0.8	7.4	145	16.9	14.9	17.5	24	14.4	0.5				

a Total abundance = $\sum z_n$, with z_n as relative amount of n-alkane or fatty acid with n carbons.

b Average chain length = $\sum z_n \times n / \sum z_n$, with z_n as relative amount of n-alkane or fatty acid with n carbons.

c Carbon preference index of n-alkanes = $[(\sum C_{17-31\text{odd}} / \sum C_{16-30\text{even}}) + (\sum C_{17-31\text{odd}} / \sum C_{18-32\text{even}})] \times 0.5$.

d Carbon preference index of long chain n-alkanes = $[(\sum C_{25-31\text{odd}} / \sum C_{24-30\text{even}}) + (\sum C_{25-31\text{odd}} / \sum C_{26-32\text{even}})] \times 0.5$.

e Ratio between short and long chain n-alkanes $R_{s/i} = \sum C_{15-24} / \sum C_{25-33}$.

f Carbon preference index of fatty acids = $[(\sum C_{10-28\text{even}} / \sum C_{9-27\text{odd}}) + (\sum C_{10-28\text{even}} / \sum C_{11-29\text{odd}})] \times 0.5$.

g Ratio between short and long chain fatty acid $R_{FA s/i} = \sum C_{10-20} / \sum C_{21-28}$.

h Percentage of unsaturated fatty acids to total fatty acid amount.

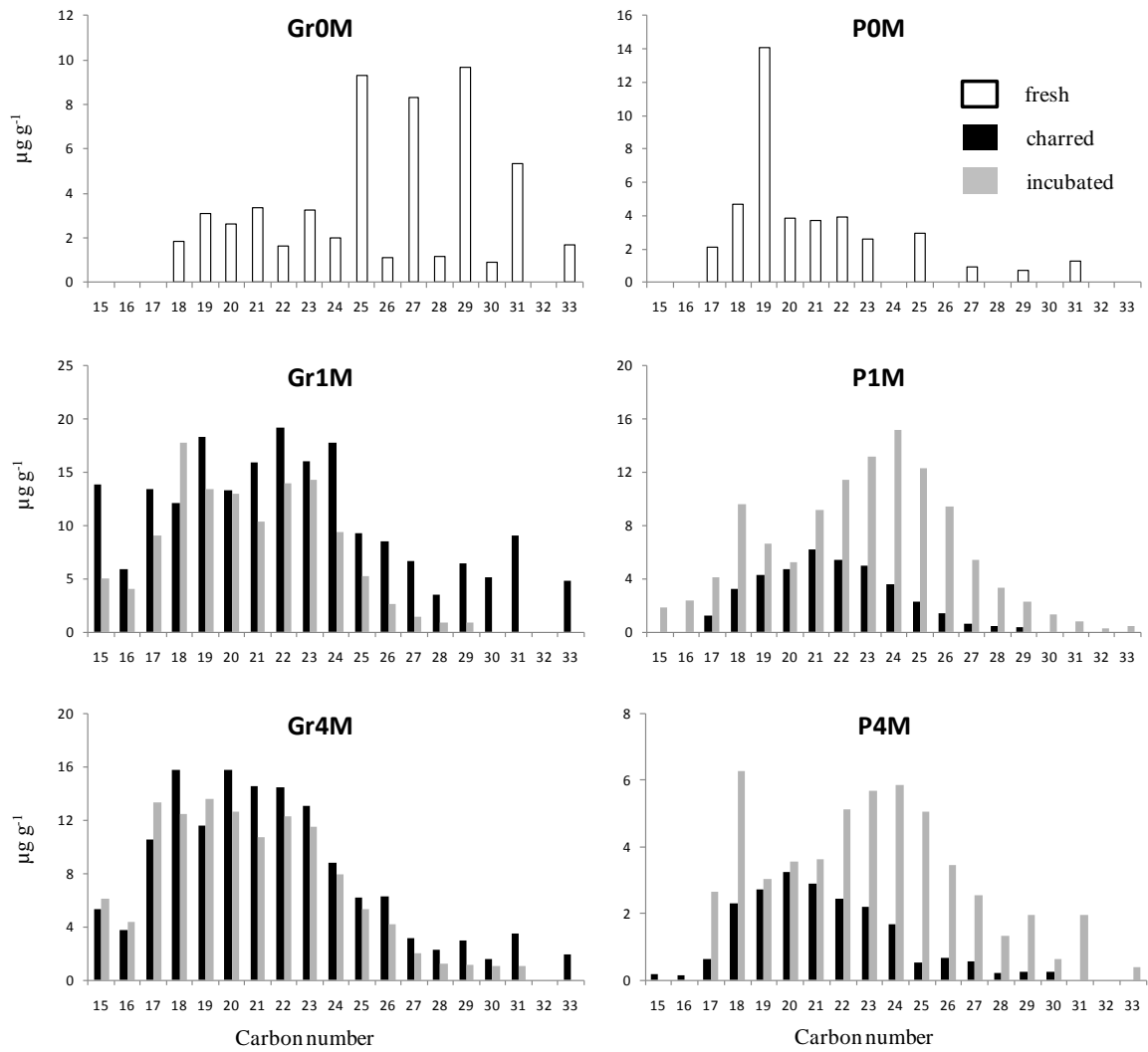


Figure 15: Abundances of n-alkanes from rye grass and pine wood and the respective fresh and incubated PyOM.

Table 9: Abundance and molecular ratios for n-alkanes and fatty acids of the incubated PyOM.

Sample	Total lipid extract			n-Alkanes				saturated FA				unsaturated FA				
	mg g ⁻¹	RC (%)	Total ^a µg g ⁻¹	RC (%) ^b	ACL ^c	CPI ^d	CPI _{long} ^e	R _{s/l} ^f	Total ^a µg g ⁻¹	RC (%) ^b	ACL ^c	CPI ^g	R _{FA s/l} ^h	Total ^a µg g ⁻¹	Portion ⁱ (%)	RC (%) ^b
Gr1M _{ink}	30	44	121	61	20.6	0.9	1.4	9.9	2540	72	16.9	8.8	7.2	145	5	71
Gr4M _{ink}	9	74	121	85	20.7	1.1	1.1	6.6	746	66	16.5	6.4	7.7	49	6	50
P1M _{ink}	10	55	53	295	22.7	0.9	1.1	2.2	319	269	16.5	6.3	7.6	140	30	225
P4M _{ink}	5	147	63	253	22.9	1.0	1.6	2.1	672	464	17.2	11.4	7.8	9	1	37

^a Total abundance = $\sum Z_n$, with Z_n as relative amount of n-alkane or fatty acid with n carbons.

^b Relative recovery of total n-alkane or fatty acid amount for the incubates.

^c Average chain length = $\sum Z_n \times n / \sum Z_n$, with Z_n as relative amount of n-alkane or fatty acid with n carbons.

^d Carbon preference index of n-alkanes = $[(\sum C_{17-31\text{odd}} / \sum C_{16-30\text{even}}) + (\sum C_{17-31\text{odd}} / \sum C_{18-32\text{even}})] \times 0.5$.

^e Carbon preference index of long chain n-alkanes = $[(\sum C_{25-31\text{odd}} / \sum C_{24-30\text{even}}) + (\sum C_{25-31\text{odd}} / \sum C_{26-32\text{even}})] \times 0.5$.

^f Ratio between short and long chain n-alkanes $R_{s/l} = \sum C_{15-24} / \sum C_{25-33}$.

^g Carbon preference index of fatty acids = $[(\sum C_{10-28\text{even}} / \sum C_{9-27\text{odd}}) + (\sum C_{10-28\text{even}} / \sum C_{11-29\text{odd}})] \times 0.5$.

^h Ratio between short and long chain fatty acid $R_{FA s/l} = \sum C_{10-20} / \sum C_{21-28}$.

ⁱ Percentage of unsaturated fatty acids on total fatty acid amount.

4.3 Free fatty acid pattern of the fresh and incubated PyOM

The free FA fraction of the fresh plant materials is mainly composed of saturated and mono- as well as di- and tri-unsaturated straight-chain homologues (Fig. 16). The total FA abundance of the fresh rye grass is 15.5 times higher than that of the pine wood (Table 8). The FAs palmitic acid ($C_{16:0}$), linoleic acid ($C_{18:2}$) and α -linolenic acid ($C_{18:3}$) were highly abundant in fresh grass with 39% of the total ion current (TIC), constituting 87% of FA extracted from rye grass (Fig. 16). This observation is in line with the findings of previous investigations of the FA abundance for grasses (Wiesenberg et al., 2004; Jansen et al., 2006; Dungait et al., 2010). Comparably, the FA distribution of the pine wood is dominated by C_{16} and C_{18} chains. These mid-chain compounds are ubiquitous in living biomass (Jaffe et al., 1996). The content of FA is with $639 \mu\text{g g}^{-1}$ in the range reported by Willför et al. (2003) for Scots pine sapwood. In contrast to the n-alkanes, the FAs of the fresh materials are characterised by a typical even to odd C-number predominance with a CPI of 24.5 (rye grass) and 40.6 (pine).

During the charring process, the amount of FA decreased by a factor of 8.1 and 3.8 for Gr4M and P4M. In general, the unsaturated FAs are more depleted in relation to the saturated counterparts (Fig. 16). With prolonging charring time, the contribution of the latter to the FA fraction reveals a sharp decline from 57% to 8% for the grass char (Table 8). Especially, linoleic acid ($C_{18:2}$) and α -linolenic acid ($C_{18:3}$) are depleted in the more severely charred Gr4M (Fig. 16), whereas oleic acid ($C_{18:1}$) is still present. An enhanced thermal decomposition with an increasing number of double bonds was also confirmed by the pyrolysis study of Ushikusa (1990). The relation of $C_{18:0}$ to the unsaturated counterparts $C_{18:1-3}$ displays a relative enrichment of saturated FA $C_{18:0}$ with increasing charring degree (Table 8). It can be concluded that severely charred plant materials will be depleted in unsaturated FA homologues. The increasing ratio $R_{\text{FA } s/1}$ of the saturated mid and short-chain FA (C_{10-20}) related to the long chain saturated FA (C_{21-28}) indicates the relative enrichment of mid chain homologues with prolonging charring time most likely due to cracking of carbon bonds (Table 8).

The reduction of the recovery of saturated FA to 72% for Gr1M and 66% for Gr4M points to their degradation and transformation to other soil organic matter groups (Table 9). The unsaturated FA followed the same trend. Comparable modification of FA occurred for the different grass chars, showing that for this material the burning degree has no visible impact on the degradation pattern (Fig. 16). In contrast, the pine chars experienced a

formation of FA with enrichment factors of 2.7 and 4.6 for the saturated FA (Table 9). The largest increase was found for FA C_{16:0} and the C₁₈ homologues (Fig. 16). An enrichment factor of 2.3 was detected for the FA C_{18:1} of the P1M incubate. The observation is in line with the detected increasing n-alkanes abundance and may be due to biosynthesis for example by fungi that are using the char as growing substrate. This assumption is supported by the fact that the FA composition of mould fungi is also dominated by saturated and unsaturated FA with 16 and 18 carbon atoms (Foppen and Griбанov, 1968; Rambo and Bean, 1969; Cooney and Proby, 1971). Note that the more severely charred P4M_{ink} shows a more expressed FA resynthesis compared to P1M_{ink} with enrichment factors of 3.1 and 3.2 for C_{16:0} and C_{18:0}, respectively (Fig. 16). During biotic incubation it was observed a more efficient oxidation of aryl structures in P4M incubates than of those in the less charred PyOM (Chapter 3.4; Hilscher et al. (2009)). This supports the idea of a higher microbial activity for P4M_{ink}. The molecular ratio ACL and CPI of all incubated PyOM is in the same range as for the fresh ones. Only the reduced ratio R_{FA s/l} indicates an enrichment of long chain FA C_{>20}. González-Pérez et al. (2008) reported a comparable trend to increase R_{FA s/l} after forest fire in soil. The authors describe a trend to reach the initial values of the control soils after 5 yrs. The present incubation study can explain that the latter is attributed by biotic *in situ* processes because no fresh plant material was added.

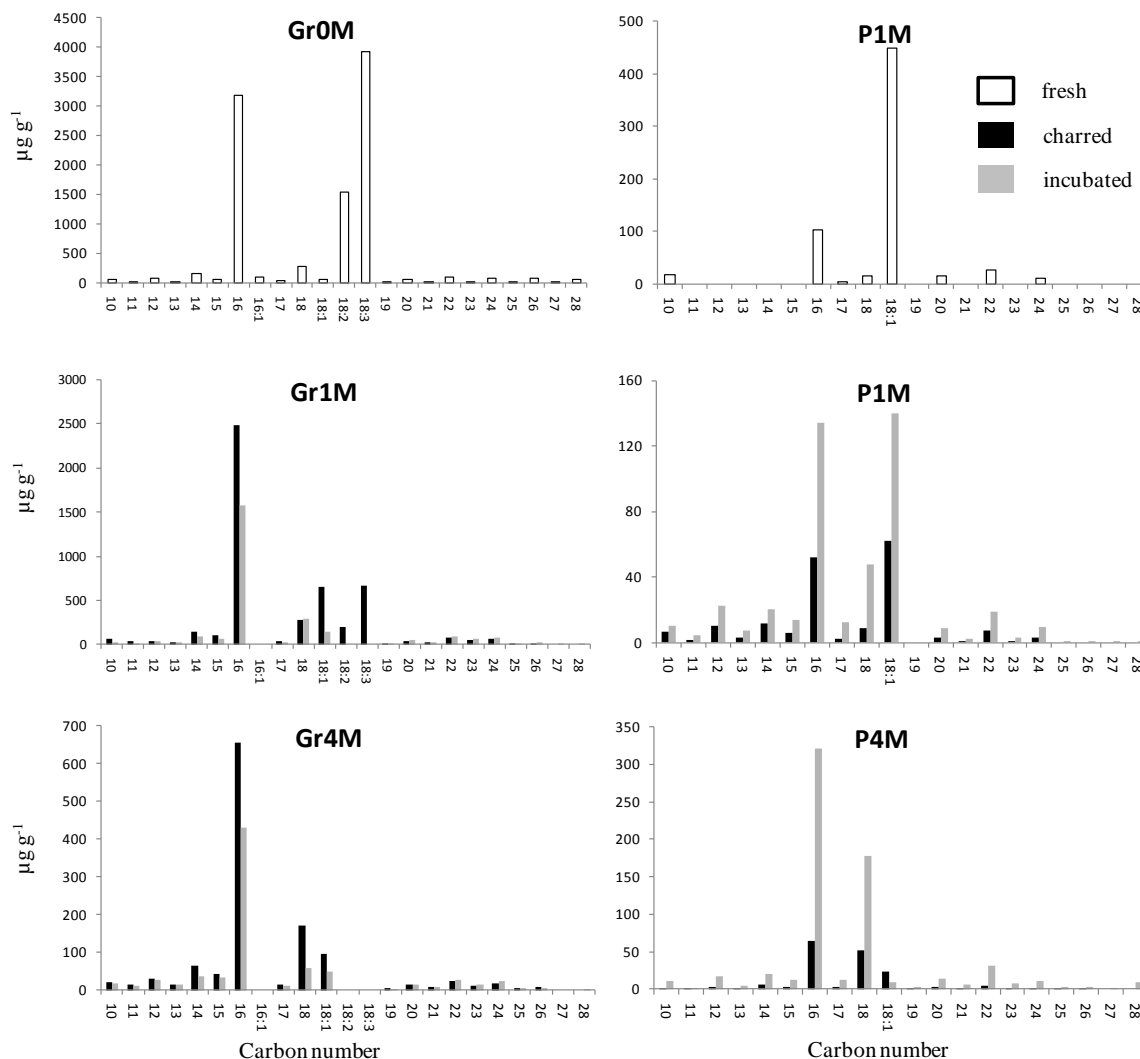


Figure 16: Abundances of fatty acids from rye grass and pine wood and the respective fresh and incubated PyOM.

4.4 Degradation of biomarkers for plant source material and biomass burning

The lipid extract of the fresh pine wood (POM) contains biomarkers such as resin acids (abietic acid, dehydroabietic acid, 7-Oxodehydroabietic acid, primeric acid; Table 10) which are typical for conifers (Willför et al., 2003; Valentin et al., 2010). In total, the resin acids account for 18.6% of the TIC, whereas dehydroabietic acid is the major resin constituent with a proportion of 70.2%. Stilbene derivatives are with 12.5% of the TIC the second main compound of the pine wood extract. The occurrence of the coniferyl alcohol vanillin, the primary aromatic alcohol monomer of gymnosperm lignin is a further typical marker for pine wood.

Table 10: Specific biomarker abundances of fresh and charred plant materials and respective recovery from the incubated PyOM.

Sample	Vanillin		Resin acids ^a		Levoglucosan ^b	
	TIC (%) ^c	RC (%) ^d	TIC (%) ^c	RC (%) ^d	TIC (%) ^c	RC (%) ^d
Gr0M	-	-	-	-	-	-
Gr1M	-	-	-	-	3.6	0
Gr4M	-	-	-	-	1.7	0
P0M	2.2	-	18.6	-	-	-
P1M	22.7	8	1.0	149	17.2	23
P4M	0.3	0	3.5	23	2.2	85

a Conifer biomarker (sum of abietic acid, dehydroabietic acid, 7-Oxodehydroabietic acid and primeric acid).

b Indicator for biomass burning.

c Percentage of the total ion chromatogram (TIC) area of the fresh PyOM.

d Total recovery of biomarkers for the incubated PyOM.

Already after 1 min of charring only a small amount of dehydroabietic acid derivatives and no other resin acids or stilbenes were detected for the pine char (Table 10), indicating a low thermal stability of these conifer biomarkers. The TIC of the P1M char shows a strong relative accumulation of vanillin with 22.7% (Table 10). This is in agreement with the study of Hilscher et al. (2009) (Chapter 3.4) reporting an accumulation of methoxyl C and O-aryl C signals in the ¹³C NMR spectrum of P1M and confirms former findings demonstrating that some lignin derivatives survives the charring process (Knicker et al., 2008a). The signal of vanillin completely disappears in the chromatogram of the sample after 4 min of charring, indicating a complete demethoxylation of the lignin structures.

Levoglucosans are detectable in all fresh PyOM, whereas P1M has with 17.2% of the TIC the highest contribution of all PyOM (Table 10). The grass-derived PyOM contains smaller contributions of LG. With prolonging charring time (4 min) the total amount of LG is decreased by 86.1% and 97.6% in relation to the respective PyOM 1M for the rye grass and the pine wood, respectively. This indicates that severely burnt plant material can be depleted in LG. The observation is in line with the study of Kuo et al. (2008) who detect LG only in low temperature char (150-350°C).

The content of resin acids of the pine-PyOM incubates shows no clear trend during incubation. Only for the P4M incubate, degradation was observed which was indicated by small recovery of 23% of the resin acid amount occurring in the fresh char. An elimination of resin acids by 80% after treatment with various white-rot fungi for 4 weeks was

described by Dorado et al. (2000) identified in acetone extractives of Scots pine sapwood. White-rot fungi could be also responsible for the degradation of resin acids of the PyOM that survived the charring.

The vanillin residues of the pine chars were efficiently decomposed during the incubation period of 7 weeks. Only 8% of the initial amount was recovered for the P1M_{ink} and the small initial content of P4M was completely degraded (Table 10). White-rot fungi attack efficiently lignin structures (Blanchette, 1991; Hatakka, 1994) and may be responsible for the observed loss.

The marker for charring of cellulose LG was completely decomposed for the grass-derived PyOM incubates and the most LG containing P1M revealed a loss by 77% (Table 10). Environmental studies dealing with the fate of LG in soils and sediments are rare. However, microbial laboratory studies confirmed that LG is fermented and metabolised by yeasts and fungi (Kitamura et al., 1991; Prosen et al., 1993). In this line, Xie et al. (2006) isolated 26 types of LG-assimilating microorganisms from four types of soil in China. This indicates that the use of LG as a tracer for burning in soil may lead to underestimation because under optimal environmental conditions of the laboratory incubation it was rapidly lost.

5. Degradation of ^{13}C and ^{15}N labelled grass-derived PyOM, transport of the residues within a soil column and distribution in soil organic matter fractions during a microcosm experiment

As described in chapter 3, PyOM was efficiently degraded during a short-time incubation. The intention of this study is to examine the degradation potential of PyOM on a long-term scale. For understanding the environmental cycling of PyOM it is important to quantify potential translocation and redistribution processes. Isotopic labels were used to determine the partitioning of PyOM into different SOM fractions and to trace the vertical movement of PyOM residues in a soil column. The availability of a co-substrate on the mineralisation, redistribution and transport of PyOM was also considered.

5.1 Characterisation of the isotopically labelled grass material during thermal treatment

After 1 min thermal treatment, PyOM 1M showed a slight increase of the C concentration and a clear relative enrichment of N (Table 11). A longer charring time of 4 min resulted in a C loss of 66%. The declining atomic C/N values in the PyOM are in line with a preferential accumulation of N, supporting the importance as a PyOM component of the latter. The proportion of NH_4^+ N in the total N of the PyOM was, with up to 0.3 g 100 g⁻¹, very low (Table 11), allowing the conclusion that most N input in the incubation study represents organically bound N. The ^{13}C and ^{15}N losses during the charring were slightly lower than the total C and N losses (Table 11). This relative isotopic enrichment was significant ($p < 0.001$) and may be a result of to the kinetic isotope effect, which results from a lower reactivity of isotopically heavier compounds. Studies dealing with the influence of burning on the ^{13}C signature of char showed conflicting results (Bird and Grocke, 1997; Czimczik et al., 2002). Turekian et al. (1998) similarly observed an enrichment of ^{15}N in burnt residues relative to the original vegetation. They suggested that different N pools of nitrogenous compounds were accessed at different temperatures of heating. The authors postulated that the initial ^{15}N enrichment of the charred residual material could be caused by the volatilisation of ^{14}N containing free ammonia within the plant material or the deamination of free amino acids. With increasing charring this N pool

becomes enriched in ^{15}N as ^{14}N is preferentially lost through kinetic isotope effects. A second pool of ^{15}N could be representative of bound amino acids which require the increased heat in order to take place for the combined hydrolysis and deamination reaction. The observed significant ^{15}N enrichment with increasing charring intensity in the present study supports the explanation of Turekian et al. (1998). The charring of the labelled grass material resulted in PyOM with an isotopic contribution of 25.2 atom% (^{13}C) and 66.0 atom% (^{15}N) allowing an effective tracing in the soil during the incubation.

Table 11: Elemental and isotopic composition of fresh and burnt rye grass and isotopic losses during charring at 350°C under oxic conditions^a.

Sample	C		N		C/N (atomic)	NH_4^+ N g/100 g	C loss g/100 g initial amount	N loss g/100 g initial amount	^{13}C atom%	^{15}N g/100 g initial amount	^{13}C loss g/100 g initial amount	^{15}N loss g/100 g initial amount
	g kg ⁻¹	g kg ⁻¹	g kg ⁻¹	g kg ⁻¹								
Fresh rye grass	382 ± 2A	19 ± 1A	17 ± 0.0A									
PyOM 1M ^b	415 ± 5B	31 ± 1B	11 ± 0.1B	0.2	53	28	23.5 ± 0.2A	62.8 ± 0.2A	50	28		
PyOM 4M ^c	377 ± 8A	34 ± 1C	9 ± 0.2C	0.3	66	37	24.8 ± 0.3B	63.2 ± 0.2A	64	34		
ANOVA <i>p</i> -value	<0.001	<0.001	<0.001	<0.001	<0.001	<0.001	<0.001	<0.001	<0.001	<0.001		

^a mean values and standard deviation (±) are calculated using 5 replicates;

elemental concentration and isotopic content with different letters were significantly different according to an one-way ANOVA and a Tukey's honest significant difference post-hoc comparison.

^b Pyrogenic organic material produced with charring time of 1 min.

^c Pyrogenic organic material produced with charring time of 4 min.

Figure 17 displays the ^{13}C NMR spectra of the fresh and charred rye grass residues. Most of the intensity in the spectrum of the fresh rye grass is in the region assigned to O/N-alkyl C between 110 and 45 ppm (Table 12). A further strong signal is observable in the alkyl-C region (45 to 0 ppm). According to a previous study (Knicker et al., 1996b), it derives mainly from peptides and peptide-like constituents rather than from paraffinic units in plant waxes.

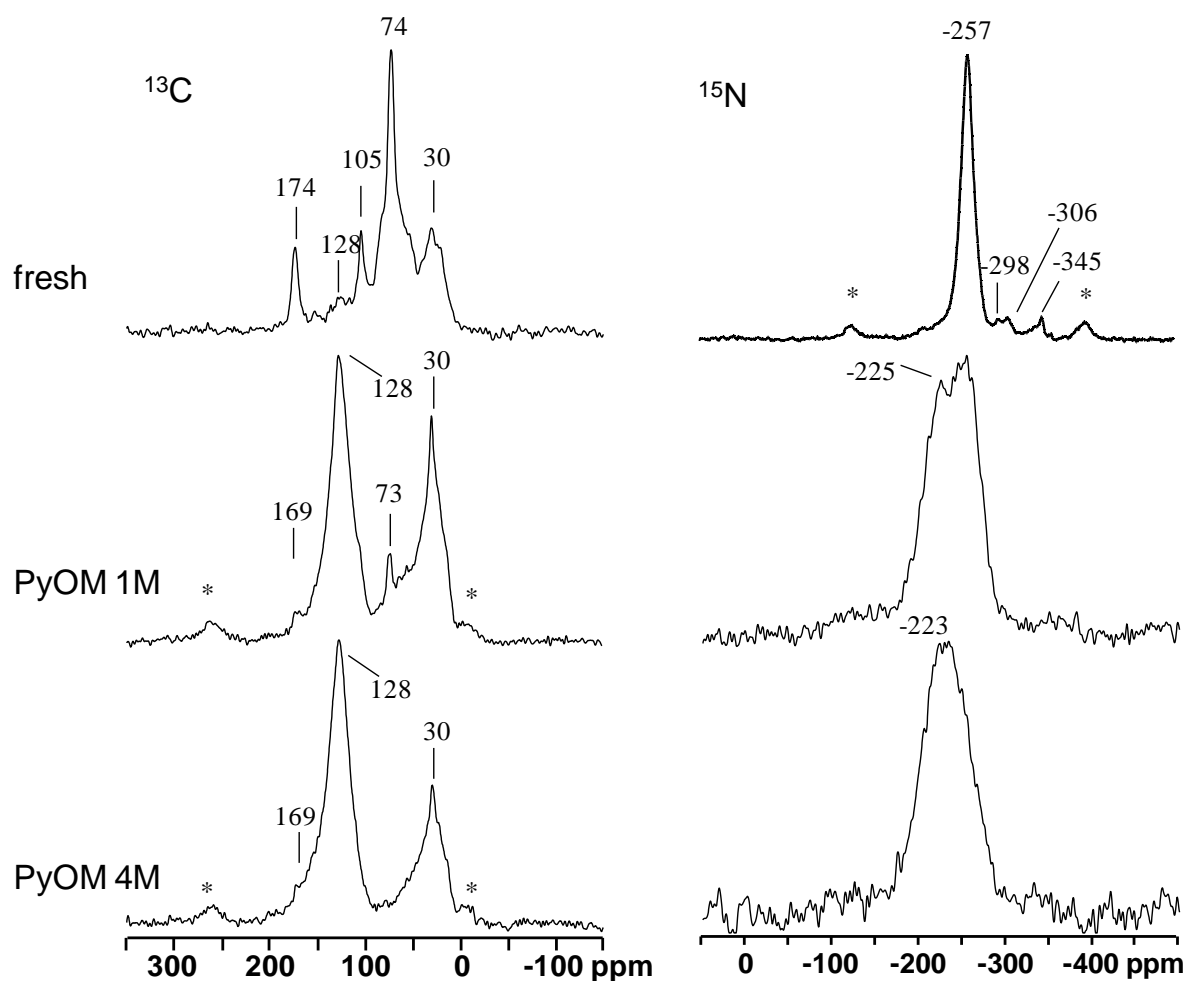


Figure 17: Solid-state ^{13}C NMR and ^{15}N NMR spectra of fresh rye grass (*Lolium perenne* L.) and charred residues produced under oxic conditions for 1 (PyOM 1M) and 4 min (PyOM 4M) at 350°C. Spinning side bands marked with asterisks.

Table 12: Intensity distribution of solid-state ¹³C and ¹⁵N NMR spectra (%) of fresh rye grass and its residue (PyOM) charred at 350°C under oxic conditions.

Sample	¹³ C NMR					¹⁵ N NMR				
	Carbonyl/ Carboxyl C 245 to 160 ppm	O-Aryl C 160 to 140 ppm	Aryl C 140 to 90 ppm	O/N-Alkyl C 90 to 45 ppm ^d	Alkyl C 45 to 0 ppm	Pyridine/ Imine-N -25 to -145 ppm	Pyrrole-N -145 to -240 ppm	Amide-N -240 to -285 ppm	Guanidine- N -285 to -325 ppm	Amino/ NH ⁴⁺ -N -325 to -375 ppm
Fresh rye grass	11 ± 0.7	3 ± 0.4	10 ± 0.9	55 ± 0.5	21 ± 0.7	0	3	83	9	4
PyOM 1M ^b	5 ± 0.4	7 ± 0.3	46 ± 0.9	15 ± 0.8	27 ± 0.3	4	56	34	3	2
PyOM 4M ^c	8 ± 0.2	11 ± 0.2	51 ± 0.5	9 ± 0.9	21 ± 0.6	5	64	25	4	3

^a Mean values and standard deviation (±) are calculated after repeating (5 x) ¹³C NMR measurement

^b Pyrogenic organic material produced with charring time 1 min.

^c Pyrogenic organic material produced with charring time 4 min.

^d Chemical shift ranges applied for PyOM, for the fresh rye grass material the O/N-alkyl region was set to 110 – 45 ppm.

The spectra of the chars show an increase in aromaticity (signal between 160 and 90 ppm) with charring time, although a high contribution of alkyl C (45 to 0 ppm) was still detectable. Considering the high peptide content of the source material, the signal is assigned to thermally altered, but relatively heat resistant, products of proteinaceous material (Knicker et al., 2008a). The ^{13}C NMR spectra of the more thermally treated char revealed no signals attributable to cellulose or carbohydrate. This, and the fact that the 128 ppm signal in the aromatic region dominates the spectrum, confirms that they can be taken as representative of severely charred material. The ^{13}C NMR spectra of the grass-derived PyOM produced for the respiration experiment (Chapter 3.1) are quite similar in general appearance and even relative areas, showing acceptable reproducibility in the preparation of the PyOM.

To test the reproducibility of the intensity distribution, the solid-state ^{13}C NMR spectra of the PyOM, aliquots of the sample material were measured five times. The total standard deviation determined for each C group is $< 1\%$ (Table 12), which confirms the good reproducibility for the NMR technique. This is in line with other recent SOM-related NMR studies (Dieckow et al., 2005; Knicker et al., 2005b).

The ^{15}N NMR spectrum of the unburned grass shows a signal at -257 ppm, typical for amide N (Fig. 17 and Table 12). With increasing burning time, its relative intensity decreases, which can be explained by thermolytic degradation of these compounds or their conversion to heterocyclic compounds (Almendros et al., 2003). The latter is confirmed by the strong increase in the relative signal intensity in the region for indoles, imidazoles and pyrroles (-145 to -240 ppm; Table 12). A detailed description of chemical modifications during the thermal treatment of plant material is provided in chapter 3.1.

5.2 Reproducibility of PyOM recovery

Although the availability of labelled plant material was limited, the reproducibility of label recovery was tested for the PyOM samples incubated for two months. For the A layer of the soil column, the absolute deviation for the ^{13}C and ^{15}N recovery ranged between 1% and 4%, corresponding to a relative deviation $< 4\%$ (Table 13). The reproducibility of the respective sub-layers was comparable. For all samples, the total deviation was between 0.0% and 0.3%. The PyOM recovery for the SOM fractions from the A layer showed comparably good reproducibility. The good reproducibility underlines the high analytical sensitivity with highly isotopically enriched PyOM. In particular, the recovery of the

PyOM, even for fractions where it occurred only in low abundance, was improved with this technique. Because of the use of homogenised sample material and controlled laboratory conditions for the incubation experiment, the experimental design discharges the scientific requirements. This is in line with the results of a PyOM respiration study by Hilscher et al. (2009), who showed that the relative deviation of 5 replicates was $< 5\%$ (Chapter 3.2).

Table 13: Reproducibility of recovery of ^{13}C and ^{15}N from isotopically enriched PyOM from 2 month incubated samples (mean values calculated from duplicates).

	PyOM ^a sample	PyOM ^a recovery (%)	
		^{13}C	^{15}N
A layer	1M ^e	91 ± 3	101 ± 4
	4M ^f	81 ± 2	81 ± 1
B layer	1M	0.3 ± 0.0	1.3 ± 0.2
	4M	0.6 ± 0.0	1.1 ± 0.0
C layer	1M	0.3 ± 0.0	0.8 ± 0.3
	4M	0.4 ± 0.1	1.0 ± 0.1
Outflow	1M	0.6 ± 0.1	0.6 ± 0.2
	4M	0.4 ± 0.1	0.4 ± 0.1
Sum	1M	93 ± 3	103 ± 4
	4M	82 ± 2	84 ± 1
SOM ^b fractions of A layer			
DOM ^c	1M	0.2 ± 0.1	1.0 ± 0.4
	4M	0.1 ± 0.0	0.6 ± 0.1
POM ^d	1M	70 ± 3	84 ± 4
	4M	68 ± 1	65 ± 0
Mineral phase	1M	11.3 ± 0.1	15.3 ± 0.4
	4M	12.3 ± 0.3	16.3 ± 0.8
Particle size fractions			
5000-63 μm	1M	0.0 ± 0.0	0.0 ± 0.0
63-20 μm	1M	0.1 ± 0.1	0.0 ± 0.0
20-6.3 μm	1M	0.3 ± 0.1	0.2 ± 0.1
6.3-2 μm	1M	2.1 ± 0.5	2.1 ± 0.8
< 2 μm	1M	10.2 ± 0.5	12.3 ± 0.9
5000-63 μm	4M	0.0 ± 0.0	0.0 ± 0.0
63-20 μm	4M	0.0 ± 0.0	0.0 ± 0.0
20-6.3 μm	4M	0.3 ± 0.1	0.2 ± 0.1
6.3-2 μm	4M	2.5 ± 0.1	3.3 ± 0.2
< 2 μm	4M	10.5 ± 0.3	14.4 ± 1.7

^a Pyrogenic organic material.^b Soil organic matter.^c Dissolved organic matter.^d Particulate organic matter.^e Charring time 1 min.^f Charring time 4 min.

5.3 Recovery of ^{13}C and ^{15}N labelled PyOM in soil column

The sum of the ^{13}C recoveries from the three sub-layers indicates a loss of PyOM, which continuously increased with prolonged incubation time (Fig. 18). This is best explained by the release of $^{13}\text{CO}_2$ during PyOM degradation. After 20 months incubation, between 65% and 73% of the initial ^{13}C input was recovered. Co-substrate applications did not enhance PyOM mineralisation ($p = 0.168$; Fig. 18). It seems that co-substrate addition had no major effect on the extent of PyOM loss, possibly because decomposable sources were already available in the starting PyOM. This is in line with the 2 month, high resolution respiration study (Hilscher et al., 2009) using similar PyOM (Chapter 3). The increasing charring degree resulted in no significant decrease in the mineralisation of PyOM ($0.428 \leq p \leq 0.772$). After 28 months, the recovery of ^{13}C was only between 62% and 65%. The respective ^{15}N recoveries followed the same trend but tended to be slightly higher (between 67% and 80%; Fig. 18). This is in line with a relative enrichment in N compounds. To explain the N losses, one has to bear in mind that N could only leave the soil column as gaseous emissions. Thus, some of the ^{15}N compounds must have been mineralised to $^{15}\text{NO}_3^-$ and subsequently denitrified to $^{15}\text{N}_2\text{O}$, ^{15}NO and $^{15}\text{NO}_2$ (Yamulki and Jarvis, 2002; Pinto et al., 2004). However, for microbial denitrification, alternate aerobic-anaerobic conditions are favourable. In fact, the soil columns were adjusted to a soil moisture content of 60% WHC which provides water-filled pore space, allowing this process.

The study reveals quick mineralisation rates for PyOM that are unexpected with respect to the commonly assumed recalcitrance of PyOM. However, Nguyen and Lehmann (2009) found comparable mineralisation rates for BC produced from corn (*Zea mays L.*) at a charring temperature of 350°C. They calculated a C loss of up to 21.2% during the first year of incubation, which was performed under comparable conditions to the present study. In contrast to the present results, the incubation study of Kuzyakov et al. (2009), who used ^{14}C -labelled grass-derived char in pure sand, revealed a lower decomposition rate of 0.5% BC per year, possibly because the material experienced more intense chemical alteration after 14 h charring. This difference supports the idea that charring conditions can affect the degradability of PyOM.

The observed fast turnover rates of PyOM in the present work could explain the unexpected small char contribution found by the field study of Dai et al. (2006). The authors described only minor effects on the size of the soil BC pool in a temperate mixed

grass savannah, although the site was affected by 2–3 fires. Comparable short residence times were obtained for Russian steppe soils where the BC stocks decreased about 25% over a century (Hammes et al., 2008). In this line, the study of Bird et al. (1999), examining sandy savannah soils, predicted for well aerated tropical soil environments that charcoal can be significantly degraded, even over a short time span. Based on the field study findings it can be concluded that the observed fast PyOM mineralisation rates of this study can also occur under natural conditions and PyOM cannot be assumed to be recalcitrant in all soils.

5.4 Relocation of PyOM in soil column

Isotopic measurements indicate that up to 2.3% of the ^{13}C PyOM was found for the B soil layer of the 4MCS treatment (Fig. 18). The fast initial vertical movement during the first 2 months may be explained by direct leaching of “water-soluble” fractions produced during the charring process and remaining in the PyOM (Table 7; Hilscher et al. (2009)). It is also possible that small clay-sized PyOM particles were physically translocated, since Skjemstad et al. (1999) showed that >90% of soil char occurs in the <53 μm fraction.

PyOM 4M and PyOM 1MCS showed a comparable or higher migration potential (Fig. 18) than PyOM 1M and PyOM 4MCS. This is remarkable because of the larger contribution of aromatic compounds, which in chars is commonly assumed to be hydrophobic and thus less mobile. A substitution of aryl C with polar functional groups as a result of degradation processes, as described by Hilscher et al. (2009) (Chapter 3.4) could be an explanation. Alternatively, the isotopic label in the deeper layers may derive from small C clusters formed by pyrolytic breakdown during the more intense thermal treatment (Czimczik et al., 2002; Knicker et al., 2005a).

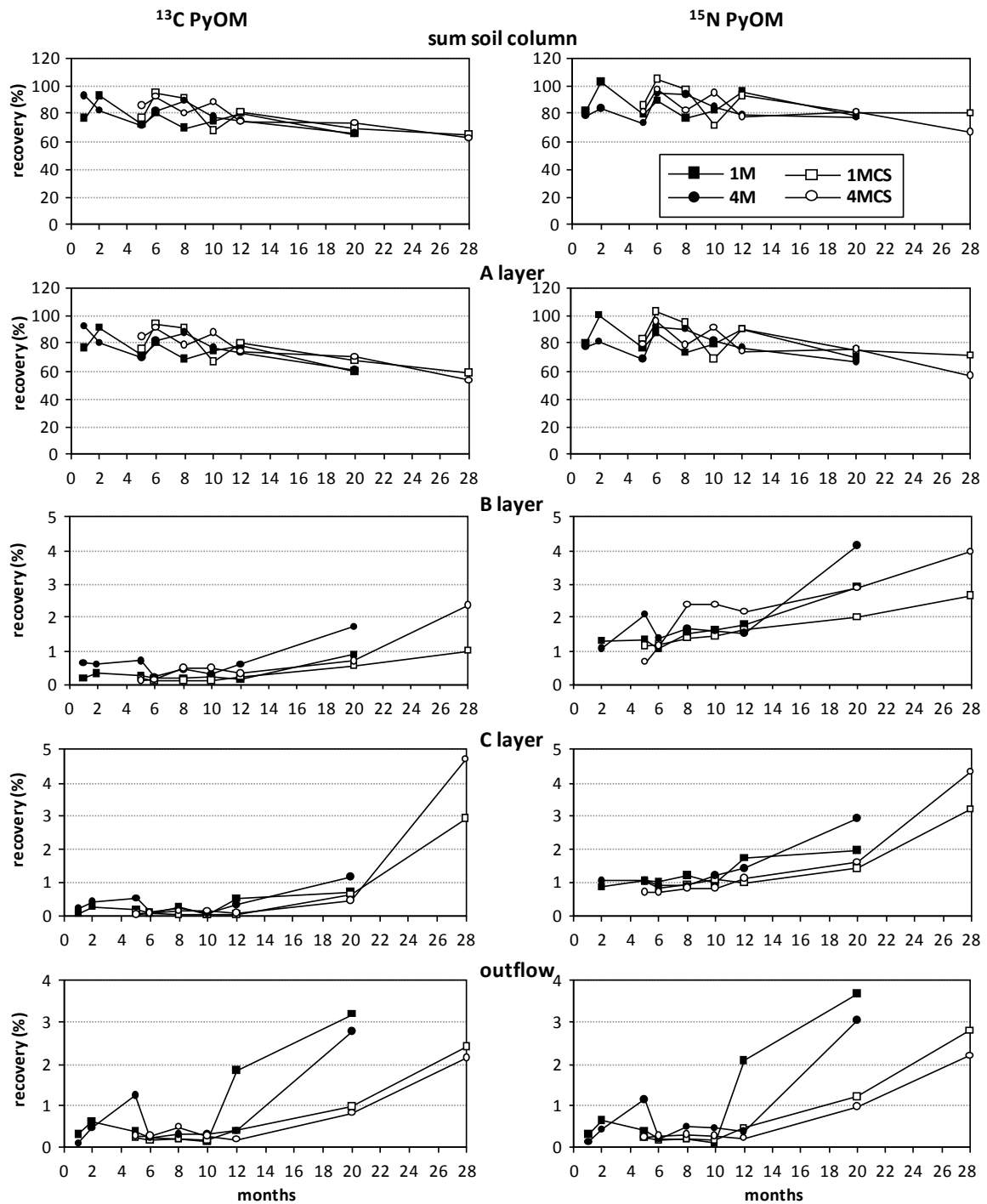


Figure 18: Recovery of ^{13}C and ^{15}N labelled PyOM in the soil layers A (0-2 cm), B (2-5 cm) and C (5-8 cm) as a function of incubation time. Values corrected by subtraction of natural ^{13}C and ^{15}N background. (1M, pyrogenic material from charring time of 1 min; 4M, pyrogenic material from charring time of 4 min; CS, addition of fresh rye grass as co-substrate; BV, blank incubated without PyOM addition)

In comparison to ^{13}C , the ^{15}N PyOM recovery was 5 to 10 times higher in the B layer after 12 months incubation, which points to a preferential transport of N containing compounds ($p < 0.001$). With progressive incubation, a clear increase of the ^{15}N label was revealed for the B layer (Fig. 18). The C layer, with a depth of 5 to 8 cm, reflected the same ^{13}C and ^{15}N PyOM incorporation pattern (Fig. 18), although the recovery was initially lower because of the longer migration pathway. At the end of the experiment, the ^{13}C and ^{15}N yields were in the same range as for the B layer. The ^{13}C and ^{15}N recoveries in the “outflow” (leachate) indicate that PyOM was transported downwards for a distance of 8 cm and even left the soil column (Fig. 18). At the end of the experiment up to 3.2% of ^{13}C and 3.7% of ^{15}N were found in the collected leachate. In total, up to 9.2% of the ^{13}C and 10.5% of the ^{15}N label were relocated downwards from the A layer to the sub-layers.

The vertical movement of PyOM during the incubation experiment is in agreement with observations by Hockaday et al. (2006) who identified charcoal degradation products in pore water of fire-affected forest soil (75 cm depth). This indicates that oxidation and dissolution of charcoal occurs on a centennial timescale. On the other hand, Skjemstad et al. (1999) have shown that $> 90\%$ of soil char is included in the $< 53 \mu\text{m}$ fraction. Hence, such fine particles should be relatively mobile. The results are also in line with the findings of Dai et al. (2006). They showed that, in a temperate mixed-grass savannah, the highest rates of accumulation of PyOM was observed at 10 – 20 cm, which suggests that PyOM was translocated to lower horizons. Another observation of the potential mobilisation of PyOM is given by Rodionov et al. (2006) for a steppe soil in Russia. They concluded that water flux transporting material from the upper soil layer may have intensified the BC maximum in the 30 to 50 cm depth range. The incubation study clearly confirms the mobilisation of PyOM (8 cm depth) and indicates that this is supported by prior microbial degradation and mineralisation activities.

5.5 ^{13}C and ^{15}N PyOM partitioning in soil fractions of the A layer

5.5.1 DOM fraction

Among the SOM fractions, DOM had the lowest contribution to total SOM (Fig. 19). During the first year of incubation, the ^{13}C recovery increased from 0.1% after 1 month to 0.4% after 12 months (Fig. 19). All incubation series followed this trend of increased PyOM mobilisation. This is best explained by pyrogenic DOC, resulting from the metabolic activity of microorganism, and physical and chemical leaching processes. After

20 and 28 months incubation, a decline to a constant recovery of 0.1% for the ^{13}C label in the DOM fraction was apparent. In comparison to ^{13}C recovery, recovery of ^{15}N was remarkable. In general, the percentages of the latter were one order of magnitude higher ($p < 0.001$), supporting a clear relative enrichment in ^{15}N (Fig. 19). The fact that the C/N ratio was approaching values < 1 after 12 months points towards an accumulation of inorganic N (Fig. 20). The respective BV-corrected $^{13}\text{C}/^{15}\text{N}$ values for the DOM followed the same trend and confirmed ^{15}N accumulation with increasing incubation time (Fig. 20). This inorganic ^{15}N enrichment must derive from ^{15}N mineralisation, since 99.7% of the ^{15}N PyOM input was organically bound ^{15}N (Table 11).

In general, the total recoveries of PyOM in DOM were low compared to the other SOM fractions. However, it has to be borne in mind that DOM can be removed by adsorption to mineral surfaces (Kaiser and Guggenberger, 2000) and/or be efficiently attacked and mineralised by considerable numbers of microorganisms (Woo and Park, 2004). This continuing process of production and consumption demonstrates that leaching of PyOM should not be underestimated. The present data support the idea that the recalcitrance may not be the rate limiting factor in soil PyOM turnover times (Hockaday et al., 2007), since PyOM contributes C to the DOM fraction within a very short time scale.

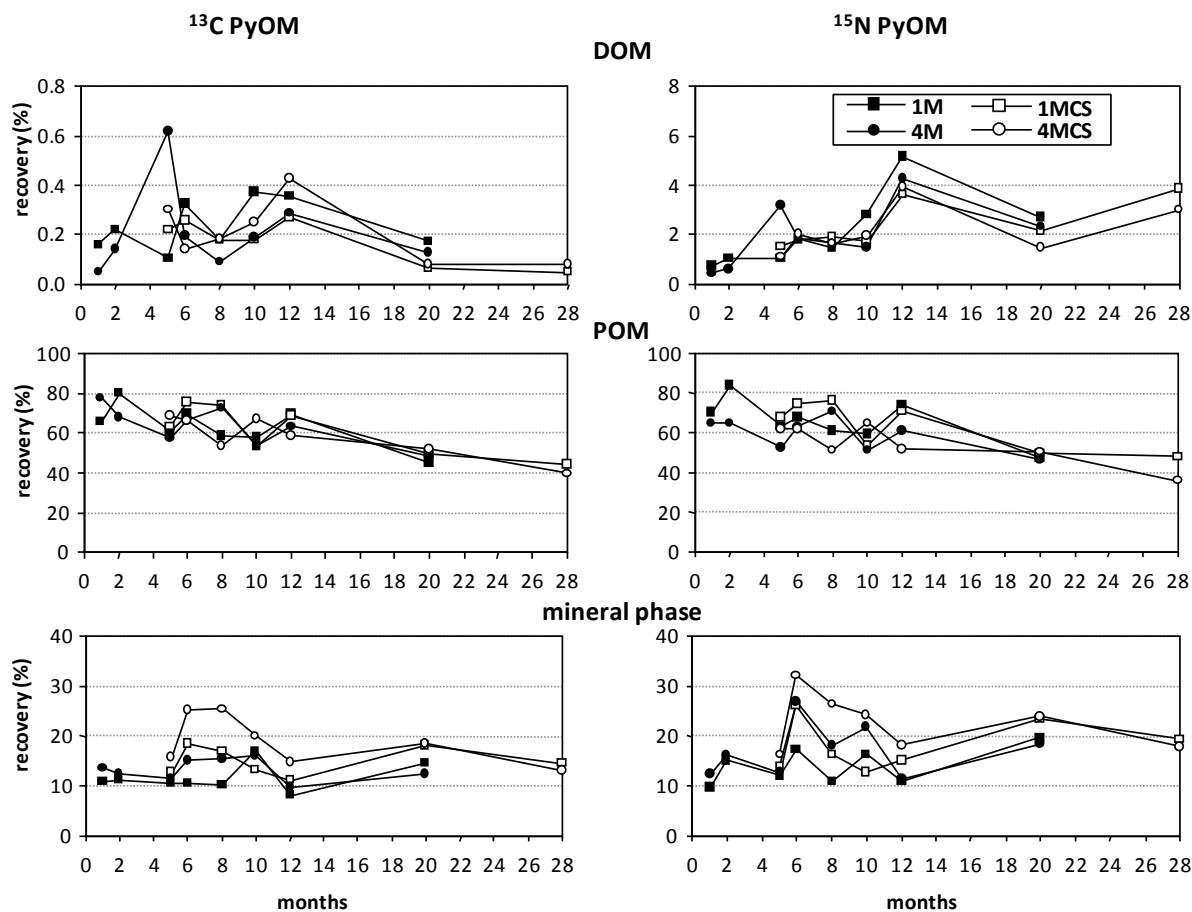


Figure 19: Temporal development of recovery of ^{13}C and ^{15}N labelled PyOM in different SOM fractions (DOM; POM and mineral associated organic matter) of A layer (0-2 cm) of a microcosm vs. incubation time. Values corrected by subtraction of natural ^{13}C and ^{15}N background (1M, pyrogenic material produced from charring time of 1 min; 4M, pyrogenic material produced from charring time of 4 min; CS, addition of fresh rye grass as co-substrate; BV, blank incubated without PyOM addition; SOM, soil organic matter; DOM, dissolve organic matter; POM, particulate organic matter).

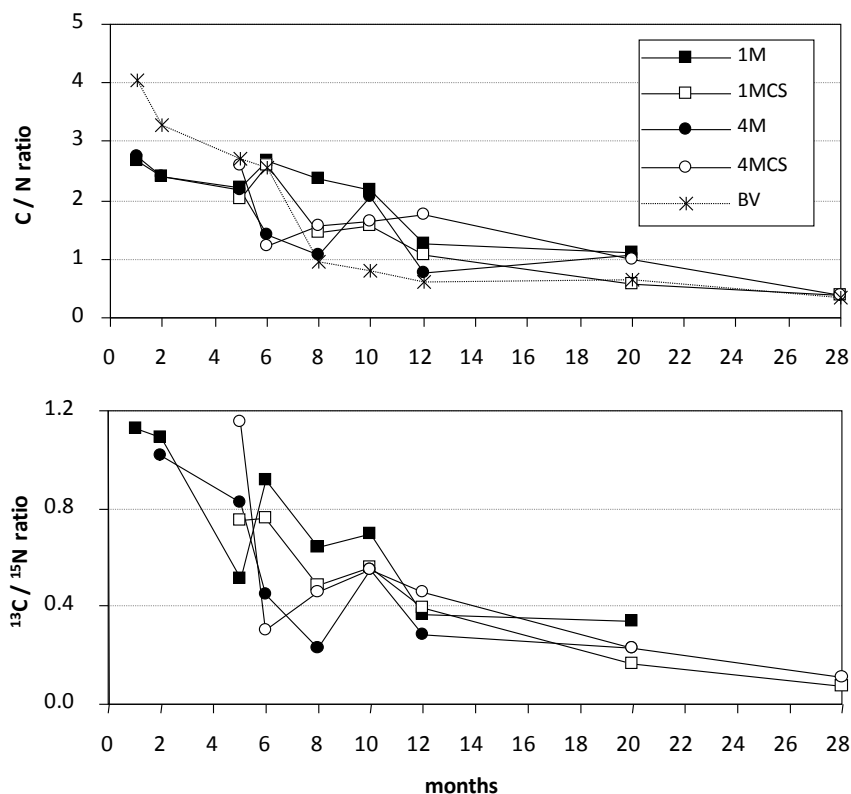


Figure 20: C/N and $^{13}\text{C}/^{15}\text{N}$ ratios of DOM fraction of A the layer. Values corrected by subtraction of natural ^{13}C and ^{15}N background; (1M, pyrogenic material produced from charring time of 1 min; 4M, pyrogenic material produced from charring time of 4 min; CS, addition of fresh rye grass as co-substrate; BV, blank incubated without PyOM addition; DOM, dissolved organic matter).

3.5.2 POM fraction

Most of the added PyOM was recovered in the POM fraction with a density $< 1.8 \text{ g cm}^{-3}$ (Fig. 19), whereby the main part of the POM fraction was obtained as the size fraction $> 20 \mu\text{m}$ (55% to 76%). During the first two months, between 84% and 65% of the ^{13}C and ^{15}N PyOM, respectively, were associated with the whole POM fraction. With prolonged incubation time, a decline in ^{13}C and ^{15}N PyOM was verifiable (Fig. 19). The mean loss of PyOM per month ranged between 0.9% and 1.3% relative to the input. Neither charring degree nor co-substrate addition seemed to affect the respective recoveries of the PyOM (p 0.566). A similar result was obtained by Kuzyakov et al. (2009) after addition of glucose. After 28 months, the PyOM recovery was reduced to half. In contrast to the total A layer, no relative enrichment in ^{15}N compounds in comparison to ^{13}C PyOM was observed for the POM fraction of the A layer (Fig. 19).

As shown in Fig. 19, the POM was the first SOM fraction affected by degradation. Fresh PyOM has a particular hydrophobic character (Hubbert et al., 2006) and provides

relatively small amounts of polar functional groups which could interact with mineral surfaces (Table 11). Therefore, the continuing decline in PyOM is very tentatively related to either interaction with the mineral phase or to conversion to other SOM fractions such as DOM, via which it may be subject to a downward transport through the soil column. Alternatively, it was converted into CO_2 via mineralisation as shown in chapter 3.

5.5.3 PyOM interactions with mineral surfaces

After one month, up to 13.8% for ^{13}C and 12.4% for the ^{15}N label were detected for the 4M PyOM, which verifies a fast association of PyOM with the mineral fraction (Fig. 19). The 1M PyOM showed a lower incorporation into the mineral phase during the first year but the trend was not significant (p 0.109 for ^{13}C and p 0.126 for ^{15}N , respectively). For a better comparison of the impact of the degree of burning, the relative recovery (Q) was calculated by setting the 1M PyOM treatments to 100% relative to the respective 4M PyOM values. A higher relative recovery of up to 152% (^{13}C) and 167% (^{15}N) was found between month 6 and month 10 for the 4M PyOM substrates (Fig. 21). However, with time, the differences in the 1M and 4M incorporation potential decreased. After 20 months, the substrates had comparable amounts of 1M and 4M PyOM associated with the mineral fraction. This could be attributed to lower 4M PyOM incorporation rates and/or a loss of former mineral-fixed PyOM (Fig. 19). This indicates that this pool is not stable and declined because of mineralisation of partly decomposed PyOM.

The recovery of ^{13}C and ^{15}N PyOM in the mineral fractions was partly decreased with prolonged incubation time (Fig. 19; month 6 to month 12). Thus, PyOM may behave comparably to unburned SOM where a low stability of young mineral-associated OC was observed (Kölbl et al., 2007).

In general, ^{15}N PyOM seems to have had a higher affinity for mineral surfaces because, with the exception of the one month incubates, all other time series tended to show higher ^{15}N accumulation in the mineral fractions (Fig. 19). An enrichment of inorganic ^{15}N (nitrate) can be excluded because it would have been removed during the DOM extraction and the following salt washing steps after the density fractionation. The higher N recovery of mineral-associated PyOM may be due to preferential mineralisation and loss of C, leading to a relative enrichment of N. Alternatively, a promoted partial oxidation of the N-containing compounds, resulting in formation of polar functional groups, may have led to a preferential adsorption to the mineral phase.

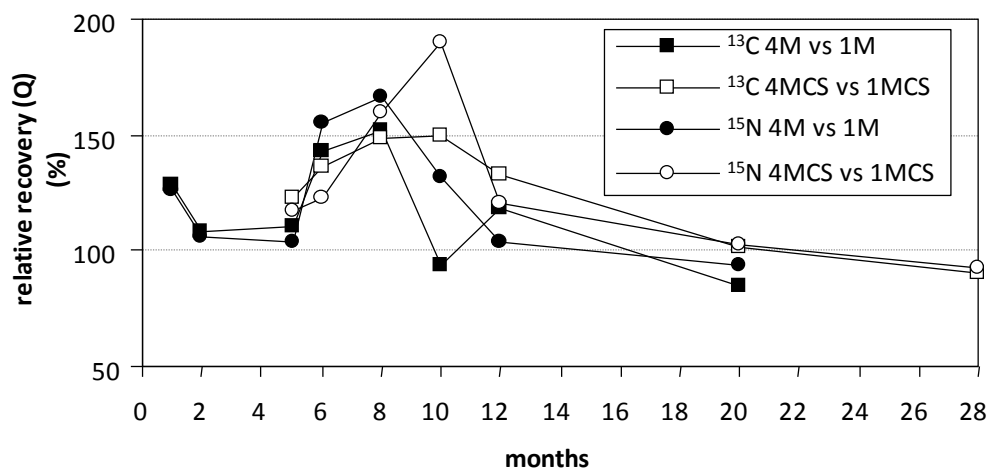


Figure 21: Influence of charring degree on association of ^{13}C and ^{15}N enriched PyOM with the mineral phase. Relative recovery(Q) was calculated by setting the recovery of the 1M PyOM treatments to 100% related to the respective 4M PyOM values; (1M, pyrogenic material produced from charring time of 1 min; 4M, pyrogenic material produced from charring time of 4 min; CS, addition of fresh rye grass as co-substrate; BV, blank value incubated without PyOM addition).

The co-substrate incubates show trends comparable to the pure ones, but the total recoveries of the isotopic labels were higher than for incubations without co-substrate (Fig. 22). Two months after the first co-substrate addition (month 6), the highest mineral-associated ^{13}C and ^{15}N PyOM amounts for the total experiment were detected for 1MCS and 4MCS. The charring degree showed no major influence (p 0.428) on the amount of additionally incorporated ^{13}C and ^{15}N PyOM (Fig. 22).

The formation of such organo-mineral complexes is favoured by partial PyOM degradation providing negative surface charges of initially hydrophobic material for organo-mineral associations (Glaser et al., 2000; Brodowski et al., 2005a; Cheng et al., 2008). Further, the higher PyOM recovery for the experiments with co-substrate addition indicates a kind of priming effect, which enhances the partial degradation of PyOM and promotes subsequently the interaction with mineral surfaces.

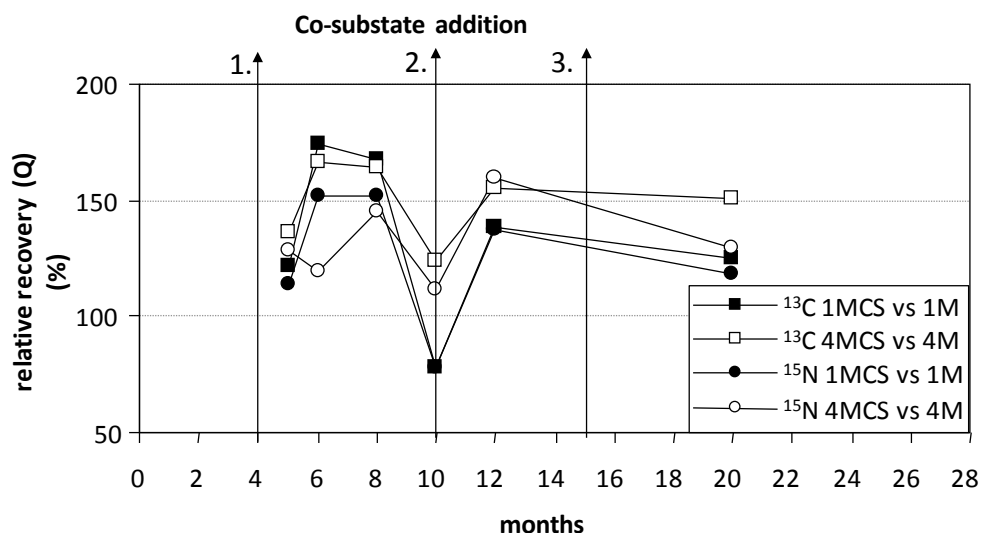


Figure 22: Influence of co-substrate addition on association of ^{13}C and ^{15}N enriched PyOM with the mineral phase. Relative recovery (Q) was calculated by setting the recovery of the PyOM incubates with co-substrate addition to 100% related to the respective PyOM incubates without co-substrate addition; (1M, pyrogenic material produced from a charring time of 1 min; 4M, pyrogenic material produced from a charring time of 4 min; CS addition of fresh rye grass as co-substrate; BV, blank incubated without PyOM addition).

5.5.4 Particle size fractions

The PyOM incorporation within the particle size fractions showed significant differences ($p < 0.001$). In general, the recovery of PyOM increased with decreasing particle size (Table 14). No PyOM was found in the sand fraction. Only small recoveries were observed for the coarse and middle silt fraction (63 to 6.3 μm ; Table 14). The main part of the mineral-associated PyOM was in the fine silt (6.3 to 2 μm) and clay fractions (< 2 μm). Comparable results were obtained by Kuzyakov et al. (2009), confirming that stabilisation within microaggregates plays a significant role in reducing BC decomposition rate. For the clay fraction, the highest PyOM recoveries were found for the more charred material with co-substrate addition (Table 14). Each particle size fraction followed the trends observed for the whole mineral fraction, leading to the conclusion that neither the burning degree nor co-substrate addition fostered preferential PyOM incorporation into a specific particle size fraction. Thus, although degradation was promoted by the increased degree of charring and co-substrate addition, the respective pathway and the partitioning remained unaltered.

For all substrates, 73% to 82% of the mineral-associated PyOM was found in the clay fraction (Table 14). No significant differences in the partitioning pattern of PyOM within the particle size fractions were observed, not only for the different incubate series,

but also with respect to the isotopic label and incubation time ($0.134 \leq p \leq 0.937$). Note that the quantitative distribution of SOM among the size fractions from the BV incubates was comparable to the PyOM incubates (Table 14). This may indicate that PyOM has degradation and mineral-binding mechanisms similar to the unburned OM of the BV incubate. The high affinity of PyOM for the clay fraction confirms the conclusion that PyOM was modified by partial degradation, resulting in products to which the soil matrix offered adsorption sites. In contrast, Rodionov et al. (2006) and Rovira et al. (2009) found the highest PyOM content in the silt fraction. However, in the present study, the light fraction (POM) was removed prior to particle size fractionation. Thus, on average, one quarter of the PyOM input was recovered with the POM fraction with a particle size $< 20 \mu\text{m}$ (data not shown), which would be in the range of the silt size fraction. This means that a considerable part of grass-derived PyOM is found in the size range $< 20 \mu\text{m}$ when counting the free POM and mineral-associated size fraction.

Table 14: Recovery of ¹³C and ¹⁵N from isotopically enriched PyOM in size fractions of A layers of the soil microcosms after 28 months incubation (size fractions with different letters were significantly different at α 0.05 according to the one-way repeated measures ANOVA and the Tukey's honest significant difference post-hoc comparison).

Sample	Range of time series ¹³ C PyOM				Range of time series ¹⁵ N PyOM			
	RC (%) ^a	SD ^c	DB (%) ^b	SD ^c	RC (%) ^a	SD	DB (%) ^b	SD ^c
PyOM 1M^d								
63-20 μ m	0.1A	0.0	1	0	0.0A	0.0	0	0
20-6.3 μ m	0.2A	0.1	2	1	0.1A	0.1	1	1
6.3-2 μ m	2.1B	0.5	19	3	2.1B	0.7	16	4
<2 μ m	9.0C	1.5	79	3	10.9C	2.0	82	5
Sum	11.4	1.9	100	-	13.1	2.6	100	-
PyOM 1MCS^{d,f}								
63-20 μ m	0.1A	0.1	0	0	0.0A	0.0	0	0
20-6.3 μ m	0.5A	0.5	4	2	0.4A	0.4	2	2
6.3-2 μ m	3.6B	1.5	22	5	3.5B	1.2	22	5
<2 μ m	10.9C	2.1	74	7	12.5C	2.4	75	7
sum	15.1	3.6	100	-	16.4	3.5	100	-
PyOM 4M^e								
63-20 μ m	0.0A	0.1	0	0	0.0A	0.0	0	0
20-6.3 μ m	0.3A	0.3	2	1	0.3A	0.2	2	1
6.3-2 μ m	2.7B	0.8	20	4	3.1B	0.9	18	4
<2 μ m	10.5C	1.8	78	5	13.4C	2.4	80	4
Sum	13.6	2.6	100	-	16.8	3.2	100	-
PyOM 4MCS^{e,f}								
63-20 μ m	0.0A	0.0	0	1	0.0A	0.0	0	0
20-6.3 μ m	0.6A	0.5	3	2	0.5A	0.4	2	2
6.3-2 μ m	4.5B	2.7	23	9	5.1B	3.0	23	7
<2 μ m	13.8C	3.0	73	10	15.8C	3.5	75	8
Sum	18.9	5.5	100	-	21.5	6.0	100	-
BV^g								
63-20 μ m	-	-	3	1	-	-	2	1
20-6.3 μ m	-	-	10	2	-	-	10	4
6.3-2 μ m	-	-	15	3	-	-	23	4
< 2 μ m	-	-	72	4	-	-	65	6
Sum	-	-	100	-	-	-	100	-

^a Recovery.^b Distribution.^c Standard deviation.^d Pyrogenic organic material produced with a charring time of 1 min.^e Pyrogenic organic material produced with a charring time of 4 min.^f Addition of fresh rye grass as co-substrate.^g Blank value incubated without PyOM addition.

5.6 Elucidation of residence time

The decomposition kinetics of incubated PyOM (Fig. 19) were fitted with a two-component model (Eq. 3). In the first phase of decomposition, preferential decay of easily degradable compounds occurred (Table 15, Pool A). In this period, 7% to 19% of the ^{13}C PyOM was mineralised with half life periods ($t_{1/2}$) 1 to 19 days (Table 15). The 1M PyOM seemed to provide more readily available C to the microorganisms, including partly charred O/N-alkyl C and alkyl C components (Table 12). However, a recent study also indicated that aryl C-containing compounds can be mineralised during this initial phase (Hilscher et al. (2009); Chapter 3.4; Table 4). The remaining pool of more stable organic material accounted for most of the PyOM (Table 15; pool B) and its constituents were decomposed much more slowly, with $t_{1/2}$ between 3.9 and 4.7 yrs. This is possibly due to the protection of some PyOM particles within soil aggregates but also to continuous preferential utilisation of PyOM compounds (e.g. very small particles, strongly oxidised parts) during initial decomposition, which are more degradable than others, and would slow down decomposition in the following stages (Kuzyakov et al., 2009). The calculated $t_{1/2}$ implies mean residence times between 26 and 31 yr for the more stable pool B. The results are in agreement with the study of Steinbeiss et al. (2009), reporting comparable short mean residence times between 4 and 29 yr, depending on soil type and quality of char. Likewise, short mean residence times of up to 19 yr for grass-derived PyOM and 56 yr for pine wood PyOM were reported for the short term respiration experiment of 2 months (Hilscher et al., 2009; Chapter 3.8).

In comparison, for fresh plant material a $t_{1/2}$ of up to 0.5 yr (Pool B) was found (Voroney et al., 1989; Kölbl et al., 2007). This means that the $t_{1/2}$ for the PyOM of this study was up to 10 times longer than for fresh plant material, but still not unlimited. No major differences in the turnover dynamics were found for the different PyOM incubates (p 0.168 for ^{13}C and p 0.658 for ^{15}N ; Table 15). The uncertainty in ^{15}N PyOM recovery was too high for fitting the kinetics, because of low total ^{15}N concentrations.

Table 15: Estimation of decomposition kinetics of PyOM^a fitted to a two-component decay model.

Sample	Pool A			Pool B			R ^{2g}	p value ^h
	mg	Portion (%)	t _{1/2} (day) ^f	mg	Portion (%)	t _{1/2} (day) ^f		
¹³ C PyOM total								
1M ^b	6	16	1	34	84	1705	0.69	0.0963
1MCS ^{b,d}	3	7	1	37	93	1424	0.68	0.1169
4M ^c	6	14	18	34	86	1666	0.73	0.0679
4MCS ^{c,d}	8	19	19	32	81	1593	0.81	0.0139
¹³ C PyOM POM ^e								
1M ^b	10	26	1	30	74	1061	0.82	0.0269
1MCS ^{b,d}	10	24	1	30	76	1142	0.81	0.0138
4M ^c	12	30	14	28	70	1325	0.86	0.0145
4MCS	11	27	13	29	73	1098	0.93	0.0007
¹⁵ N PyOM POM ^e								
1M ^b	2	23	1	7	77	1024	0.79	0.0391
1MCS ^{b,d}	2	20	1	7	80	1106	0.81	0.0148
4M ^c	3	34	1	6	66	1455	0.85	0.0174
4MCS ^{c,d}	3	33	1	6	67	1119	0.93	0.0007

^a Pyrogenic organic material.^b Charring time 1 min.^c Charring time 4 min.^d Addition of fresh rye grass as co-substrate.^e Particulate organic matter of the A layer.^f Half-time period.^g Coefficient of determination.^h Probability level.

Because PyOM was added as particulate material, the initial PyOM input was set as POM. The strong decline in ^{13}C and ^{15}N POM within the first 2 months was followed by a distinctly slower decrease (Fig. 19). The degradation kinetics indicate a more expressed portion of decomposable PyOM (Pool A) of 24% to 30% of the ^{13}C POM fraction in comparison with the whole PyOM incubate (Table 15). This suggests that the C pool represents PyOM lost by way of mineralisation and incorporation into the mineral phase.

In this context, it is important to note that the calculated $t_{1/2}$ values represent minimum turnover times since they are based on 28 months incubation under more or less optimal and controlled aerobic conditions. Such conditions would certainly not be available in natural environments. Cold and dry periods can result in much slower degradation rates. Assuming that fungi increase the degradation efficiency of aromatic constituents (Hofrichter et al., 1997; Wengel et al., 2006), anaerobic conditions, for example in fossil horizons, archaeological sites and sediments may contribute to the preservation PyOM residues on the long term. On the other hand, preservation by way of oxygen deficiency is also a common feature of other organic compounds such as lignin and paraffinic structures. Consequently, PyOM may not necessarily be as important for the long term C sequestration within the global C cycle as commonly assumed. The relatively fast degradation times of plant char estimated in this and other studies (Bird et al., 1999; Hamer et al., 2004; Hammes et al., 2008) could contribute to the unexpectedly low PyOM abundance reported in different field studies (Czimczik et al., 2003; Solomon et al., 2007).

Furthermore, the mineralisation kinetic of the pure PyOM demonstrates that microbial degradation of even strongly charred residues can occur in the initial post-fire phase. This implies that, after intensive fires leaving almost no thermally unaltered plant residues, the newly developed microorganism communities may not need additional nourishing substrate, at least during the very early post-fire phase.

6. Carbon and nitrogen degradation on molecular scale of grass-derived pyrogenic organic material during incubation in soil

A continuous mineralisation of PyOM was described in chapter 5 during the incubation of more than 2 years in soil. This chapter discusses the aging process of PyOM on molecular scale. Therefore, solid-state ^{13}C and ^{15}N NMR studies were conducted at different stages of the incubation to identify the degradation and humification mechanisms.

6.1 Efficiency of HF treatment of PyOM-enriched mineral fractions on NMR sensitivity

The HF treatment of the fine silt (6.3 to 2 μm) and clay fraction (< 2 μm) resulted in high C-enrichment factors ($E_c = 4 \pm 1$; Table 16), leading to C concentrations between 20 and 40 mg C g^{-1} for the clay fraction and between 6 and 13 mg C g^{-1} for the fine silt fraction. During the demineralisation step $83 \pm 2\%$ of the mineral phase was removed. High recoveries of the ^{13}C label ($88 \pm 7\%$) underline that HF treatment did not change the chemical composition of the PyOM samples. For the ^{15}N -labelled and HF-treated mineral samples, the recovery of $71 \pm 8\%$ was lower compared to the ^{13}C label, which is explained by large losses of inherent N of the used soil (BV; Table 16). This is supported by a higher loss of soil derived ^{14}N and a relative enrichment of the PyOM-derived ^{15}N label (Table 16). Relative mean ^{15}N -enrichment factors ($E_{15\text{N}}$) were calculated as 2.5 and 2.0 for the fine silt fraction (6.3 to 2 μm) and clay fraction (< 2 μm), respectively.

Selected clay fractions were analysed by solid-state ^{13}C NMR spectroscopy before and after HF treatment (Fig. 23). In line with the results of Goncalves et al. (2003), the HF treatment induced no major alteration of the intensity distribution, but the quality of the NMR spectra was improved by removal of paramagnetic material and relative enrichment of PyOM. Only 60,000 scans were necessary for the acquisition of the HF-treated clay fraction. The NMR spectra of the HF-treated clay fraction reveal a higher alkyl contribution compared to the respective NMR spectra of the untreated ones (Fig. 23). The observation can be explained by alkyl-C signal suppression in the untreated samples due to presence of paramagnetic compounds (Fe, Cu, Mn) which leads to ineffective CP and line broadening (Chapter 1.4.2.).

Table 16: Elemental composition and isotopic ^{13}C and ^{15}N contents before and after HF treatment of the mineral fraction with C and N-enrichment factors E_C and E_N . Data represent mean values ($n = 6$) with standard deviation (\pm).

PyOM ^a Treatment	Fraction	Mineral loss (%)	C _{before} (mg g ⁻¹)	C _{after} (mg g ⁻¹)	E_C	^{13}C _{before} (atom%)	^{13}C _{after} (atom%)	^{13}C recovery (%)	N _{before} (mg g ⁻¹)	N _{after} (mg g ⁻¹)	E_N	^{15}N _{before} (atom%)	^{15}N _{after} (atom%)	$E_{^{15}\text{N}}$	^{15}N recovery (%)
BV ^b	6.3-2 μm	87	2.1	11.9	6	1.1	1.1	71	1.7	2.3	1	0.3	0.3	1.0	23
	<2 μm	83	7.1	25.5	4	1.1	1.1	60	2.3	4.6	2	0.3	0.3	1.0	40
1M ^c	6.3-2 μm	83.7 \pm 2.0	2.0 \pm 0.2	10.0 \pm 1.6	4.9 \pm 0.8	3.1 \pm 0.4	3.6 \pm 0.4	91.6 \pm 3.3	1.5 \pm 0.1	2.4 \pm 0.4	1.6 \pm 0.3	0.9 \pm 0.2	2.4 \pm 0.5	2.8 \pm 0.6	69.6 \pm 6.5
	<2 μm	81.8 \pm 2.1	6.8 \pm 0.2	25.8 \pm 3.5	3.8 \pm 0.5	3.0 \pm 0.3	3.7 \pm 0.4	85.8 \pm 3.2	2.3 \pm 0.1	4.2 \pm 0.7	1.9 \pm 0.4	1.7 \pm 0.2	3.5 \pm 0.7	2.0 \pm 0.3	68.1 \pm 8.7
1MCS ^{c,e}	6.3-2 μm	83.5 \pm 1.8	2.3 \pm 0.3	11.6 \pm 1.5	5.0 \pm 0.9	4.2 \pm 0.9	4.7 \pm 1.2	90.6 \pm 6.2	1.4 \pm 0.1	2.6 \pm 0.7	1.9 \pm 0.6	1.4 \pm 0.3	3.8 \pm 2.0	2.6 \pm 0.8	74.3 \pm 7.2
	<2 μm	83.3 \pm 0.8	8.0 \pm 0.4	34.5 \pm 2.0	4.3 \pm 0.2	3.1 \pm 0.2	3.7 \pm 0.2	85.3 \pm 2.5	2.3 \pm 0.1	5.3 \pm 0.9	2.3 \pm 0.3	1.9 \pm 0.2	3.8 \pm 0.4	2.0 \pm 0.2	75.2 \pm 7.2
4M ^d	6.3-2 μm	83.5 \pm 2.0	2.2 \pm 0.3	10.3 \pm 1.7	4.7 \pm 1.0	3.4 \pm 0.7	4.1 \pm 0.9	91.4 \pm 5.6	1.5 \pm 0.2	2.5 \pm 0.5	1.7 \pm 0.4	1.3 \pm 0.5	3.2 \pm 1.5	2.4 \pm 0.5	66.0 \pm 5.4
	<2 μm	81.6 \pm 2.1	7.1 \pm 0.5	27.1 \pm 4.7	3.8 \pm 0.5	3.1 \pm 0.6	3.9 \pm 0.7	87.0 \pm 4.2	2.3 \pm 0.2	4.6 \pm 1.0	2.0 \pm 0.4	2.2 \pm 0.6	4.5 \pm 1.6	2.0 \pm 0.2	74.2 \pm 9.8
4MCS ^{d,e}	6.3-2 μm	84.8 \pm 1.4	2.3 \pm 0.9	11.3 \pm 4.0	5.0 \pm 0.9	4.8 \pm 0.9	5.6 \pm 1.3	88.0 \pm 11.6	1.4 \pm 0.1	2.9 \pm 0.9	2.1 \pm 0.6	2.3 \pm 1.0	4.9 \pm 1.3	2.3 \pm 0.5	68.5 \pm 9.5
	<2 μm	83.1 \pm 0.8	8.5 \pm 0.7	36.2 \pm 2.8	4.3 \pm 0.3	3.4 \pm 0.2	4.0 \pm 0.4	86.2 \pm 0.4	2.4 \pm 0.1	5.6 \pm 1.0	2.3 \pm 0.4	2.7 \pm 0.4	5.2 \pm 0.7	1.9 \pm 0.2	75.5 \pm 6.3

a Pyrogenic organic material.

b Without PyOM addition.

c Charring time 1 min.

d Charring time 4 min.

e Addition of fresh rye grass as co-substrate.

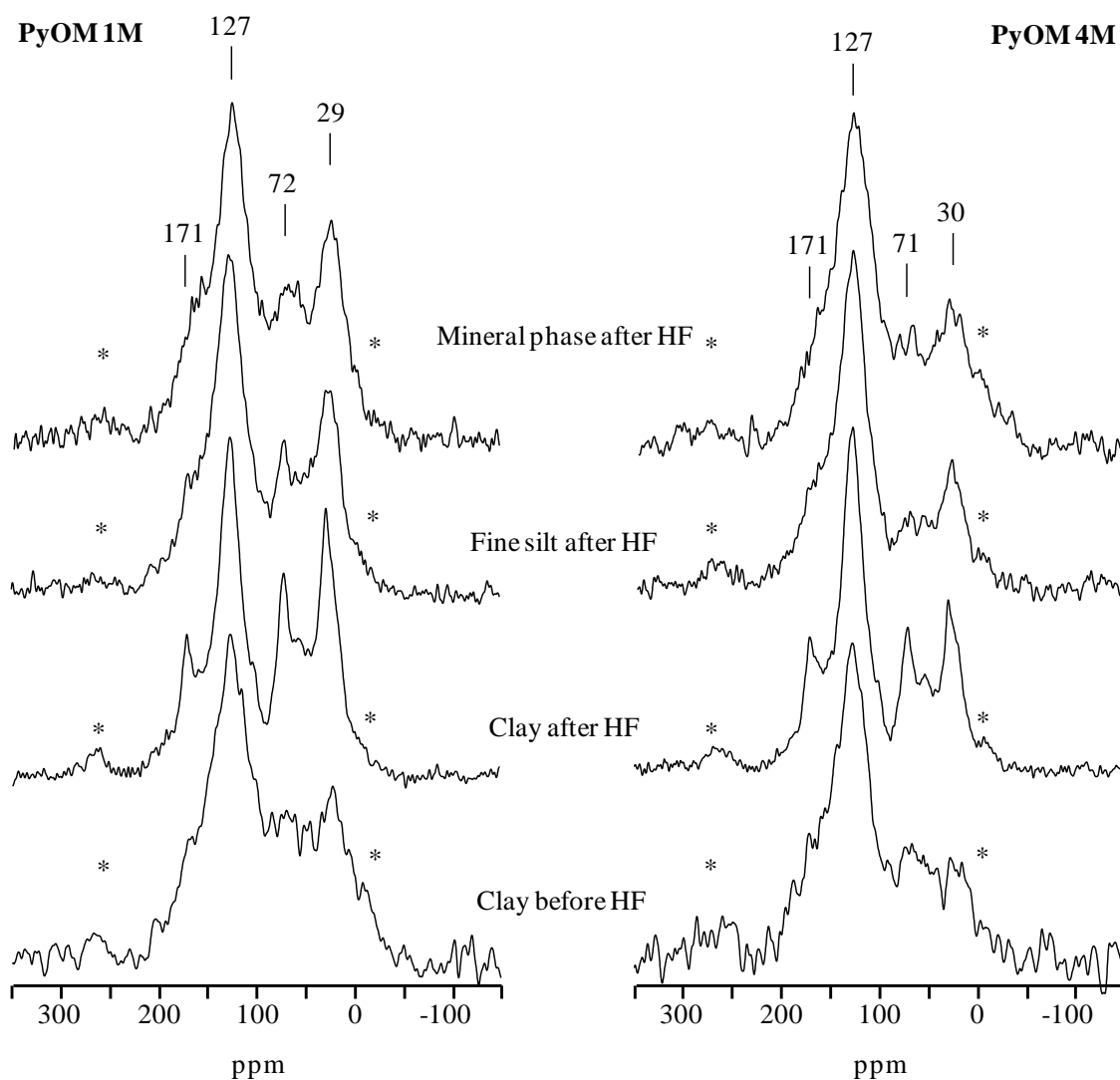


Figure 23: Solid-state ^{13}C NMR spectra of HF-treated and untreated mineral-associated PyOM. Spinning side bands are marked with asterisks. PyOM 1M = charring time 1 min.; PyOM 4M = charring time 4 min.

6.2 Reproducibility of C group recovery

The PyOM samples which had been incubated for two months were prepared in replicates and the reproducibility of their chemical composition was analysed. For the different C groups, the absolute standard deviation of the contribution to total C ranged between 0 and 1.6% (Table 17). These good agreements support the improved analytical sensitivity accomplished by using PyOM that was highly enriched with isotopic labels. The findings are in line with the results of the short-term incubation study (Chapter 3, Fig. 12) which shows that the relative standard deviation of the amount of mineralised PyOM of 5 replicates was smaller than 5%.

Table 17: Reproducibility of the intensity distribution and the total recovery for PyOM C groups after 2 months of incubation. Mean values and standard deviations (\pm) were calculated from duplicates.

Sample	Carbonyl/ Carboxyl C	O-aryl C	Aryl C	O/N-alkyl C	Alkyl C	Sum
<i>Relative contribution (%)</i>						
PyOM ^a 1M ^b	9.1 \pm 0.0	8.4 \pm 0.0	36.7 \pm 0.1	18.5 \pm 0.0	27.3 \pm 0.1	100
PyOM ^a 4M ^c	8.7 \pm 1.0	9.8 \pm 0.6	47.1 \pm 1.6	10.4 \pm 0.2	24.0 \pm 0.1	100
<i>Total recovery (mg ¹³C)</i>						
PyOM ^a 1M ^b	3.3 \pm 0.1	3.1 \pm 0.1	13.5 \pm 0.4	6.8 \pm 0.2	10.1 \pm 0.2	36.9 \pm 1.0
PyOM ^a 4M ^c	2.8 \pm 0.3	3.2 \pm 0.1	15.4 \pm 0.8	3.4 \pm 0.0	7.8 \pm 0.2	32.7 \pm 0.6

a Pyrogenic organic material.

b Charring time 1 min.

c Charring time 4 min.

6.3 C-group distribution of incubated PyOM

Besides aryl C, the alkyl C represents a quantitatively important fraction of grass-derived PyOM. It showed no major alteration of its contribution to the bulk PyOM C (Fig. 24A). After 20 months, the alkyl-C contribution for all incubates decreased slightly by 5% with respect to the fresh PyOM, but the change is not significant ($0.130 \leq p \leq 0.998$). Co-substrate addition did not change the alkyl-C contribution to total C ($0.866 \leq p \leq 1.000$; Fig 24A). At all stages of the incubation, higher alkyl-C contents of the PyOM 1M compared to that of the PyOM 4M treatments was detected ($p < 0.001$).

Compared to the unburned plant material, the O/N-alkyl C content of the fresh PyOM was small (15 and 9%; Table 12, Chapter 3.1), indicating a minor relevance for the C flux. Starting after 10 months of incubation, the O/N-alkyl-C contribution to the total C of the different PyOM treatments decreased significantly ($p \leq 0.022$; Fig. 24B). At month 20, O/N-alkyl C was only 6% of the total C for the PyOM 1M, revealing a higher loss of O/N-alkyl C compared to other C groups. The initial differences in O/N-alkyl C content in the two types of PyOM decreased, but were still present ($0.006 \leq p \leq 0.032$; Fig. 24B). No significant effect of co-substrate addition on the O/N-alkyl C distribution was observed ($0.976 \leq p \leq 0.999$).

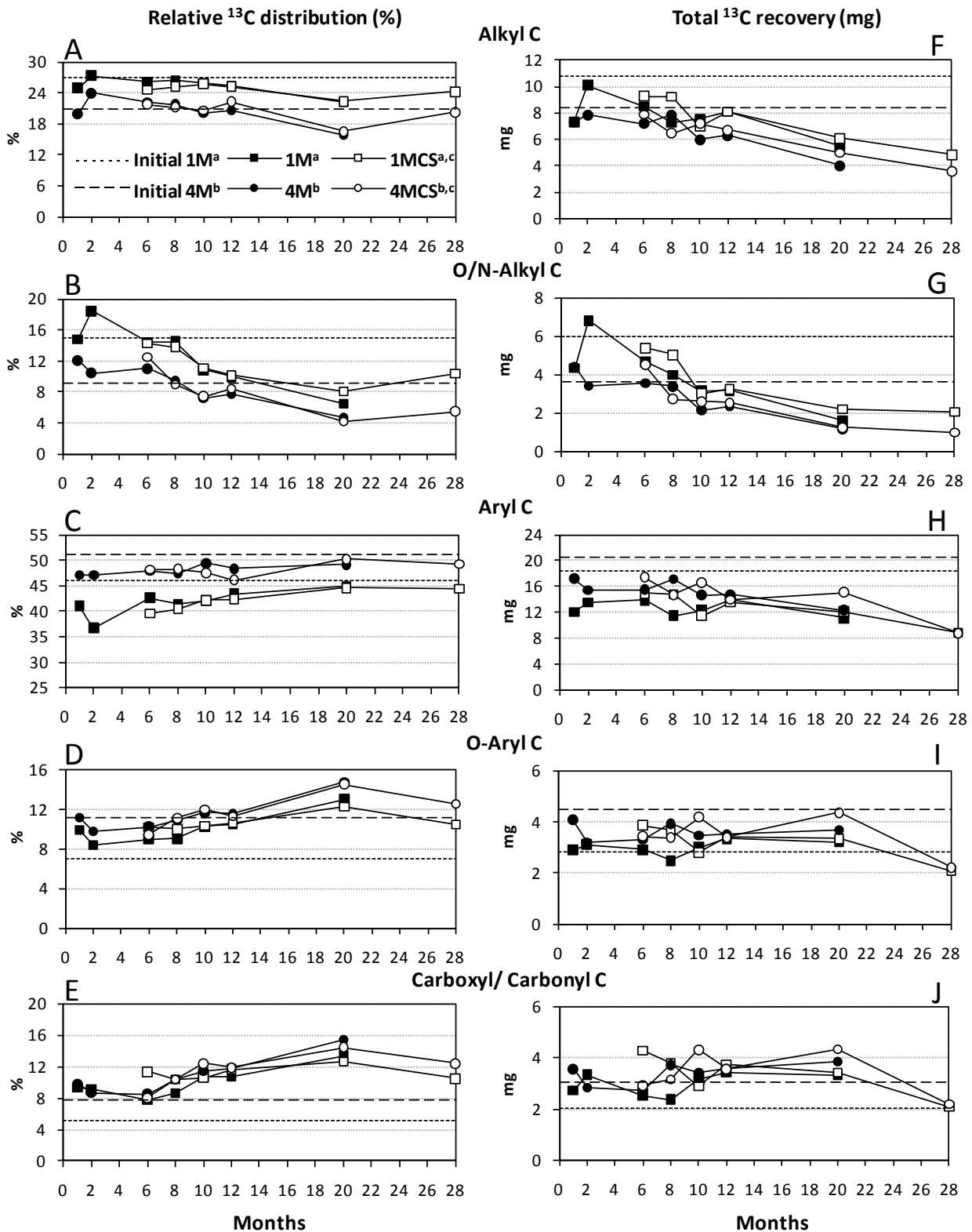


Figure 24: Time course of the relative distribution and total recovery of the different PyOM C groups during the 28 months of incubation. ^acharring time 1 min.; ^b charring time 4 min.; ^c addition of fresh rye grass as co-substrate.

The aryl-C group represented the main fraction of the PyOM-C with 46% for PyOM 1M and 51% for PyOM 4M (Table 12, Chapter 3.1). The large percentages confirm the effective charring of the plant material. No significant differences of the aryl-C contents were detected for the incubates with and without co-substrate addition ($p \geq 0.999$; Fig. 17C). During the first year, the aryl-C proportion was smaller than at the beginning of the experiment. In the second year, the aryl-C distribution reached initial values ($0.080 \leq p \leq 0.454$; Fig. 24C).

The initial O-aryl-C fraction of PyOM 4M was with 11% slightly larger than that of PyOM 1M with 7% (Fig. 24D). For the whole incubation period, a constant increase of the O-aryl-C contribution was observed for the PyOM 1M and PyOM 1MCS incubates ($p \leq 0.001$). For this C group, enrichment factors of up to 1.9 relative to the fresh PyOM 1M were found. The respective PyOM 4M and PyOM 4MCS incubates did not show a significant enrichment of O-aryl-C groups ($p \geq 0.890$). The PyOM 1M and 4M incubates with CS addition did not differ from the untreated ones ($0.923 \leq p \leq 0.998$) and were in line with the aryl-C behaviour. At the end of the incubation experiment, there were only small differences in the O-aryl-C contributions between the PyOM with different charring degree. Considering the sum of aryl C and O-aryl C, their contribution to the total PyOM C was comparable to the respective fresh PyOM ($0.421 \leq p \leq 1.000$).

The carboxyl/carbonyl-C pool showed the largest relative enrichment of all C groups during the incubation (Fig. 24E). Already after one month of incubation the carboxyl/carbonyl-C content of the PyOM 1M incubates reached the level of those of PyOM 4M (Fig. 24E). For the following period, a constant increase of the carboxyl/carbonyl-C contribution was observed for all PyOM 1M and PyOM 4M treatments ($p \leq 0.001$). After 20 months, up to 15% of the PyOM C was assigned to carboxyl/carbonyl-C groups. For the other C groups no influence of CS addition on the C contribution was found for the PyOM incubates ($p \geq 0.646$). All different PyOM treatments showed comparable relative carboxyl/carbonyl-C enrichments at the end of the incubation ($0.702 \leq p \leq 0.991$). Enrichment factors between 1.6 and 2.6 were calculated in comparison with the fresh PyOM.

6.4 Degradation of PyOM-derived C

In contrast to the contribution of alkyl C to the PyOM, the total alkyl-C recovery was efficiently reduced during the incubation (Fig. 24F). After 20 months, the alkyl-C loss

ranged between 41 and 53%. At the end of the incubation up to 57% of the initial alkyl C was mineralised or converted into other C groups. Neither the burning intensity nor the availability of a co-substrate showed a significant influence on the degradation rate ($p \geq 0.323$). The decomposition kinetics $t_{1/2}$ of the alkyl-C group was in the range of 2.1 and 2.5 years (Table 18). In comparison with the alkyl-C decomposition rate for fresh grass material that have been calculated from data published by Knicker and Lüdemann (1995), the respective $t_{1/2}$ are higher by the factor 6 to 7 (Table 18).

Among all C groups, O/N-alkyl C showed the largest loss (Fig. 24G). In general, up to 73% of the initial amount was mineralised for PyOM 4M CS. In comparison with alkyl C, the total O/N-alkyl-C loss related to the bulk PyOM C was up to 10% lower than for the alkyl C with up to 15% for the lower charred PyOM 1M. Comparable to the pattern of alkyl C, the degradation rate was neither affected by the burning degree nor by the availability of a fresh co-substrate ($p \geq 0.572$). The calculated $t_{1/2}$ was the shortest of all C groups with only up to 1.3 years (Table 18). Compared to fresh rye grass, the biodegradability of this potentially readily decomposable C source was strongly reduced by a factor between 34 and 45 (Table 18).

The reduced microbial availability of O/N-alkyl C and alkyl-C residues of the PyOM can be explained by the chemical alteration induced by charring, as e.g. formation of anhydrosugars (Elias et al., 2001). Alternatively, some of those compounds may have been physically protected by entrapment of more charred domains (Knicker et al., 1996b). However, as indicated in the present study, those alkyl C and O/N-alkyl C residues will be primarily decomposed during the initial stage of char degradation. Concerning the O/N-alkyl and alkyl-C decomposition dynamics, significant correlations were found for all PyOM treatments (Table 19). This denotes comparable degradation behaviour for both C groups.

Table 18: Decomposition kinetics for the different C groups of fresh rye grass and PyOM revealed by fitting with a first order decay model.

C group	$t_{1/2}^a$ (y)	R^{2b}	p value ^c	F_{slow}^d
<i>Alkyl C</i>				
Fresh rye grass	0.4	0.84	0.011	-
1M ^e	2.3	0.69	0.026	6
1MCS ^{e,g}	2.5	0.70	0.006	7
4M ^f	2.1	0.79	0.003	6
4MCS ^{f,g}	2.4	0.87	0.000	6
<i>O/N-alkyl C</i>				
Fresh rye grass	0.0	0.94	0.001	-
1M ^e	1.0	0.78	0.004	34
1MCS ^{e,g}	1.3	0.74	0.003	45
4M ^f	1.2	0.80	0.003	40
4MCS ^{f,g}	1.3	0.78	0.002	42
<i>Aryl C</i>				
Fresh rye grass	0.4	0.87	0.017	-
1M ^e	3.8	0.32	0.147	10
1MCS ^{e,g}	3.6	0.50	0.033	10
4M ^f	3.0	0.68	0.012	8
4MCS ^{f,g}	3.0	0.69	0.006	8
<i>O-aryl and aryl C</i>				
Fresh rye grass	0.4	0.79	0.004	-
1M ^e	5.1	0.26	0.198	14
1MCS ^{e,g}	4.1	0.48	0.037	11
4M ^f	3.3	0.61	0.023	9
4MCS ^{f,g}	3.4	0.62	0.012	9

a Half-time period.

b Coefficient of determination.

c Probability level.

d Slowing factor related to degradation rate of fresh rye grass.

e Charring time 1 min.

f Charring time 4 min.

g Addition of fresh rye grass as co-substrate.

Table 19: Correlation coefficients between total recoveries of the PyOM C groups during 28 months of incubation. The values in parentheses represent the p value.

Sample		1M	1MCS	4M	4MCS
O/N-Alkyl C					
1M ^a	Alkyl C	0.902 (0.002)			
1MCS ^{a,c}			0.936 (0.006)		
4M ^b				0.870 (0.005)	
4MCS ^{b,c}					0.908 (0.012)
Aryl C					
1M ^a	Alkyl C	0.852 (0.007)			
1MCS ^{a,c}			0.963 (0.002)		
4M ^b				0.856 (0.007)	
4MCS ^{b,c}					0.872 (0.024)
O-Aryl C					
1M ^a	Carboxyl/	0.769 (0.026)			
1MCS ^{a,c}	Carbonyl C		0.925 (0.008)		
4M ^b				0.861 (0.018)	
4MCS ^{b,c}					0.992 (0.001)

a Charring time 1 min.

b Charring time 4 min.

c Addition of fresh rye grass as co-substrate.

The total aryl-C group recovery of the PyOM decreased significantly during the 28 months of incubation ($p \leq 0.001$; Fig. 24H). After 20 months between 26 and 40% of the initial aryl-C amount was mineralised or converted to other C groups. At the 28th month the aryl-C loss reached up to 57% for the PyOM 4MCS incubate. At this stage, the low total recovery can be partly attributed to an increasing vertical movement of PyOM into the two sub soil layers that was demonstrated by the isotopic PyOM recovery studies (Fig. 18, Chapter 5.3; Hilscher and Knicker, 2011b). However, the ¹³C enrichment of the sub soil layers was too small to accomplish ¹³C NMR measurements.

In general, in the top layer the aryl-C fraction showed the largest total C loss of all PyOM-C groups. At month 20, the loss accounted from 13 to 20% of the initial total PyOM C. Examining the turnover of this group, remarkable short $t_{1/2}$ between 3.0 and 3.8 years can be noticed (Table 18). Compared to the decomposition rate obtained for lignin-derived aryl structures of fresh rye grass material, they are 10 times lower for the PyOM 1M and 8 times lower for the more charred PyOM 4M treatments (Table 18). This

indicates that comparable to aryl structures in lignin, also those of the PyOM can be microbially decomposed.

In contrast to aryl C, the amounts of O-aryl C show no alteration for PyOM 1M and PyOM 1MCS ($p = 0.216$) or only small losses for PyOM 4M and PyOM 4MCS ($p \leq 0.005$). This behaviour may point to a steady state between degradation and formation of that C species (Fig. 24I). Considering the sum of the O-aryl C and aryl-C pool, the respective $t_{1/2}$ are with 3.3 to 5.1 years slightly higher compared to those obtained for the aryl-C pool alone. With $t_{1/2}$ of 2.5 years the decomposition for the fresh rye grass indicated a faster degradation of O-aryl C under unburnt conditions.

Related to the initial carboxyl and carbonyl-C amount, a significantly higher recovery of this group (146% for PyOM 1M and 165% for PyOM 1MCS) was observed ($p \leq 0.008$; Fig. 24J). The PyOM 4M treatments, on the other hand, did not reveal significant changes of the total carboxyl and carbonyl C amounts ($p \geq 0.846$). Note that the ^{13}C -label technique allows exclusively the observation of PyOM-derived polar functional groups. Thus, the detected large carboxyl/carbonyl-C amounts are not a result of a possible sorption of non-BC-derived polar groups.

It can be concluded that the observed degradation of aromatic C may include two simultaneous processes: (i) complete mineralisation to CO_2 and (ii) conversion to other C groups by partial oxidation. The relevance of the latter process is supported by the fact that oxygen-substituted aryl structures (O-aryl C) showed little if any decrease in spite of the considerable aryl C and total C losses (Fig. 24D). Oxidation reactions during the degradation of charcoal and coals have already been reported by Potter (1908). Thus, we propose the concept that the partial oxidation of aryl structures is composed of two main steps. As a first reaction, the aryl rings are modified by substitution of the aryl C with hydroxyl groups to catechol-like structures. The formation of O-aryl C may be caused by enzymatic hydroxylation of aromatic structures (Ullrich and Hofrichter, 2007). A significant correlation ($p \leq 0.026$) between the oxygen-substituted aryl structures and carboxyl/carbonyl-C groups (Table 19; Fig. 24 I and J) supports that in a second step the O-aryl ring structures are partly oxygenated and cleaved, resulting in carboxyl/carbonyl-C (Kojima et al., 1961). The enrichment of O-containing groups in aged PyOM has also been described in other recent field (Knicker et al., 2006; Solomon et al., 2007) and laboratory studies (Lehmann et al., 2005; Cheng et al., 2006), supporting the suggested degradation mechanisms. Additionally, microbial resynthesis of PyOM may be responsible for the

observed enrichment of O-containing functional groups as described by Rumpel and Kögel-Knabner (2004) for the degradation of lignite coals.

The presence of a co-substrate (fresh plant material) did neither significantly affect the degradation kinetics of the respective C groups nor the chemical quality of the aged PyOM (Fig. 24 and 26). An explanation may be the availability of decomposable C sources in the starting PyOM. In line with the findings of the present study, it was not found a co-metabolic enhancement for a 7 week short-time incubation with PyOM derived from different plant source materials (Chapter 3).

6.5 Chemical structure of leached PyOM

Up to 3.2% of ^{13}C and 3.7% of the ^{15}N label were recovered with the leachate after 20 and 28 months. The respective ^{13}C NMR spectra revealed strong differences to the fresh PyOM (Fig. 25). Most of the ^{13}C signal intensity was observed in the aryl-C region, indicating that PyOM was vertically moved. Between 46 and 49% of the total C of the leachate of the PyOM 1M treatments and up to 53% of that of the PyOM 4M incubates are assignable to aryl domains. This implicates that during the last 8 months of incubation between 0.7 and 2.8% of the initial aryl C was relocated. The chemical composition of the leachate showed a relative increase of O-aryl-C and carboxyl/carbonyl-C (Fig. 25). Possibly, the larger contribution of those polar C groups was responsible for the increased water solubility and thus mobility of this fraction.

The alkyl-C portion is depleted in the PyOM leachate. For the PyOM 1M treatments between 19 and 21% and for the PyOM 4M up to 16% of the total leachate C is alkyl C. Furthermore, the shift of the aryl-C signal from around 29 ppm to 22 ppm in the spectra of PyOM 1M and PyOM 4M indicates the formation of acetyl groups (Fig. 25), possibly caused by degradation processes and accumulation of short alkyl-C chains. The contribution of O/N-alkyl C to the total C pool of the PyOM-derived leachate is only 4%.

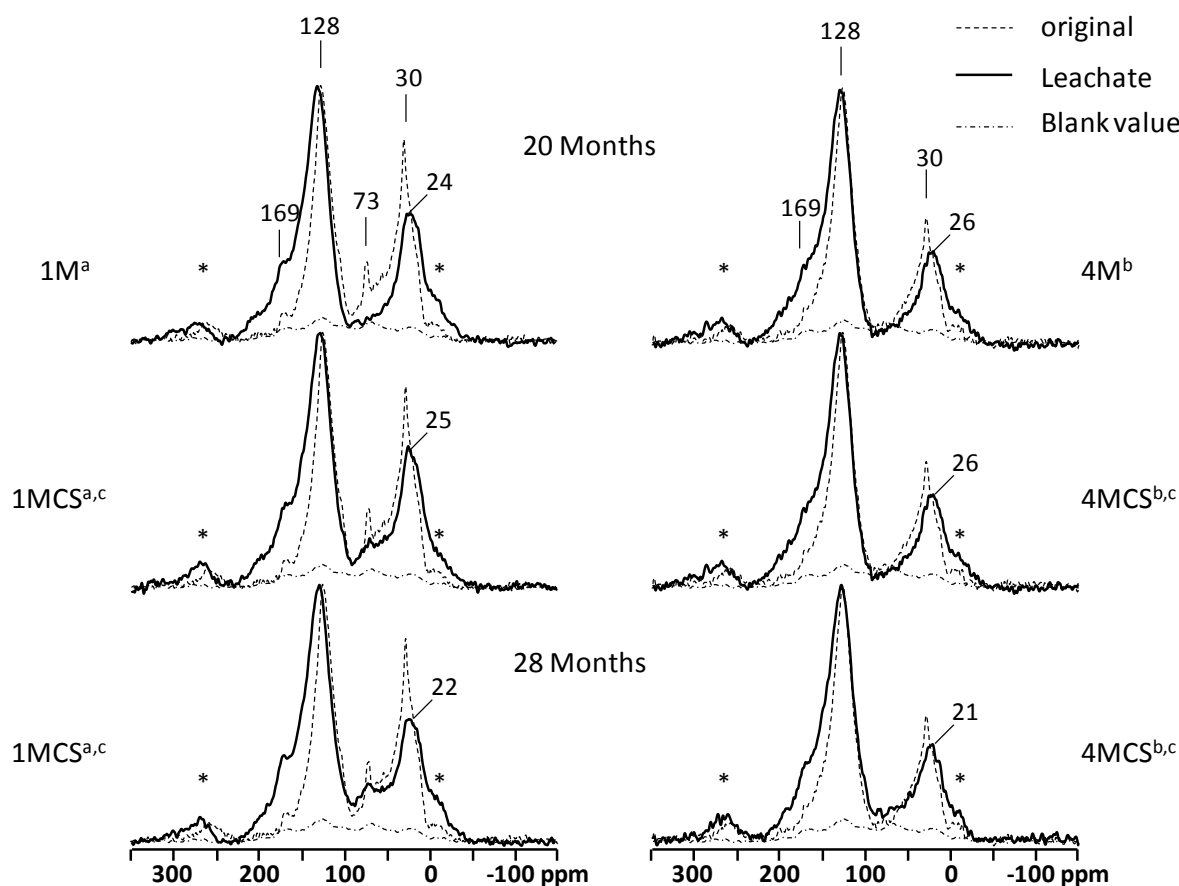


Figure 25: Solid-state ^{13}C NMR spectra of the vertical down moved PyOM fraction for the last 8 months of incubation. ^a Charring time 1 min.; ^b charring time 4 min.; ^c addition of fresh rye grass as co-substrate.

6.6 Turnover of pyrogenic N

The solid-state ^{15}N NMR spectra of the fresh PyOM confirm that most of the organic N is bound in heterocyclic aryl compounds such as pyrrole and indole-like structures. The compounds contribute to 62 and 72% of the total ^{15}N pools in PyOM 1M and PyOM 4M, respectively (Fig. 17, Chapter 5.1). No major alteration of the organic matter composition was detected for the A layer of the PyOM 1M incubates at any stage of the incubation (Fig. 26A and B). However, a relative decrease of proportion of heterocyclic N was observed for the PyOM 4M (Fig. 26B). After 28 months of incubation, no significant difference in the chemical N composition related to the PyOM 1M treatments was monitored (p 0.472). This trend is confirmed by an increase of the amide to heterocyclic N ratio which is in the range of 0.6 to 0.8 for the PyOM 4M incubates compared to 0.4 for the fresh PyOM 4M. It was not possible to calculate the N-group balances of the sub layers because the ^{15}N content was too low to obtain evaluable ^{15}N NMR spectra. Nevertheless, it is likely that

heterocyclic N compounds are decomposed because for the whole soil column a total ^{15}N loss up to 33% was found (Fig. 18, Chapter 5.3).

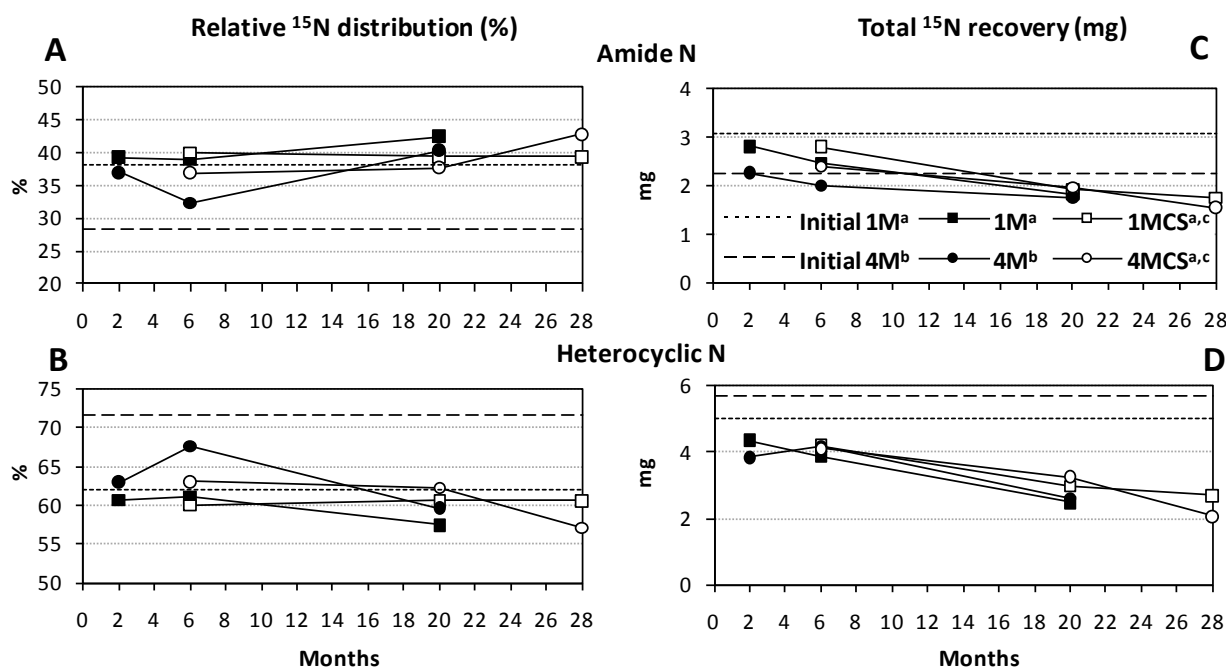


Figure 26: Time course of the relative distribution and total recovery of the different PyOM N groups for the A layer during the 28 months of incubation. ^acharring time 1 min.; ^b charring time 4 min.; ^c addition of fresh rye grass as co-substrate.

For the A soil layer, a continuous loss of total amide N and heterocyclic N for the A layer was detected (Fig. 26C and D). After 20 months, for all incubates only 49 to 59% of heterocyclic N compounds were recovered. The respective amide-N recoveries were larger (59 to 87%). For the more charred PyOM 4M treatments, the trend of larger losses of heterocyclic N than amide N is significant at all stages of the incubation ($p \leq 0.001$). Similar to PyOM C, co-substrate addition showed no significant impact on the degradation rate of organic N ($0.148 \leq p \leq 0.761$). The same pattern was observed for PyOM 4M ($0.259 \leq p \leq 0.452$).

For the 28-month incubates, the ^{15}N enrichment of the leachate was large enough to perform ^{15}N NMR spectroscopy. However, due to the low signal to noise ratio of the spectra we disclaim quantification. The spectrum is dominated by the signal in the region of heterocyclic N (Fig. 27). In total, 2.8 and 2.2% of the ^{15}N PyOM input was recovered in the leachate, indicating that up to 3.5% of the total remaining ^{15}N PyOM can be heterocyclic N.

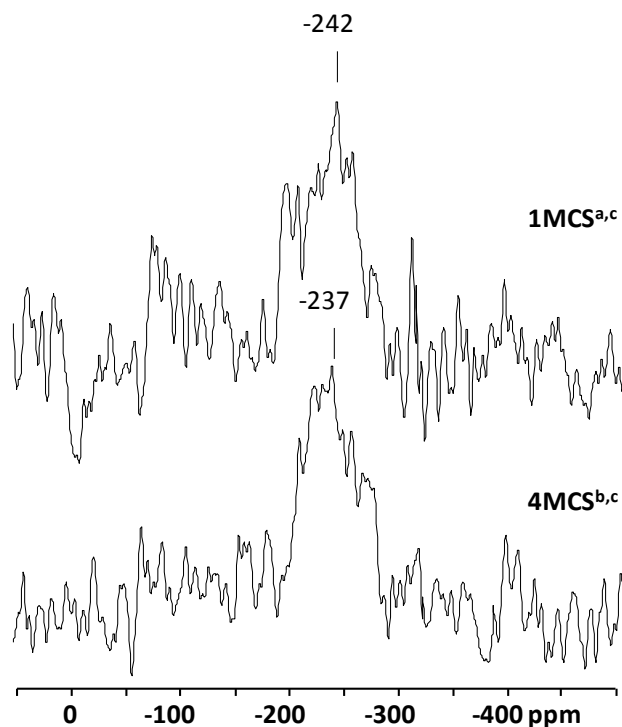


Figure 27: Solid-state ^{15}N NMR spectra of the vertical relocated PyOM leachate fraction after 28 months of incubation. ^acharring time 1 min.; ^b charring time 4 min; ^c addition of fresh rye grass as co-substrate.

6.7 Is black nitrogen (BN) a recalcitrant N pool?

The charring process of rye grass produced a narrow aryl C to heterocyclic N ratio of 0.9 for the respective PyOM. This implicates concomitantly an increasing heterocyclic N content. The finding is in line with Knicker (2010) who demonstrated that BN is an important constituent of grass-derived char.

The present study shows that in spite of its heteroaromatic structure BN can be degraded. The observed N loss is attributed to the conversion into mineral N forms and amide N (Fig. 26). The latter is confirmed by an increase of the amide to heterocyclic N ratio for the aged PyOM and occurred most likely by the uptake and incorporation of mineralised N derived from BN into microbial biomass, the preferential decomposition or/and their vertical movement of heterocyclic N. This finding is important for the N cycle of fire-affected environments in terms of N availability for plants and microorganisms on the long-term scale.

6.8 Structural alteration of PyOM by degradation

With respect to the investigated structural modifications of the PyOM and the calculated degradation dynamics, it can be concluded that aged PyOM is characterised by an aryl backbone which is highly substituted with carboxylic and oxygen groups. Such aged PyOM was observed for Chinese modern and ancient paddy soils (Hu et al., 2009) and could also explain the increased cation exchange capacity of Amazonian Terra preta soils (Liang et al., 2006; Solomon et al., 2007). The increased proportion of polar functional groups promotes the formation of organo-mineral complexes found by Brodowski et al. (2005a) and may also explain the PyOM-mineral interaction (Fig. 19, chapter 5.5.3). Furthermore, the hydrophobicity may be reduced by partial oxidation of PyOM, allowing an increased vertical movement through the soil column or export to aquatic systems as recently described by Hockaday et al. (2007) and Guggenberger et al. (2008).

6.9 Stability of PyOM and environmental implications

The present study indicates that PyOM is composed of C and N pools with different chemical structure and stability (Table 18, Fig. 24 and 26, Hilscher and Knicker (2011a)). In general, the degradation rate of PyOM is reduced compared to rates reported for fresh plant material. However, their $t_{1/2}$ are still in a range 3.0 to 3.8 yrs, which indicate a low to medium recalcitrance. Additionally, the study demonstrates that a more intensive thermal alteration, resulting in increased aromaticity, does not necessarily reduce the degradation efficiency of the aryl C pool (Table 18). An explanation may be that during the charring process instead of larger polycondensed structures, relatively small C clusters were formed due to pyrolytic breakdown processes (Kramer et al., 2004; Knicker et al., 2005a).

Associated with the mineralisation process (Fig. 12, Chapter 3.2; Fig. 18, Chapter 5.3), the detected structural modifications of PyOM, especially the formation of oxygen-containing polar groups, are an important factor influencing the chemical properties of the fire-affected SOM. The resulting aged PyOM is characterised by high aryl-C content and has a similar structure as the humic-like substances produced by Trompowsky et al. (2005) by chemical oxidation of eucalyptus charcoal. Such aged PyOM is being held responsible for organic matter accumulation and consequently higher soil fertility potential, especially for tropical soils (Glaser et al., 2002).

When translating the findings of the present study to natural or managed landscapes it is important to note, that the experimental conditions were more or less optimal and controlled. Such conditions will certainly not be present in natural environments. However, it was used a natural soil and simulated the incorporation of fresh plant material by adding fresh rye grass as a co-substrate. With this experimental design, possible organo-mineral interactions (von Lützow et al., 2006; Wiseman and Püttmann, 2006) and priming effects (Hamer et al., 2004) are considered, allowing a more realistic view on the fate of PyOM in soils and sediments.

7. Conclusions and outlook

The present research work has highlighted that PyOM is involved in the degradation and humification process of organic matter in soil.

The incubation experiments reveal that PyOM can be already attacked by microorganism shortly after its production and accumulation at the soil surface. It was shown that such PyOM can be mineralised at rates that are comparable to those for soil organic matter. In this context, the application of PyOM (biochar) to soil in order to sequester C on a long-term scale has to be considered critically. Most likely the disintegration of biochar will be enhanced by intensive agricultural practices (ploughing, tilling, harrowing), leading to even shorter residence times. On the other hand the present studies showed that the degradation of PyOM also results in mineralisation of black nitrogen which turns it into a plant available form. The gradual slow N release minimises N loss by leaching. Therefore, N-rich PyOM may be considered as an efficient N fertiliser for cultivation of crop plants.

There are considerations to use the n-alkanes composition of the lipid fraction as a tracer for biomass burning in soils and sediments. However, the present study demonstrates that this lipid fraction is quickly modified by biotic activities, most likely by degradation and *in situ* biosynthesis. For this reason, the preservation of such thermally modified lipids will be limited in well-aerated soils. The application of the molecular marker levoglucosan (LG) can also lead to underestimation of PyOM in soil. Severely charred plant remains were depleted in LG and it was shown to be efficiently decomposed during the initial degradation of PyOM. Therefore, the application of such specific biomarkers for PyOM quantification in soil and sediment cannot be recommended. In general, the use of a lot of different quantification techniques in PyOM research is problematic. Studies which apply different PyOM detection approaches are limited their comparability.

The PyOM is also subjected to an aging process and contributes to the SOM. The observed enrichment of polar functional groups by partial oxidation of aromatic PyOM structures has an important impact on the respective SOM quality. The presence of such PyOM-derived functional groups may increase the cation exchange capacity which results in an improved nutrient supply for plants as observed in PyOM-rich “Terra preta” soils (Glaser et al., 2001; Liang et al., 2006). Moreover, the supply of fresh plant residues promotes the partial oxidation of PyOM, which results in provision of a larger amount of organic source material for mineral association. The formation of PyOM-mineral complexes could

contribute to stabilisation against further microbial attack. However, the organo-mineral stabilisation potential of humified PyOM residues depends on soil properties like texture and mineralogy. The stabilisation of PyOM may be responsible for reported residence times of thousands of years in soils and sediments (Saldarriaga and West, 1986; Middelburg et al., 1999; Glaser et al., 2001). Thus, such a preservation of PyOM may be explained by physical protection (hydrophobicity, occlusion and encapsulation) or conservation (e.g. oxygen exclusion) mechanisms against biotic and non-biotic degradation as observed for other SOM fractions (von Lützow et al., 2006). This means that PyOM preservation is not based on a chemical persistence of PyOM. This view allows to understand the found fast PyOM turnover in savannah and steppe soils (Bird et al., 1999; Hammes et al., 2008). The stabilisation potential of PyOM in such sandy well-aerated soils will be limited, leading to faster mineralisation of PyOM residues on a decadal to centennial time scale. Therefore, there must be no discrepancy in the large difference of the reported residence times of PyOM.

An additional loss of PyOM is caused by mobilisation and transport to deeper soil horizons or into aquatic systems. The export of PyOM from fire-impacted ecosystems is linked to geographic and climatic factors such as slope and rainfall frequency. Such PyOM fluxes are often neglected in C-circle balances. The consideration of these fluxes would show that PyOM is involved in the global C and N cycle.

With regard to the climate change, an increase of warmer climates with extended dry periods is predicted. Such conditions favour a higher fire risk, leading to an increase of fire-affected ecosystem areas. It was postulated that the expected larger PyOM loads may count as an important C sink for long-term reduction of CO₂ in the atmosphere. However, it has to bear in mind that under wildfire conditions most of the biomass is even converted to CO₂ and only 1 to 3% remains as PyOM. The PyOM residues can be effectively mineralised which clearly disproves the often postulated long-term C sequestration potential.

It can be concluded that the assumption PyOM is a highly refractory constituent within the SOM is oversimplified. PyOM does not generally count to a “passive” SOM pool with turnover rates of more than 1,000 yrs. Therefore, C and N flux models for soils should take into account that some PyOM may have turnover times on a decade scale. The increase of soil temperature due to the climate change could induce a higher microbial activity, which causes in a forced PyOM degradation in the future. This would imply increasing CO₂

emissions by mineralisation of PyOM and other SOM together with an increased fire-induced CO₂ release on the other hand.

8. References

- Aleman, L.B., Grant, D.M., Alger, T.D. and Pugmire, R.J., 1983. Cross polarization and magic angle sample spinning NMR spectra of model organic compounds. 3. Effect of the ^{13}C - ^1H dipolar interaction on cross polarization and carbon-proton dephasing. *Journal of the American Chemical Society* 105, 6697-6704.
- Almendros, G., Martin, F. and Gonzalez-Vila, F.J., 1988. Effects of fire on humic and lipid fractions in a dystic Xerocherpt in Spain. *Geoderma* 42, 115-127.
- Almendros, G., Gonzalez-Vila, F.J. and Martin, F., 1990. Fire-induced transformation of soil organic matter from an oak forest - an experimental approach to the effects of fire on humic substances. *Soil Science* 149, 158-168.
- Almendros, G., Knicker, H. and Gonzalez-Vila, F.J., 2003. Rearrangement of carbon and nitrogen forms in peat after progressive thermal oxidation as determined by solid-state ^{13}C and ^{15}N NMR spectroscopy. *Organic Geochemistry* 34, 1559-1568.
- Ambles, A., Parlanti, E., Jambu, P., Mayoungou, P. and Jacquesy, J.C., 1994. n-Alkane oxidation in soil - formation of internal monoalkenes. *Geoderma* 64, 111-124.
- Baldock, J.A., Oades, J.M., Waters, A.G., Peng, X., Vassallo, A.M. and Wilson, M.A., 1992. Aspects of the chemical-structure of soil organic materials as revealed by solid-state ^{13}C NMR spectroscopy. *Biogeochemistry* 16, 1-42.
- Baldock, J.A. and Smernik, R.J., 2002. Chemical composition and bioavailability of thermally altered *Pinus resinosa* (red pine) wood. *Organic Geochemistry* 33, 1093-1109.
- Ben Said, O., Goni-Urriza, M.S., El Bour, M., Dellali, M., Aissa, P. and Duran, R., 2008. Characterization of aerobic polycyclic aromatic hydrocarbon-degrading bacteria from Bizerte lagoon sediments, Tunisia. *Journal of Applied Microbiology* 104, 987-997.
- Bird, M.I. and Grocke, D.R., 1997. Determination of the abundance and carbon isotope composition of elemental carbon in sediments. *Geochimica Et Cosmochimica Acta* 61, 3413-3423.

- Bird, M.I., Moyo, C., Veenendaal, E.M., Lloyd, J. and Frost, P., 1999. Stability of elemental carbon in a savanna soil. *Global Biogeochemical Cycles* 13, 923-932.
- Bird, M.I. and Ascough, P.L., 2010. Isotopes in pyrogenic carbon: A review. *Organic Geochemistry*, doi:10.1016/j.orggeochem.2010.09.005.
- Blanchette, R.A., 1991. Delignification by wood-decay fungi. *Annual Review of Phytopathology* 29, 381-398.
- Bloch, F., Hansen, W.W. and Packard, M., 1946. The nuclear induction experiment. *Physical Review* 70, 474-485.
- Bortiatynski, J.M., Hatcher, P.G. and Knicker, H., 1996. NMR techniques (C, N, and H) in studies of humic substances. In: J.S. Gaffney, N.A. Marley and S.B. Clark (Editors), *Humic and Fulvic Acids - Isolation, Structure, and Environmental Role*. Acs Symposium Series, pp. 57-77.
- Brodowski, S., Amelung, W., Haumaier, L., Abetz, C. and Zech, W., 2005a. Morphological and chemical properties of black carbon in physical soil fractions as revealed by scanning electron microscopy and energy-dispersive X-ray spectroscopy. *Geoderma* 128, 116-129.
- Brodowski, S., Rodionov, A., Haumaier, L., Glaser, B. and Amelung, W., 2005b. Revised black carbon assessment using benzene polycarboxylic acids. *Organic Geochemistry* 36, 1299-1310.
- Brunnauer, S., Emmett, P.H. and Teller, E., 1938. Adsorption of gases in multimolecular layers. *Journal of the American Chemical Society* 60, 309 - 319.
- Buchan, G.D., Grewal, K.S., Claydon, J.J. and McPherson, R.J., 1993. A comparison of sedigraph and pipette methods for soil particle-size analysis. *Australian Journal of Soil Research* 31, 407-417.
- Cao, Z.H., Ding, J.L., Hu, Z.Y., Knicker, H., Kögel-Knabner, I., Yang, L.Z., Yin, R., Lin, X.G. and Dong, Y.H., 2006. Ancient paddy soils from the Neolithic age in China's Yangtze river delta. *Naturwissenschaften* 93, 232-236.

- Cheng, C.H., Lehmann, J., Thies, J.E., Burton, S.D. and Engelhard, M.H., 2006. Oxidation of black carbon by biotic and abiotic processes. *Organic Geochemistry* 37, 1477-1488.
- Cheng, C.H., Lehmann, J. and Engelhard, M.H., 2008. Natural oxidation of black carbon in soils: Changes in molecular form and surface charge along a climosequence. *Geochimica Et Cosmochimica Acta* 72, 1598-1610.
- Cheshire, M.V., Williams, B.L., Benzingpurdie, L.M., Ratcliffe, C.I. and Ripmeester, J.A., 1990. Use of NMR spectroscopy to study transformations of nitrogenous substances during incubation of peat. *Soil Use and Management* 6, 90-92.
- Cook, R.L., Langford, C.H., Yamdagni, R. and Preston, C.M., 1996. A modified cross-polarization magic angle spinning ^{13}C NMR procedure for the study of humic materials. *Analytical Chemistry* 68, 3979-3986.
- Cooney, J.J. and Proby, C.M., 1971. Fatty acid composition of *cladosporium-resinae* grown on glucose and on hydrocarbons. *Journal of Bacteriology* 108, 777-781.
- Cornelissen, G., Gustafsson, O., Bucheli, T.D., Jonker, M.T.O., Koelmans, A.A. and Van Noort, P.C.M., 2005. Extensive sorption of organic compounds to black carbon, coal, and kerogen in sediments and soils: Mechanisms and consequences for distribution, bioaccumulation, and biodegradation. *Environmental Science & Technology* 39, 6881-6895.
- Covington, W.W. and Sackett, S.S., 1992. Soil mineral nitrogen changes following prescribed burning in ponderosa pine. *Forest Ecology and Management* 54, 175-191.
- Czimczik, C.I., Preston, C.M., Schmidt, M.W.I., Werner, R.A. and Schulze, E.D., 2002. Effects of charring on mass, organic carbon, and stable carbon isotope composition of wood. *Organic Geochemistry* 33, 1207-1223.
- Czimczik, C.I., Preston, C.M., Schmidt, M.W.I. and Schulze, E.D., 2003. How surface fire in Siberian Scots pine forests affects soil organic carbon in the forest floor: Stocks, molecular structure, and conversion to black carbon (charcoal). *Global Biogeochemical Cycles* 17, 1020.

- Dai, K.H. and Johnson, C.E., 1999. Applicability of solid-state C-13 CP/MAS NMR analysis in Spodosols: chemical removal of magnetic materials. *Geoderma* 93, 289-310.
- Dai, X., Boutton, T.W., Hailemichael, M., Ansley, R.J. and Jessup, K.E., 2006. Soil carbon and nitrogen storage in response to fire in a temperate mixed-grass savanna. *Journal of Environmental Quality* 35, 1620-1628.
- de Boer, J.H., Lippens, B.C., Linsen, B.G., Broekhoff, J.C.P., van den Heuvel, A. and Osinga, T.J., 1966. The t-curve of multimolecular N₂-adsorption. *Journal of Colloid and Interface Science* 21, 404-414.
- De la Rosa, J.M., Knicker, H., Lopez-Capel, E., Manning, D.A.C., Gonzalez-Perez, J.A. and Gonzalez-Vila, F.J., 2008. Direct detection of black carbon in soils by Py-GC/MS, carbon-13 NMR spectroscopy and thermogravimetric techniques. *Soil Science Society of America Journal* 72, 258-267.
- De la Rosa, J.M., Gonzalez-Vila, F.J., Lopez-Capel, E., Manning, D.A.C., Knicker, H. and Gonzalez-Perez, J.A., 2009. Structural properties of non-combustion-derived refractory organic matter which interfere with BC quantification. *Journal of Analytical and Applied Pyrolysis* 85, 399-407.
- deJonge, H. and MittelmeijerHazeleger, M.C., 1996. Adsorption of CO₂ and N₂ on soil organic matter: Nature of porosity, surface area, and diffusion mechanisms. *Environmental Science & Technology* 30, 408-413.
- Dell'Abate, M.T., Benedetti, A. and Sequi, P., 2000. Thermal methods of organic matter maturation monitoring during a composting process. *Journal of Thermal Analysis and Calorimetry* 61, 389-396.
- Dell'Abate, M.T., Benedetti, A. and Brookes, P.C., 2003. Hyphenated techniques of thermal analysis for characterisation of soil humic substances. *Journal of Separation Science* 26, 433-440.
- Dieckow, J., Mielniczuk, J., Knicker, H., Bayer, C., Dick, D.P. and Kögel-Knabner, I., 2005. Composition of organic matter in a subtropical Acrisol as influenced by land use, cropping and N fertilization, assessed by CPMAS ¹³C NMR spectroscopy. *European Journal of Soil Science* 56, 705-715.

- Dorado, J., Claassen, F.W., van Beek, T.A., Lenon, G., Wijnberg, J. and Sierra-Alvarez, R., 2000. Elimination and detoxification of softwood extractives by white-rot fungi. *Journal of Biotechnology* 80, 231-240.
- Dubinin, M.M. and Radushkevich, L.V., 1947. Teoriya Dinamiki Adsorbtsii Na Realnom Zernenom Adsorbente. *Doklady Akademii Nauk Sssr* 55, 331.
- Dungait, J.A.J., Docherty, G., Straker, V. and Evershed, R.P., 2010. Seasonal variations in bulk tissue, fatty acid and monosaccharide $\delta^{13}\text{C}$ values of leaves from mesotrophic grassland plant communities under different grazing managements. *Phytochemistry* 71, 415-428.
- Eckmeier, E. and Wiesenberg, G.L.B., 2009. Short-chain n-alkanes (C16-20) in ancient soil are useful molecular markers for prehistoric biomass burning. *Journal of Archaeological Science* 36, 1590-1596.
- Eglinton, G., Gonzalez, A.G., Hamilton, R.J. and Raphael, R.A., 1962. Hydrocarbon constituents of the wax coatings of plant leaves - a taxonomic survey. *Phytochemistry* 1, 89-102.
- Eglinton, G. and Hamilton, R.J., 1967. Leaf epicuticular waxes. *Science* 156, 1322-1335.
- Elias, V.O., Simoneit, B.R.T., Cordeiro, R.C. and Turcq, B., 2001. Evaluating levoglucosan as an indicator of biomass burning in Carajas, Amazonia: A comparison to the charcoal record. *Geochimica Et Cosmochimica Acta* 65, 267-272.
- Eusterhues, K., Rumpel, C., Kleber, M. and Kögel-Knabner, I., 2003. Stabilisation of soil organic matter by interactions with minerals as revealed by mineral dissolution and oxidative degradation. *Organic Geochemistry* 34, 1591-1600.
- Fang, X.W., Chua, T., Schmidt-Rohr, K. and Thompson, M.L., 2010. Quantitative ^{13}C NMR of whole and fractionated Iowa Mollisols for assessment of organic matter composition. *Geochimica Et Cosmochimica Acta* 74, 584-598.
- Fontaine, S., Mariotti, A. and Abbadie, L., 2003. The priming effect of organic matter: a question of microbial competition? *Soil Biology & Biochemistry* 35, 837-843.

- Foppen, F.H. and Griбанov, O., 1968. Lipids produced by *Epicoccum nigrum* in submerged culture. *Biochemical Journal* 106, 97-100.
- Freitas, J.C.C., Bonagamba, T.J. and Emmerich, F.G., 1999. ¹³C High-resolution solid-state NMR study of peat carbonization. *Energy & Fuels* 13, 53-59.
- Gärdenäs, A.I., Ågren, G.I., Bird, J.A., Clarholm, M., Hallin, S., Ineson, P., Kätterer, T., Knicker, H., Nilsson, S.I., Näsholm, T., Ogle, S., Paustian, K., Persson, T. and Stendahl, J., 2011. Knowledge gaps in soil carbon and nitrogen interactions – From molecular to global scale. *Soil Biology & Biochemistry* doi:10.1016/j.soilbio.2010.04.006.
- Gelinas, Y., Baldock, J.A. and Hedges, J.I., 2001. Demineralization of marine and freshwater sediments for CP/MAS C-13 NMR analysis. *Organic Geochemistry* 32, 677-693.
- Glaser, B., Haumaier, L., Guggenberger, G. and Zech, W., 1998. Black carbon in soils: the use of benzenecarboxylic acids as specific markers. *Organic Geochemistry* 29, 811-819.
- Glaser, B., Balashov, E., Haumaier, L., Guggenberger, G. and Zech, W., 2000. Black carbon in density fractions of anthropogenic soils of the Brazilian Amazon region. *Organic Geochemistry* 31, 669-678.
- Glaser, B., Haumaier, L., Guggenberger, G. and Zech, W., 2001. The 'Terra Preta' phenomenon: a model for sustainable agriculture in the humid tropics. *Naturwissenschaften* 88, 37-41.
- Glaser, B., Lehmann, J. and Zech, W., 2002. Ameliorating physical and chemical properties of highly weathered soils in the tropics with charcoal - a review. *Biology and Fertility of Soils* 35, 219-230.
- Glaser, B. and Knorr, K.H., 2008. Isotopic evidence for condensed aromatics from non-pyrolytic sources in soils - implications for current methods for quantifying soil black carbon. *Rapid Communications in Mass Spectrometry* 22, 935-942.

- Goncalves, C.N., Dalmolin, R.S.D., Dick, D.P., Knicker, H., Klamt, E. and Kögel-Knabner, I., 2003. The effect of 10% HF treatment on the resolution of CPMAS ^{13}C NMR spectra and on the quality of organic matter in Ferralsols. *Geoderma* 116, 373-392.
- González-Pérez, J.A., González-Vila, F.J., González-Vázquez, R., Arias, M.E., Rodríguez, J. and Knicker, H., 2008. Use of multiple biogeochemical parameters to monitor the recovery of soils after forest fires. *Organic Geochemistry* 39, 940-944.
- González-Vila, F.J., Tinoco, P., Almendros, G. and Martin, F., 2001. Pyrolysis-GC-MS analysis of the formation and degradation stages of charred residues from lignocellulosic biomass. *Journal of Agricultural and Food Chemistry* 49, 1128-1131.
- González-Vila, F.J., Polvillo, O., Boski, T., Moura, D. and de Andres, J.R., 2003. Biomarker patterns in a time-resolved holocene/terminal Pleistocene sedimentary sequence from the Guadiana river estuarine area (SW Portugal/Spain border). *Organic Geochemistry* 34, 1601-1613.
- Grassi, M. and Gatti, G., 1995. Nuclear magnetic resonance methods in environmental chemistry. *Annali Di Chimica* 85, 487-502.
- Guggenberger, G., Rodionov, A., Shibistova, O., Grabe, M., Kasansky, O.A., Fuchs, H., Mikheyeva, N., Zrazhevskaya, G. and Flessa, H., 2008. Storage and mobility of black carbon in permafrost soils of the forest tundra ecotone in Northern Siberia. *Global Change Biology* 14, 1367-1381.
- Gustafsson, O., Haghseta, F., Chan, C., MacFarlane, J. and Gschwend, P.M., 1997. Quantification of the dilute sedimentary soot phase: Implications for PAH speciation and bioavailability. *Environmental Science & Technology* 31, 203-209.
- Gustafsson, O., Bucheli, T.D., Kukulska, Z., Andersson, M., Largeau, C., Rouzaud, J.N., Reddy, C.M. and Eglinton, T.I., 2001. Evaluation of a protocol for the quantification of black carbon in sediments. *Global Biogeochemical Cycles* 15, 881-890.
- Hamer, U., Marschner, B., Brodowski, S. and Amelung, W., 2004. Interactive priming of black carbon and glucose mineralisation. *Organic Geochemistry* 35, 823-830.

- Hammes, K., Smernik, R.J., Skjemstad, J.O., Herzog, A., Vogt, U.F. and Schmidt, M.W.I., 2006. Synthesis and characterisation of laboratory-charred grass straw (*Oryza sativa*) and chestnut wood (*Castanea sativa*) as reference materials for black carbon quantification. *Organic Geochemistry* 37, 1629-1633.
- Hammes, K., Schmidt, M.W.I., Smernik, R.J., Currie, L.A., Ball, W.P., Nguyen, T.H., Louchouart, P., Houel, S., Gustafsson, O., Elmquist, M., Cornelissen, G., Skjemstad, J.O., Masiello, C.A., Song, J., Peng, P., Mitra, S., Dunn, J.C., Hatcher, P.G., Hockaday, W.C., Smith, D.M., Hartkopf-Froeder, C., Boehmer, A., Luer, B., Huebert, B.J., Amelung, W., Brodowski, S., Huang, L., Zhang, W., Gschwend, P.M., Flores-Cervantes, D.X., Largeau, C., Rouzaud, J.N., Rumpel, C., Guggenberger, G., Kaiser, K., Rodionov, A., Gonzalez-Vila, F.J., Gonzalez-Perez, J.A., de la Rosa, J.M., Manning, D.A.C., Lopez-Capel, E. and Ding, L., 2007. Comparison of quantification methods to measure fire-derived (black/elemental) carbon in soils and sediments using reference materials from soil, water, sediment and the atmosphere. *Global Biogeochemical Cycles* 21.
- Hammes, K., Torn, M.S., Lapenas, A.G. and Schmidt, M.W.I., 2008. Centennial black carbon turnover observed in a Russian steppe soil. *Biogeosciences* 5, 1339-1350.
- Hatakka, A., 1994. Lignin-modifying enzymes from selected white-rot fungi: production and role in lignin degradation. *Fems Microbiology Reviews* 13, 125-135.
- Hedges, J.I., Eglinton, G., Hatcher, P.G., Kirchman, D.L., Arnosti, C., Derenne, S., Evershed, R.P., Kögel-Knabner, I., de Leeuw, J.W., Littke, R., Michaelis, W. and Rullkotter, J., 2000. The molecularly-uncharacterized component of nonliving organic matter in natural environments. *Organic Geochemistry* 31, 945-958.
- Hilscher, A., Heister, K., Siewert, C. and Knicker, H., 2009. Mineralisation and structural changes during the initial phase of microbial degradation of pyrogenic plant residues in soil. *Organic Geochemistry* 40, 332-342.
- Hilscher, A. and Knicker, H., 2011a. Carbon and Nitrogen degradation on molecular scale of grass-derived pyrogenic organic material during 28 months of incubation in soil. *Soil Biology & Biochemistry* 43, 261-270.

- Hilscher, A. and Knicker, H., 2011b. Degradation of grass-derived pyrogenic organic material, transport of the residues within a soil column and distribution into soil organic matter fractions during a microcosm experiment of 28 months. *Organic Geochemistry* 42, 42-54.
- Hockaday, W.C., Grannas, A.M., Kim, S. and Hatcher, P.G., 2006. Direct molecular evidence for the degradation and mobility of black carbon in soils from ultrahigh-resolution mass spectral analysis of dissolved organic matter from a fire-impacted forest soil. *Organic Geochemistry* 37, 501-510.
- Hockaday, W.C., Grannas, A.M., Kim, S. and Hatcher, P.G., 2007. The transformation and mobility of charcoal in a fire-impacted watershed. *Geochimica Et Cosmochimica Acta* 71, 3432-3445.
- Hofrichter, M., Bublitz, F. and Fritsche, W., 1997. Fungal attack on coal: I. modification of hard coal by fungi. *Fuel Processing Technology* 52, 43-53.
- Hu, L.C., Li, X., Liu, B.D., Gu, M. and Dai, J.Y., 2009. Organic structure and possible origin of ancient charred paddies at Chuodun site in southern China. *Science in China Series D-Earth Sciences* 52, 93-100.
- Hubbert, K.R., Preisler, H.K., Wohlgemuth, P.M., Graham, R.C. and Narog, M.G., 2006. Prescribed burning effects on soil physical properties and soil water repellency in a steep chaparral watershed, southern California, USA. *Geoderma* 130, 284-298.
- Jaffe, R., Elisme, T. and Cabrera, A.C., 1996. Organic geochemistry of seasonally flooded rain forest soils: Molecular composition and early diagenesis of lipid components. *Organic Geochemistry* 25, 9-17.
- Jansen, B., Nierop, K.G.J., Hageman, J.A., Cleef, A.M. and Verstraten, J.M., 2006. The straight-chain lipid biomarker composition of plant species responsible for the dominant biomass production along two altitudinal transects in the Ecuadorian Andes. *Organic Geochemistry* 37, 1514-1536.
- Jones, J.G., 1969. Studies on lipids of soil micro-organisms with particular reference to hydrocarbons. *Journal of General Microbiology* 59, 145-152.

- Kaiser, K. and Guggenberger, G., 2000. The role of DOM sorption to mineral surfaces in the preservation of organic matter in soils. *Organic Geochemistry* 31, 711-725.
- Keeler, C. and Maciel, G.E., 2003. Quantitation in the solid-state ^{13}C NMR analysis of soil and organic soil fractions. *Analytical Chemistry* 75, 2421-2432.
- Kim, E.J., Oh, J.E. and Chang, Y.S., 2003. Effects of forest fire on the level and distribution of PCDD/Fs and PAHs in soil. *Science of the Total Environment* 311, 177-189.
- Kim, S.W., Kaplan, L.A., Benner, R. and Hatcher, P.G., 2004. Hydrogen-deficient molecules in natural riverine water samples - evidence for the existence of black carbon in DOM. *Marine Chemistry* 92, 225-234.
- Kitamura, Y., Abe, Y. and Yasui, T., 1991. Metabolism of levoglucosan (1,6-anhydro-beta-d-glucopyranose) in microorganisms. *Agricultural and Biological Chemistry* 55, 515-521.
- Knicker, H., 1993. Quantitative ^{15}N - und ^{13}C -CPMAS-Festkörper- und ^{15}N Flüssigkeits-NMR-Spektroskopie an Pflanzenkomposten und natürlichen Böden. Ph.D. thesis. Universität Regensburg, Regensburg, Germany.
- Knicker, H. and Lüdemann, H.D., 1995. ^{15}N and ^{13}C CPMAS and solution NMR-studies of ^{15}N enriched plant material during 600 days of microbial degradation. *Organic Geochemistry* 23, 329-341.
- Knicker, H., Hatcher, P.G. and Scaroni, A.W., 1996a. A solid-state ^{15}N NMR spectroscopic investigation of the origin of nitrogen structures in coal. *International Journal of Coal Geology* 32, 255-278.
- Knicker, H., Almendros, G., Gonzalez-Vila, F.J., Martin, F. and Lüdemann, H.D., 1996b. ^{13}C and ^{15}N NMR spectroscopic examination of the transformation of organic nitrogen in plant biomass during thermal treatment. *Soil Biology & Biochemistry* 28, 1053-1060.

- Knicker, H., Bruns-Nagel, D., Drzyzga, O., Von Löw, E. and Steinbach, K., 1999. Characterization of ^{15}N -TNT residues after an anaerobic/aerobic treatment of soil/molasses mixtures by solid state ^{15}N NMR spectroscopy. 1. Determination and optimization of relevant NMR spectroscopic parameters. *Environmental Science & Technology* 33, 343-349.
- Knicker, H., Schmidt, M.W.I. and Kögel-Knabner, I., 2000. Nature of organic nitrogen in fine particle size separates of sandy soils of highly industrialized areas as revealed by NMR spectroscopy. *Soil Biology & Biochemistry* 32, 241-252.
- Knicker, H., 2000. Biogenic nitrogen in soils as revealed by solid-state ^{13}C and ^{15}N nuclear magnetic resonance spectroscopy. *Journal of Environmental Quality* 29, 715-723.
- Knicker, H., 2002. The feasibility of using DCPMAS ^{15}N ^{13}C NMR spectroscopy for a better characterization of immobilized ^{15}N during incubation of ^{13}C - and ^{15}N -enriched plant material. *Organic Geochemistry* 33, 237-246.
- Knicker, H., 2003. Incorporation of N-15-TNT transformation products into humifying plant organic matter as revealed by one- and two-dimensional solid state NMR spectroscopy. *Science of the Total Environment* 308, 211-220.
- Knicker, H., Totsche, K.U., Almendros, G. and Gonzalez-Vila, F.J., 2005a. Condensation degree of burnt peat and plant residues and the reliability of solid-state VACP MAS ^{13}C NMR spectra obtained from pyrogenic humic material. *Organic Geochemistry* 36, 1359-1377.
- Knicker, H., Gonzalez-Vila, F.J., Polvillo, O., Gonzalez, J.A. and Almendros, G., 2005b. Fire-induced transformation of C- and N-forms in different organic soil fractions from a Dystric Cambisol under a Mediterranean pine forest (*Pinus pinaster*). *Soil Biology & Biochemistry* 37, 701-718.
- Knicker, H., Almendros, G., Gonzalez-Vila, F.J., Gonzalez-Perez, J.A. and Polvillo, O., 2006. Characteristic alterations of quantity and quality of soil organic matter caused by forest fires in continental Mediterranean ecosystems: a solid-state ^{13}C NMR study. *European Journal of Soil Science* 57, 558-569.
- Knicker, H., 2007. How does fire affect the nature and stability of soil organic nitrogen and carbon? A review. *Biogeochemistry* 85, 91-118.

- Knicker, H., Müller, P. and Hilscher, A., 2007. How useful is chemical oxidation with dichromate for the determination of "black carbon" in fire-affected soils? *Geoderma* 142, 178-196.
- Knicker, H., Hilscher, A., Gonzalez-Vila, F.J. and Almendros, G., 2008a. A new conceptual model for the structural properties of char produced during vegetation fires. *Organic Geochemistry* 39, 935-939.
- Knicker, H., Wiesmeier, M. and Dick, D.R., 2008b. A simplified method for the quantification of pyrogenic organic matter in grassland soils via chemical oxidation. *Geoderma* 147, 69-74.
- Knicker, H., 2010. "Black nitrogen" – An important fraction in determining the recalcitrance of charcoal. *Organic Geochemistry* 41, 947-950.
- Kögel-Knabner, I., 1997. ^{13}C and ^{15}N NMR spectroscopy as a tool in soil organic matter studies. *Geoderma* 80, 243-270.
- Kojima, Y., Itada, N. and Hayaishi, O., 1961. Metapyrocatechase: a new catechol-cleaving enzyme. *Journal of Biological Chemistry* 236, 2223-2228.
- Kölbl, A. and Kögel-Knabner, I., 2004. Content and composition of free and occluded particulate organic matter in a differently textured arable Cambisol as revealed by solid-state ^{13}C NMR spectroscopy. *Journal of Plant Nutrition and Soil Science* 167, 45-53.
- Kölbl, A., von Lützow, M., Rumpel, C., Munch, J.C. and Kögel-Knabner, I., 2007. Dynamics of ^{13}C -labeled mustard litter (*Sinapis alba*) in particle-size and aggregate fractions in an agricultural cropland with high- and low-yield areas. *Journal of Plant Nutrition and Soil Science-Zeitschrift Für Pflanzenernährung und Bodenkunde* 170, 123-133.
- Kramer, R.W., Kujawinski, E.B. and Hatcher, P.G., 2004. Identification of black carbon derived structures in a volcanic ash soil humic acid by Fourier transform ion cyclotron resonance mass spectrometry. *Environmental Science & Technology* 38, 3387-3395.

- Kruege, M.A., Stankiewicz, B.A., Crelling, J.C., Montanari, A. and Bensley, D.F., 1994. Fossil charcoal in cretaceous-tertiary boundary strata - evidence for catastrophic firestorm and megawave. *Geochimica Et Cosmochimica Acta* 58, 1393-1397.
- Kuhlbusch, T.A.J. and Crutzen, P.J., 1995. Toward a global estimate of black carbon in residues of vegetation fires representing a sink of atmospheric CO₂ and a source of O₂. *Global Biogeochemical Cycles* 9, 491-501.
- Kuhn, T.K., Krull, E.S., Bowater, A., Grice, K. and Gleixner, G., 2010. The occurrence of short chain n-alkanes with an even over odd predominance in higher plants and soils. *Organic Geochemistry* 41, 88-95.
- Kuo, L.J., Herbert, B.E. and Louchouart, P., 2008. Can levoglucosan be used to characterize and quantify char/charcoal black carbon in environmental media? *Organic Geochemistry* 39, 1466-1478.
- Kuzyakov, Y., Subbotina, I., Chen, H.Q., Bogomolova, I. and Xu, X.L., 2009. Black carbon decomposition and incorporation into soil microbial biomass estimated by ¹⁴C labeling. *Soil Biology & Biochemistry* 41, 210-219.
- Kwon, S. and Pignatello, J.J., 2005. Effect of natural organic substances on the surface and adsorptive properties of environmental black carbon (char): Pseudo pore blockage by model lipid components and its implications for N₂-probed surface properties of natural sorbents. *Environmental Science & Technology* 39, 7932-7939.
- Lakshman, C.M. and Hoelsche, H.E., 1970. Production of levoglucosan by pyrolysis of carbohydrates - pyrolysis in hot inert gas stream. *Industrial & Engineering Chemistry Product Research and Development* 9, 57-59.
- Lehmann, J., Liang, B.Q., Solomon, D., Lerotic, M., Luizao, F., Kinyangi, J., Schafer, T., Wirick, S. and Jacobsen, C., 2005. Near-edge X-ray absorption fine structure (NEXAFS) spectroscopy for mapping nano-scale distribution of organic carbon forms in soil: Application to black carbon particles. *Global Biogeochemical Cycles* 19.
- Lehmann, J., 2007. A handful of carbon. *Nature* 447, 143-144.

- Liang, B., Lehmann, J., Solomon, D., Kinyangi, J., Grossman, J., O'Neill, B., Skjemstad, J.O., Thies, J., Luizao, F.J., Petersen, J. and Neves, E.G., 2006. Black carbon increases cation exchange capacity in soils. *Soil Science Society of America Journal* 70, 1719-1730.
- Lund, N.A., Robertson, A. and Whalley, W.B., 1953. The chemistry of fungi. 21. Asperxanthone and a preliminary examination of aspergillin. *Journal of the Chemical Society*, 2434-2439.
- Maciel, G.E., Kolodziejski, W.L., Bertran, M.S. and Dale, B.E., 1982. ^{13}C NMR and order in cellulose. *Macromolecules* 15, 686-687.
- Mao, J.D., Hu, W.G., Schmidt-Rohr, K., Davies, G., Ghabbour, E.A. and Xing, B.S., 2000. Quantitative characterization of humic substances by solid-state ^{13}C nuclear magnetic resonance. *Soil Science Society of America Journal* 64, 873-884.
- Marseille, F., Disnar, J.R., Guillet, B. and Noack, Y., 1999. n-alkanes and free fatty acids in humus and Al horizons of soils under beech, spruce and grass in the Massif-Central (Mont-Lozere), France. *European Journal of Soil Science* 50, 433-441.
- Masiello, C.A., 2004. New directions in black carbon organic geochemistry. *Marine Chemistry* 92, 201-213.
- Mathers, N.J., Xu, Z.H., Berners-Price, S.J., Perera, M.C.S. and Saffigna, P.G., 2002. Hydrofluoric acid pre-treatment for improving C-13 CPMAS NMR spectral quality of forest soils in south-east Queensland, Australia. *Australian Journal of Soil Research* 40, 655-674.
- Merdinger, E. and Devine, E.M., 1965. Lipids of *Debaryomyces hansenii*. *Journal of Bacteriology* 89, 1488-1493.
- Merdinger, E., Kohn, P. and McClain, R.C., 1968. Composition of lipids in extracts of *Pullularia pullulans*. *Canadian Journal of Microbiology* 14, 1021-1027.
- Middelburg, J.J., Nieuwenhuize, J. and van Breugel, P., 1999. Black carbon in marine sediments. *Marine Chemistry* 65, 245-252.
- Nguyen, B.T. and Lehmann, J., 2009. Black carbon decomposition under varying water regimes. *Organic Geochemistry* 40, 846-853.

- Nguyen, T.H., Brown, R.A. and Ball, W.P., 2004. An evaluation of thermal resistance as a measure of black carbon content in diesel soot, wood char, and sediment. *Organic Geochemistry* 35, 217-234.
- Nordgren, A., 1988. Apparatus for the continuous, long-term monitoring of soil respiration rate in large numbers of samples. *Soil Biology & Biochemistry* 20, 955-957.
- Oades, J.M., Vassallo, A.M., Waters, A.G. and Wilson, M.A., 1987. Characterization of organic-matter in particle-size and density fractions from a red-brown earth by solid-state ^{13}C NMR. *Australian Journal of Soil Research* 25, 71-82.
- Otto, A., Gondokusumo, R. and Simpson, M.J., 2006. Characterization and quantification of biomarkers from biomass burning at a recent wildfire site in Northern Alberta, Canada. *Applied Geochemistry* 21, 166-183.
- Pastor-Villegas, J., Pastor-Valle, J.F., Rodriguez, J.M.M. and Garcia, M.G., 2006. Study of commercial wood charcoals for the preparation of carbon adsorbents. *Journal of Analytical and Applied Pyrolysis* 76, 103-108.
- Pastor-Villegas, J., Rodriguez, J.M.M., Pastor-Valle, J.F. and Garcia, M.G., 2007. Changes in commercial wood charcoals by thermal treatments. *Journal of Analytical and Applied Pyrolysis* 80, 507-514.
- Peersen, O.B., Wu, X.L., Kustanovich, I. and Smith, S.O., 1993. Variable-amplitude cross-polarization MAS NMR. *Journal of Magnetic Resonance Series A* 104, 334-339.
- Pinto, M., Merino, P., del Prado, A., Estavillo, J.M., Yamulki, S., Gebauer, G., Piertzak, S., Lauf, J. and Oenema, O., 2004. Increased emissions of nitric oxide and nitrous oxide following tillage of a perennial pasture. *Nutrient Cycling in Agroecosystems* 70, 13-22.
- Plante, A.F., Fernandez, J.M. and Leifeld, J., 2009. Application of thermal analysis techniques in soil science. *Geoderma* 153, 1-10.
- Potter, M.C., 1908. Bacteria as agents in the oxidation of amorphous carbon. *Proceedings of the Royal Society of London Series B-Containing Papers of a Biological Character*, 239-259.

- Preston, C.M., Dudley, R.L., Fyfe, C.A. and Mathur, S.P., 1984. Effects of variations in contact times and copper contents in a ^{13}C CPMAS NMR-study of samples of 4 organic soils. *Geoderma* 33, 245-253.
- Preston, C.M., 1996. Applications of NMR to soil organic matter analysis: History and prospects. *Soil Science* 161, 144-166.
- Preston, C.M. and Schmidt, M.W.I., 2006. Black (pyrogenic) carbon: a synthesis of current knowledge and uncertainties with special consideration of boreal regions. *Biogeosciences* 3, 397-420.
- Prieto-Fernandez, A., Carballas, M. and Carballas, T., 2004. Inorganic and organic N pools in soils burned or heated: immediate alterations and evolution after forest wildfires. *Geoderma* 121, 291-306.
- Prosen, E.M., Radlein, D., Piskorz, J., Scott, D.S. and Legge, R.L., 1993. Microbial utilization of levoglucosan in wood pyrolysate as a carbon and energy-source. *Biotechnology and Bioengineering* 42, 538-541.
- Rabi, II, Zacharias, J.R., Millman, S. and Kusch, P., 1938. A new method of measuring nuclear magnetic moment. *Physical Review* 53, 318-318.
- Rambo, G.W. and Bean, G.A., 1969. Fatty acids of mycelia and conidia of *Fusarium oxysporum* and *Fusarium roseum*. *Canadian Journal of Microbiology* 15, 967-968.
- Rennert, T., Gockel, K.F. and Mansfeldt, T., 2007. Extraction of water-soluble organic matter from mineral horizons of forest soils. *Journal of Plant Nutrition and Soil Science-Zeitschrift Für Pflanzenernährung und Bodenkunde* 170, 514-521.
- Ripmeester, J.A., Hawkins, R.E., Macphee, J.A. and Nandi, B.N., 1986. On the interaction between pyridine and coal as studied by CP/MAS ^{15}N NMR. *Fuel* 65, 740-742.
- Rodionov, A., Amelung, W., Haumaier, L., Urusevskaja, I. and Zech, W., 2006. Black carbon in the zonal steppe soils of Russia. *Journal of Plant Nutrition and Soil Science* 169, 363-369.
- Rositani, F., Antonucci, P.L., Minutoli, M. and Giordano, N., 1987. Infrared-analysis of carbon-blacks. *Carbon* 25, 325-332.

- Rovira, P., Duguay, B. and Vallejo, V.R., 2009. Black carbon in wildfire-affected shrubland Mediterranean soils. *Journal of Plant Nutrition and Soil Science* 172, 43-52.
- Rumpel, C. and Kögel-Knabner, I., 2004. Microbial use of lignite compared to recent plant litter as substrates in reclaimed coal mine soils. *Soil Biology & Biochemistry* 36, 67-75.
- Saldarriaga, J.G. and West, D.C., 1986. Holocene fires in the northern Amazon basin. *Quaternary Research* 26, 358-366.
- Sanchez, J.P. and Lazzari, M.A., 1999. Impact of fire on soil nitrogen forms in central semiarid Argentina. *Arid Soil Research and Rehabilitation* 13, 81-90.
- Schaefer, J. and Stejskal, E.O., 1976. ^{13}C Nuclear magnetic-resonance of polymers spinning at magic Aangle. *Journal of the American Chemical Society* 98, 1031-1032.
- Schmid, E.M., Knicker, H., Bäumler, R. and Kögel-Knabner, I., 2001. Chemical composition of the organic matter in neolithic soil material as revealed by CPMAS ^{13}C NMR spectroscopy, polysaccharide analysis, and CuO oxidation. *Soil Science* 166, 569-584.
- Schmidt, M.W.I., Knicker, H., Hatcher, P.G. and Kögel-Knabner, I., 1997. Improvement of ^{13}C and ^{15}N CPMAS NMR spectra of bulk soils, particle size fractions and organic material by treatment with 10% hydrofluoric acid. *European Journal of Soil Science* 48, 319-328.
- Schmidt, M.W.I. and Noack, A.G., 2000. Black carbon in soils and sediments: Analysis, distribution, implications, and current challenges. *Global Biogeochemical Cycles* 14, 777-793.
- Schmidt, M.W.I., Skjemstad, J.O., Czimeczik, C.I., Glaser, B., Prentice, K.M., Gelinas, Y. and Kuhlbusch, T.A.J., 2001. Comparative analysis of black carbon in soils. *Global Biogeochemical Cycles* 15, 163-167.
- Schöning, I., Knicker, H. and Kögel-Knabner, I., 2005. Intimate association between O/N-alkyl carbon and iron oxides in clay fractions of forest soils. *Organic Geochemistry* 36, 1378-1390.

- Sharma, R.K., Chan, W.G., Seeman, J.I. and Hajaligol, M.R., 2003. Formation of low molecular weight heterocycles and polycyclic aromatic compounds (PACs) in the pyrolysis of alpha-amino acids. *Journal of Analytical and Applied Pyrolysis* 66, 97-121.
- Sharma, R.K., Wooten, J.B., Baliga, V.L., Lin, X.H., Chan, W.G. and Hajaligol, M.R., 2004. Characterization of chars from pyrolysis of lignin. *Fuel* 83, 1469-1482.
- Shneour, E.A., 1966. Oxidation of graphitic carbon in certain soils. *Science* 151, 991-992.
- Simoneit, B.R.T., Schauer, J.J., Nolte, C.G., Oros, D.R., Elias, V.O., Fraser, M.P., Rogge, W.F. and Cass, G.R., 1999. Levoglucosan, a tracer for cellulose in biomass burning and atmospheric particles. *Atmospheric Environment* 33, 173-182.
- Simoneit, B.R.T. and Elias, V.O., 2001. Detecting organic tracers from biomass burning in the atmosphere. *Marine Pollution Bulletin* 42, 805-810.
- Simpson, M.J. and Hatcher, P.G., 2004. Determination of black carbon in natural organic matter by chemical oxidation and solid-state ^{13}C nuclear magnetic resonance spectroscopy. *Organic Geochemistry* 35, 923-935.
- Skjemstad, J.O., Janik, L.J., Head, M.J. and McClure, S.G., 1993. High-energy ultraviolet photooxidation - A novel technique for studying physically protected organic-matter in clay-sized and silt-sized aggregates. *Journal of Soil Science* 44, 485-499.
- Skjemstad, J.O., Clarke, P., Taylor, J.A., Oades, J.M. and Newman, R.H., 1994. The removal of magnetic-materials from surface soils - a solid-state ^{13}C CPMAS NMR study. *Australian Journal of Soil Research* 32, 1215-1229.
- Skjemstad, J.O., Clarke, P., Taylor, J.A., Oades, J.M. and McClure, S.G., 1996. The chemistry and nature of protected carbon in soil. *Australian Journal of Soil Research* 34, 251-271.
- Skjemstad, J.O., Taylor, J.A. and Smernik, R.J., 1999. Estimation of charcoal (char) in soils. *Communications in Soil Science and Plant Analysis* 30, 2283-2298.
- Smernik, R.J. and Oades, J.M., 2000a. The use of spin counting for determining quantitation in solid state ^{13}C NMR spectra of natural organic matter 1. Model systems and the effects of paramagnetic impurities. *Geoderma* 96, 101-129.

- Smernik, R.J. and Oades, J.M., 2000b. The use of spin counting for determining quantitation in solid state ^{13}C NMR spectra of natural organic matter 2. HF-treated soil fractions. *Geoderma* 96, 159-171.
- Smernik, R.J., Skjemstad, J.O. and Oades, J.M., 2000. Virtual fractionation of charcoal from soil organic matter using solid state ^{13}C NMR spectral editing. *Australian Journal of Soil Research* 38, 665-683.
- Smernik, R.J., Baldock, J.A. and Oades, J.M., 2002. Impact of remote protonation on ^{13}C CPMAS NMR quantitation of charred and uncharred wood. *Solid State Nuclear Magnetic Resonance* 22, 71-82.
- Solomon, D., Lehmann, J., Thies, J., Schafer, T., Liang, B.Q., Kinyangi, J., Neves, E., Petersen, J., Luizao, F. and Skjemstad, J., 2007. Molecular signature and sources of biochemical recalcitrance of organic C in Amazonian Dark Earths. *Geochimica Et Cosmochimica Acta* 71, 2285-2298.
- Song, J.Z., Peng, P.A. and Huang, W.L., 2002. Black carbon and kerogen in soils and sediments. 1. Quantification and characterization. *Environmental Science & Technology* 36, 3960-3967.
- Steinbeiss, S., Gleixner, G. and Antonietti, M., 2009. Effect of biochar amendment on soil carbon balance and soil microbial activity. *Soil Biology & Biochemistry* 41, 1301-1310.
- Teeaar, R. and Lippmaa, E., 1984. Solid-state ^{13}C NMR of cellulose - A relaxation study. *Polymer Bulletin* 12, 315-318.
- Tinoco, P., Almendros, G., Sanz, J., Gonzalez-Vazquez, R. and Gonzalez-Vila, F.J., 2006. Molecular descriptors of the effect of fire on soils under pine forest in two continental Mediterranean soils. *Organic Geochemistry* 37, 1995-2018.
- Trompowsky, P.M., Benites, V.D., Madari, B.E., Pimenta, A.S., Hockaday, W.C. and Hatcher, P.G., 2005. Characterization of humic like substances obtained by chemical oxidation of eucalyptus charcoal. *Organic Geochemistry* 36, 1480-1489.

- Tu, T.T.N., Derenne, S., Largeau, C., Mariotti, A. and Bocherens, H., 2001. Evolution of the chemical composition of Ginkgo biloba external and internal leaf lipids through senescence and litter formation. *Organic Geochemistry* 32, 45-55.
- Turekian, V.C., Macko, S., Ballentine, D., Swap, R.J. and Garstang, M., 1998. Causes of bulk carbon and nitrogen isotopic fractionations in the products of vegetation burns: laboratory studies. *Chemical Geology* 152, 181-192.
- Ullrich, R. and Hofrichter, M., 2007. Enzymatic hydroxylation of aromatic compounds. *Cellular and Molecular Life Sciences* 64, 271-293.
- Ushikusa, T., 1990. Pyrolysis mechanism of fatty-acids for thin solid films prepared by physical vapor-deposition. *Japanese Journal of Applied Physics Part 1-Regular Papers Short Notes & Review Papers* 29, 1143-1148.
- Valentin, L., Kluczek-Turpeinen, B., Willfor, S., Hemming, J., Hatakka, A., Steffen, K. and Tuomela, M., 2010. Scots pine (*Pinus sylvestris*) bark composition and degradation by fungi: Potential substrate for bioremediation. *Bioresource Technology* 101, 2203-2209.
- Veeman, W.S., 1997. Nuclear magnetic resonance, a simple introduction to the principles and applications. *Geoderma* 80, 225-242.
- von Lützow, M., Kögel-Knabner, I., Ekschmitt, K., Matzner, E., Guggenberger, G., Marschner, B. and Flessa, H., 2006. Stabilization of organic matter in temperate soils: mechanisms and their relevance under different soil conditions - a review. *European Journal of Soil Science* 57, 426-445.
- Voroney, R.P., Paul, E.A. and Anderson, D.W., 1989. Decomposition of wheat straw and stabilization of microbial products. *Canadian Journal of Soil Science* 69, 63-77.
- Wengel, M., Kothe, E., Schmidt, C.M., Heide, K. and Gleixner, G., 2006. Degradation of organic matter from black shales and charcoal by the wood-rotting fungus *Schizophyllum commune* and release of DOC and heavy metals in the aqueous phase. *Science of the Total Environment* 367, 383-393.

- Wiesenberg, G.L.B., Schwarzbauer, J., Schmidt, M.W.I. and Schwark, L., 2004. Source and turnover of organic matter in agricultural soils derived from n-alkane/n-carboxylic acid compositions and C-isotope signatures. *Organic Geochemistry* 35, 1371-1393.
- Wiesenberg, G.L.B., Lehdorff, E. and Schwark, L., 2009. Thermal degradation of rye and maize straw: Lipid pattern changes as a function of temperature. *Organic Geochemistry* 40, 167-174.
- Willför, S., Hemming, J., Reunanen, M. and Holmbom, B., 2003. Phenolic and lipophilic extractives in Scots pine knots and stemwood. *Holzforschung* 57, 359-372.
- Wiseman, C.L.S. and Püttmann, W., 2006. Interactions between mineral phases in the preservation of soil organic matter. *Geoderma* 134, 109-118.
- Wolbach, W.S. and Anders, E., 1989. Elemental carbon in sediments - determination and isotopic analysis in the presence of kerogen. *Geochimica Et Cosmochimica Acta* 53, 1637-1647.
- Woo, S.H. and Park, J.M., 2004. Microbial degradation and enhanced bioremediation of polycyclic aromatic hydrocarbons. *Journal of Industrial and Engineering Chemistry* 10, 16-23.
- Wu, C., Zhang, X.L. and Li, G.B., 2007. Effects of humic acid coatings on phenanthrene sorption to black carbon. *Journal of Environmental Sciences-China* 19, 1189-1192.
- Xie, H.J., Zhuang, X.L., Bai, Z.H., Qi, H.Y. and Zhang, H.X., 2006. Isolation of levoglucosan-assimilating microorganisms from soil and an investigation of their levoglucosan kinases. *World Journal of Microbiology & Biotechnology* 22, 887-892.
- Yamulki, S. and Jarvis, S.C., 2002. Short-term effects of tillage and compaction on nitrous oxide, nitric oxide, nitrogen dioxide, methane and carbon dioxide fluxes from grassland. *Biology and Fertility of Soils* 36, 224-231.

- Yokelson, R.J., Susott, R., Ward, D.E., Reardon, J. and Griffith, D.W.T., 1997. Emissions from smoldering combustion of biomass measured by open-path Fourier transform infrared spectroscopy. *Journal of Geophysical Research-Atmospheres* 102, 18865-18877.

9. Danksagung

Zum Gelingen dieser Arbeit haben zahlreiche Personen beigetragen, bei denen ich mich an dieser Stelle herzlich bedanken möchte. Insbesondere auch all jenen, die an dieser Stelle nicht namentlich genannt werden, gilt mein Dank.

Meine besondere Anerkennung gilt meiner Doktormutter Frau Prof. Dr. Heike Elisabeth Knicker für die Überlassung des anspruchsvollen Themas, ihrer Geduld und ihrer steten Diskussionsbereitschaft, welche maßgebend zum Abschluss dieser Arbeit beigetragen haben. Bei Frau Prof. Dr. Ingrid Kögel-Knabner bedanke ich mich für die Übernahme des Prüfungsvorsitzes sowie bei Herrn Prof. Dr. Jörg Völkel und Herrn Prof. Dr. Christian Siewert für die Begutachtung der Dissertation.

Der Deutschen Forschungsgemeinschaft (DFG), der International Humic Substances Society (IHSS), der European Science Foundation (ESF), sowie der Kooperationsgemeinschaft des Deutschen Akademischen Austausch Dienstes (DAAD) und des Coordenação de Aperfeiçoamento de Pessoal de Nível Superior (CAPES) wird für die Finanzierung der Projekte gedankt.

Für die ausgezeichnete Laborarbeit danke ich Xiao Chen (Xiao, ich hoffe deinen Namen nun endlich richtig geschrieben zu haben), Olivia Kreyling, Petra Müller und Christoph Grausam.

Der gesamten Laborbelegschaft und allen Mitarbeitern des Lehrstuhles für Bodenkunde spreche ich an dieser Stelle meinen herzlichen Dank für die schöne gemeinsame Zeit und all die unterhaltsamen Momente aus.

Für die unbürokratische Hilfe in Bezug auf Computer und Posterdruck danke ich Brigitte Eberle, Elfriede Schuhbauer und dem Flo (Florian Schmalzl). Frau Dr. Katja Heister, Frau Dr. Angelika Kölbl und Herrn Prof. Dr. Jörg Prietzel sei nochmals für das Korrekturlesen der Manuskripte meine Anerkennungen ausgesprochen.

Meinen Mit-Doktoranden und ehemaligen Mitstreitern Josefine Beck, Carolin Bimüller, Olivia Kreyling, Pascale S. Naumann, Geertje Pronk, Dr. Sandra Spielvogel, Nora Tyufekchieva, Sven Bachmann, Dr. Thomas Caspari, Dominik Christophel, Dr. Alexander B. Dümig, Dr. Andreas Fritzsche, Dr. Steffen Jann; Dr. Carsten W. Müller, Dr.

Ingo Schöning, Dr. Markus Steffens, Dr. Markus Wehrer und Dr. Martin Wiesmeier gilt mein Dank für all die kleinen und großen Hilfen. Besonders möchte ich mich bei meiner langjährigen Zimmerkollegin Britt Pagels und Liv (Livia Wissing) für ihren lebensfrohen und erfrischenden Umgang bedanken.

Herrn Florian Steinbacher vom Lehrstuhl für Zierpflanzenbau des Gewächshauslaborzentrums Dürnast sei für die Bereitstellung einer Klimakammer und seiner Hilfsbereitschaft mein Dank ausgesprochen. In diesem Zusammenhang bedanke ich mich bei Joseph Fischer für seine Mithilfe an der Konstruktion der Plexiglas-Anzuchtbox.

Frau Prof. Dr. Déborah Pinheiro Dick und Herrn Prof. Dr. Cimélio Bayer von der Univeridade Federal do Rio Grande do Sul (UFRGS) in Porto Alegre (Brasilien) bedanke ich mich für die hervorragende fachliche und freundschaftliche Zusammenarbeit. In diesem Zusammenhang danke ich allen Mitarbeitern der Faculdade de Agronomia und des Instituto de Quimica für ihre herzliche Aufnahme und die vielen schönen Momente während meines 6-monatigen Aufenthaltes, welche meinem Leben mehr Farbe verliehen haben. Ganz besonders möchte ich an diese Stelle Suzana Caixeta, Marquel Holzschuh und Gustavo Portz hervorheben. Obrigado!

Herrn Prof. Dr. Francisco Javier González Vila, Trinidad Verdejo Robles, Dr. José Antonio González Pérez und Carlos Marfil Daza vom Instituto de Recursos Naturales y Agrobiología de Sevilla (IRNAS-CSIC) in Sevilla (Spanien) sei herzlichst für die erfolgreiche 10-monatige Zusammenarbeit und das familiäre Arbeitsklima gedankt. Quico, dir möchte ich an dieser Stelle nochmals besonders meine Anerkennung aussprechen, ich freue mich schon darauf dich zu treffen! Meinen WG-Mitbewohnern und Freunden David, Fran und Oñi sei an dieser Stelle für Ihre offene und freundschaftliche Art gedankt. Ich werde die vielen verrückten Aktionen nie vergessen. Gracias y hasta pronto!

Frau Prof. Dr. Cornelia Rumpel vom Laboratoire Biogéochimie et écologie des milieux continentaux (Bioemco; CNRS-INRA) in Thiverval-Grignon (Frankreich) sei für ihre Unterstützung bei isotopenspezifischen Messungen gedankt. Merci beaucoup!

Meinen Freunden und ehemaligen Studienmitstreitern Christopher Freund (in Fachkreisen als Fritz bekannt) und Jens Habermann danke ich für das Korrekturlesen der deutschsprachigen Kapitel meiner Dissertation.

Mein größter Dank gilt meinen Eltern Brigitte und Günter, meinen Großeltern Ruth und Reinhold, meiner Familie und meinen Freunden. Ihr habt in guten und in schlechten Zeiten immer hinter mir gestanden und mir das Gefühl vermittelt, dass ihr an mich glaubt. Ich werde euch immer verbunden sein!

Curriculum Vitae

Personal data

Name André Hilscher
Sex male
Date and Place of Birth 29/01/1978 - Werdau - Germany
Nationality German
Address Bismarckstraße 24
D-85356 Freising
E-Mail: hilscher@wzw.tum.de

Academic education and titles

Since 04/2010 Research associate at the Chair of Soil Science, Technische Universität München, Freising-Weihenstephan, Germany.

Project: CO₂-Binding of ammonoxidized lignins and their use as soil improvers.

10/2009 –07/2010 Research visit to the Instituto de Recursos Naturales y Agrobiología de Sevilla (IRNAS-CSIC), Seville, Spain.

Project: Modification of plant biomarkers by charring and during the initial phase of biodegradation of pyrogenic organic matter in soils, funded by the International Humic Substances Society (IHSS) and the European Science Foundation (ESF).

03/2009 – 07/2009 Assistant lecturer at the Institute of Landscape Architecture, University of Applied Sciences Weihenstephan, Freising-Weihenstephan, Germany.

- 06/2008 – 02/2009 Laboratory assistant at the Chair of Soil Science, Technische Universität München, Freising-Weihenstephan, Germany.
- Project: Structures and processes of the initial ecosystem development phase.*
- 09/2007 – 02/2008 Research visit to the Universidade Federal Do Rio Grande Do Sul (UFRGS), Porto Alegre, Brazil.
- Project: Dynamics and stabilisation mechanisms of the organic matter in Brazilian soils under no-tillage, supported by CAPE and DAAD.*
- 10/2004 – 09/2007 Research assistant at the Chair of Soil Science, Technische Universität München, Freising-Weihenstephan, Germany.
- Project: Degradation and humification of charred necromass in soil.*
- 10/1997 – 09/2003 Graduation in Geoecology (Diploma)
Interdisciplinary Environmental Research Center (IÖZ)
Technische Universität Bergakademie Freiberg, Germany.
Main subjects: Geochemistry, Microbiology
- Diploma thesis: Trace elements in vegetables and wild plants grown on former mining sites in Eastern Germany.*
- 07 – 09/2001 Practical work at the Volkswagen Sachsen GmbH, Mosel, Germany.
- Project: Setup of an environmental information system (UIS).*
- 11/1996 – 08/1997 Military service

06/1996

Abitur, Julius-Motteler-Gymnasium, Crimmitschau, Germany.

Membership

International Humic Substances Society

Deutsche Bodenkundliche Gesellschaft

Publications

Peer reviewed journals

- HILSCHER, A., GONZÁLEZ-VILA, F.J., VERDEJO ROBLES T. AND KNICKER, H.** (2011). Modification of plant biomarkers by charring and during the initial phase of biodegradation of pyrogenic organic matter in soils. *submitted*.
- HILSCHER, A. AND KNICKER, H.** (2011). Carbon and Nitrogen degradation on molecular scale of grass-derived pyrogenic organic material during 28 months of incubation in soil. *Soil Biology & Biochemistry* 43, 261-270.
- HILSCHER, A. AND KNICKER, H.** (2011). Degradation of grass-derived pyrogenic organic material, transport of the residues within a soil column and distribution into soil organic matter fractions during a microcosm experiment of 28 months. *Organic Geochemistry* 42, 42-54.
- HILSCHER, A., HEISTER, K., SIEWERT, S., KNICKER, H.** (2009). Mineralisation and structural changes during the initial phase of microbial degradation of pyrogenic plant residues in soil. *Organic Geochemistry* 40, 332-342.
- WIESMEIER M., DICK, D.P., RUMPEL, C., DALMOLIN, R.S.D., HILSCHER, A., KNICKER, H.** (2009). Depletion of soil organic carbon and nitrogen under *Pinus taeda* plantations in Southern Brazilian (*Campos*). *European Journal of Soil Science* 60, 347-359.
- KNICKER, H., HILSCHER, A., GONZÁLEZ-VILA, F.J., ALMENDROS, G.** (2008). A new conceptual model for the structural properties of char produced during vegetation fires. *Organic Geochemistry* 39, 935-939.
- KNICKER, H., MÜLLER, P., HILSCHER, A.** (2007). How useful is chemical oxidation with dichromate for the determination of “Black Carbon” in fire-affected soils? *Geoderma* 142(1-2), 178 - 196.

MATSCHULLAT, J., BIRMANN, K., BORBA, R.P., CIMINELLI, V., DESCHAMPS, E.M., FIGUEIREDO, B.R., GABRIO, T., HASSLER, S., **HILSCHER, A.**, JUNGHÄNEL, I., DE OLIVEIRA, N., RASSBACH, K., SCHMIDT, H., SCHWENK, M., DE OLIVEIRA VILHENA, M.J., WEIDNER, U. (2007). Long-term environmental impact of As-dispersion in Minas Gerais, Brazil. In: Bhattacharya P, Mukherjee AB, Bundschuh, J, Zevenhoven, R, Loeppert RH (eds) Arsenic in soil and groundwater environments: biogeochemical interactions. Trace metals and other contaminants in the environment 9, Elsevier, 365 - 382.

Oral presentations

HILSCHER, A., SIEWERT, S., KNICKER, H. (2009): Degradation of plant chars in soil. Guest lecture at the Instituto de Recursos Naturales y Agrobiología de Sevilla, Spain, November 2009.

HILSCHER, A., SIEWERT, S., KNICKER, H. (2009): Degradation of pyrogenic organic plant residues in soil. II International Meeting "Forest Fire Effects in Soils" FUEGORED, Sevilla – Cortegana, Spain, November 2009. *Member of the Organisation Committee.*

HILSCHER, A., SIEWERT, S., KNICKER, H. (2009): Abbau und Humifizierung pyrogener Pflanzenmaterialien im Boden. DBG Jahrestagung, Bonn, Germany, September 2009.

KNICKER, H., **HILSCHER, A.**, DE LA ROSA, J.M. (2008): How reliable is chemical oxidation with dichromate for the determination of pyrogenic organic matter in fire-affected soils? Reunión Internacional, Jornadas de la Red Temática, Efectos de los Incendios Forestales sobre los Suelos. Valencia, Spain, December 2008.

HILSCHER, A., SIEWERT, S., KNICKER, H. (2008): Mineralisation and structural modifications of different pyrogenic materials by microbiology activities. Joint meeting between the Geological Society of America (GSA), Soil Science Society of America (SSSA), American Society of Agronomy (ASA), Crop Science Society of America (CSSA), and the Gulf Coast Association of Geological Societies, Houston, USA, October 2008.

HILSCHER, A., SIEWERT, S., KNICKER, H. (2008): Short time humification and mineralisation of different pyrogenic materials under controlled laboratory conditions. 14th Meeting of the International Humic Substances Society, Moscow, Russia, September 2008.

KNICKER, H., HILSCHER, A., GONZÁLEZ-VÁZQUEZ, R., ALMENDROS, G., GONZÁLEZ-VILA, F.J. (2008): “Black nitrogen” – An important fraction of the stable soil organic matter pool? Eurosoil, Vienna, Austria, August 2008.

HILSCHER, A., KNICKER, H. (2007): Wie refraktär ist Holzkohle aus Vegetationsbränden? – Abbaustudien mit isopenangereicherten pflanzlichen Verbrennungsrückständen. DBG Jahrestagung, Dresden, Germany, September 2007.

KNICKER, H., MÜLLER, P., HILSCHER, A. (2007): Wie verlässlich ist die chemische Oxidation mit Kaliumdichromat zur Bestimmung des Holzkohleanteils in feuerbeeinflussten Böden?, Jahrestagung der Deutschen Bodenkundlichen Gesellschaft, Dresden, Deutschland, September 2007.

KNICKER, H., HILSCHER, A., GONZALEZ-VILA, F.J., GONZALEZ-PEREZ, J.A., ALMENDROS, G. (2007): Where is all the charcoal gone? – Structure and stability of charred plant residues and their role in refractory soil organic matter formation. International meeting of fire effects on soil properties, Barcelona, Spain, January 2007.

HILSCHER, A., KNICKER, H. (2006): Degradation of isotopically labelled black carbon. 3rd European Symposium on NMR Spectroscopy in Soil, Geo and Environmental Sciences, Freising, Germany, August 2006.

KNICKER H., HILSCHER, A., ALMENDROS, G., GONZÁLEZ-VILA, F.J., GONZÁLEZ-PÉREZ, J.A. (2006): The fate of charcoal in soils. Seminar at the Geographical institute of the University of Zurich, Zurich, Switzerland, January 2006.

KNICKER, H., HILSCHER, A., ALMENDROS, G., GONZÁLEZ-VILA, F.J. (2005): Cluster-size of aromatic domains in charred humic material and its impact on the stability of pyromorphic soil organic matter. 22nd International Meeting on Organic Geochemistry, Seville, Spain, September, 2005.

HILSCHER, A., GONZÁLEZ-VILA, F.J., GONZÁLEZ, J.A., BOSKI, T., KNICKER, H. (2005): Black Carbon ein wichtiger Bestandteil der Partikulären Organischen Substanz in Feuerbeeinflussten Arenosolen. Jahrestagung der Deutschen Bodenkundlichen Gesellschaft, Marburg, Deutschland, September 2005.

KNICKER, H., HILSCHER, A., ALMENDROS, G., GONZÁLEZ-VILA, F.J., GONZÁLEZ-PÉREZ, J.A. (2005): Charakteristische Zusammensetzung pyrogener Nekromasse in feuerbeeinflussten Waldböden. Jahrestagung der Deutschen Bodenkundlichen Gesellschaft, Marburg, Deutschland, September 2005.

KNICKER, H., HILSCHER, A., ALMENDROS, G., GONZÁLEZ-VILA, F.J., GONZÁLEZ-PÉREZ, J.A., POLVILLO, O. (2005): Humification and stability of charcoal in soils. ESF LESC Exploratory workshop: charcoal to black carbon. St. Andrew, United Kingdom, September 2005.

Poster presentations

HILSCHER A., GONZÁLEZ-VILA, F.J., VERDEJOB T., KNICKER H. (2010): Modification of plant biomarkers by charring and during the initial phase of biodegradation of pyrogenic organic matter in soils. III International Meeting "Forest Fire Effects in Soils" FUEGORED, Santiago de Compostela, Spain, October 2010.

HILSCHER, A., KNICKER, H. (2010): Carbon and nitrogen dynamics of grass-derived pyrogenic organic material during 2.3 years of incubation in soil. 3rd International Biochar Conference, Rio de Janeiro, Brazil, September 2010.

KNICKER, H., HILSCHER, A. (2010): Impact of Impact of Structural Heterogeneity of Pyrogenic Organic Material (PyOM) on Humification Processes in Fire-Affected Soils. 15th IHSS Meeting, Puerto de la Cruz, Tenerife, Spain, June 2010.

HILSCHER, A., KNICKER, H. (2010): Humification of pyrogenic organic plant residues in soil. 15th IHSS Meeting, Puerto de la Cruz, Tenerife, Spain, June 2010. *Member of the Organisation Committee.*

HILSCHER, A., KNICKER, H. (2010): NMR spectroscopic study of the carbon and nitrogen dynamics of grass-derived pyrogenic organic material during 2.3 years of incubation in soil. European Geosciences Union: EGU General Assembly, Vienna, Austria, April 2010.

- DE LA ROSA, GONZÁLEZ-VILA, F.J., KNICKER, H., **HILSCHER, A.**, RODRÍGUEZ-RODRÍGUEZ, A., ARBELO, C.D., VERDEJO, T., GONZÁLEZ-PÉREZ, J.A. (2009): Analytical characterization of soil organic matter changes exerted by wildfires in an Andosol from North East Tenerife (Canary Islands). II International Meeting on Forest Fire Effects on Soils, FUEGORED, Sevilla-Cortegana, November 2009.
- KNICKER, H., **HILSCHER, A.**, DE LA ROSA, J.M., GONZÁLEZ-VILA, F.J., ALMENDROS, G. (2009): “Black nitrogen” – its impact on size and quality of the refractory soil organic N and C pool. Soil Organic Matters – Rothamsted Research, West Common, Harpenden, Hertfordshire, UK, June 2009.
- HILSCHER, A.**, SIEWERT, S., KNICKER, H. (2008): Black Carbon loss and structural modifications of different pyrogenic materials by microbiology activities. European Geosciences Union: EGU General Assembly, Vienna, Austria, April 2008.
- KNICKER, H., **HILSCHER, A.**, GONZÁLEZ-VILA, F.J., ALMENDROS, G. (2007): A new conceptual model for the structural properties of char produced during vegetation fires. 23rd International Meeting on Organic Geochemistry, Torquay, United Kingdom, September 2007.
- HILSCHER, A.**, KNICKER, H. (2007): Degradation and Relocation of isotopically labelled Char subjected to incubation under controlled laboratory conditions. 22nd International Meeting on Organic Geochemistry, Torquay, Devon, United Kingdom, September 2007.
- WIESMEIER, M., RUMPEL, C., **HILSCHER, A.**, DICK, D., KNICKER, H., (2007): Veränderungen der organischen Bodensubstanz nach Aufforstungen brasilianischer Grasländer mit *Pinus spp.* Jahrestagung der Deutschen Bodenkundlichen Gesellschaft, Dresden, Deutschland, September 2007.
- HILSCHER, A.**, KNICKER, H. (2007): How stable is Black Carbon? - An incubation experiment. European Geosciences Union: EGU General Assembly, Vienna, Austria, April 2007.
- HILSCHER, A.**, GONZÁLEZ-VILA, F.J., GONZÁLEZ, J.A., BOSKI, T., KNICKER, H. (2006): Transport of Pyrogenic Humic Substances by Particulate Organic Matter in Fire-Affected Arenosols. 13th Meeting of the International Humic Substances Society, Karlsruhe, Germany, July 2006.

HILSCHER, A., HAGEDORN, F., KNICKER, H. (2006): Incorporation of black carbon into soil organic matter of forested high-elevation soils in Switzerland. European Geosciences Union: EGU General Assembly, Vienna, Austria, April 2006.

HILSCHER, A., GONZÁLEZ-VILA, F.J., GONZÁLEZ, J.A, BOSKI, T., KNICKER, H. (2005): Particulate Organic Matter as a Means for Transport of Black Carbon in Fire-Affected Arenosols - In: F.J. González-Vila, J.A. González-Pérez and G. Almendros (Eds): 22nd International Meeting on Organic Geochemistry, Seville, Spain, September 2005, Organic Geochemistry: Challenges for the 21st Century, Book of Abstracts, Vol. 2, 1069-1070, ISBN 84-689-3661-8.

HILSCHER, A., MATSCHULLAT, J. (2005): Trace Elements in Vegetables and Wild Plants grown on former Mining Sites in Eastern Germany. 3rd International Conference on Soils of Urban, Industrial, Traffic, Mining and Military Areas, Cairo, Egypt, November 2005.

KNICKER, H., HILSCHER, A., GONZÁLEZ-VILA F.J., GONZÁLEZ-PEREZ, J.A., ALMENDROS, G. (2005): Transport of Black Carbon in Soil. EGU, Vienna, Austria, April 2005.